

Conceptual Design of a Sustainable Waste Burning Molten Salt Reactor

THÈSE N° 8570 (2018)

PRÉSENTÉE LE 11 JUILLET 2018

À LA FACULTÉ DES SCIENCES DE BASE

LABORATOIRE DE PHYSIQUE DES RÉACTEURS ET DE COMPORTEMENT DES SYSTÈMES

PROGRAMME DOCTORAL EN PHYSIQUE

ÉCOLE POLYTECHNIQUE FÉDÉRALE DE LAUSANNE

POUR L'OBTENTION DU GRADE DE DOCTEUR ÈS SCIENCES

PAR

Boris Aviv HOMBOURGER

acceptée sur proposition du jury:

Prof. V. Savona, président du jury

Prof. A. Pautz, Dr J. Křepel, directeurs de thèse

Prof. E. Merle, rapporteuse

Dr J. Frýbort, rapporteur

Prof. H.-M. Prasser, rapporteur



ÉCOLE POLYTECHNIQUE
FÉDÉRALE DE LAUSANNE

Suisse
2018

Acknowledgements

I would first of all like to thank my thesis director Prof. Pautz for offering me early on the possibility of performing this research at his laboratory on a subject that is dear to me.

I would like to thank my co-supervisor Dr. Křepel for allowing such an unruly student to work with him and spend hours arguing over molten salt reactors, debating the optimum amount of hop in beer, introducing me to dršť'ková polévka as well as sharing his graphical skills with me.

This thesis would not have been possible without the funding of the Swiss National Fund for Research (SNF/FNS) and the Project and Study Fund of the Electricity Industry (PSEL) of the Association of Swiss Electricity Producers (VSE). I am very grateful for their financial support. Prof. Merle, Dr. Frýbort and Prof. Prasser have accepted to be part of my jury and their interest in this work and willingness to spend their precious time reviewing it is gratefully acknowledged.

The other permanent members of the recently renamed FAST group Konstantin and Sandro as well as those that were part of the group for a shorter time including Manuele, Carlo, Sara, Matteo and Alexander, as well as other NES people I have had the pleasure of discussing with at length on profound topics such as Hakim, Philippe and Omar, have all contributed to making my time at PSI more enjoyable through both serious and much less serious discussions.

This list would not be complete without the students that have been great office mates and that have been missed: Miquel, Valerio, Jongsoo, Evžen, Nikoleta, Hyemin, Alžběta, Eirik, Kajetan, Fanny, Emeline, Ahmed, Marianna, Simone, Marco, Byungho and Václav.

Thanks are due to the NES Ph.D. students whose adventures overlapped with mine in space and time: Ting, Damar, Vladimir, Petra, Cornelia, Dionysios, Petros, Valentyn, Anne-Laurène, Benoît, Rodrigo, and János. I wish them all the best and good luck to those that have not finished yet.

I would like to thank my mother Véronique and sister Laura for their unwavering support and for reminding me of also taking (some) care of myself.

Finally, I would like to thank Sarah for being awesome and providing much needed encouragements, motivation, and moral support.

B. A. H.

Abstract

For an energy source to qualify as sustainable, it must maximize the efficiency with which it uses natural resources while minimizing the amounts of waste it produces. Currently deployed nuclear power plants however use a very limited amount of the energy contained in natural nuclear fuels such as Uranium and Thorium and produce long-lived nuclear waste that must be dealt with.

Molten Salt Reactors (MSRs) are one family of advanced reactors designs with the potential for safe and sustainable energy production due to their use of a liquid molten salt fuel. This thesis aimed at reviewing MSR designs that have been proposed in the past, investigating alternative design possibilities and proposing a concept capable of disposing of existing waste in a sustainable manner. One possibility to do so is to design a reactor to run on an isobreeding closed fuel cycle while using existing actinide waste as a start-up inventory, which is the route investigated in this thesis.

For this purpose, the EQL0D fuel cycle procedure was developed using the MATLAB environment and the Serpent 2 Monte Carlo neutron transport code to simulate the start-up, transition and equilibrium of MSRs.

The procedure was then applied to investigate the performance at equilibrium of several candidate fuel salts and moderators in an infinite lattice and in a closed Uranium-Plutonium and Thorium-Uranium fuel cycle. The results showed that only an isobreeding closed Uranium-Thorium fuel cycle can be achieved in moderated MSRs, while both isobreeding Uranium-Plutonium and Thorium-Uranium closed fuel cycles can be sustained in fast-spectrum MSRs, which additionally show a substantial reactivity margin that enable them to dispose of poorly fissile nuclides.

The transition behavior of selected fluoride- and chloride-fueled reactors was then investigated. The fluoride-fueled cores all feature a closed Thorium-Uranium fuel cycle and included two historical graphite-moderated designs (the single- and two-fluid Molten Salt Breeder Reactors) and a modern fast-spectrum design (Molten Salt Fast Reactor). The chloride-fueled cores were proposed based on the results obtained in the infinite lattice study. The results obtained indicated that the transuranic-burning capabilities of fluoride-fueled reactors are substantially limited by the low solubility of transuranic trifluorides in fluoride salt mixtures, while no such limitation was found in chloride salts. On the other hand, chloride salts necessitate substantially larger cores and inventories.

Finally, the possibility of operating MSRs on two types of open cycles without fuel processing, breed-and-burn and once-through, was investigated to alleviate concerns related to the

Acknowledgements

uncertainties related to the technical feasibility of molten salt fuel processing in closed fuel cycles. The results obtained show that it is possible to operate chloride-fueled MSR in a sustainable breed-and-burn fuel cycle and also on an open cycle with appreciable burn-ups achieved.

Keywords: Molten Salt Reactor, Nuclear Fuel Cycle, Breed-and-Burn

Résumé

Pour qu'une source d'énergie soit durable, son efficacité d'utilisation des ressources naturelles doit être maximisée tout en produisant le moins possible de déchets. Pourtant, les centrales nucléaires actuelles n'utilisent qu'une faible fraction de l'énergie contenue dans les combustibles nucléaires naturels tels que l'Uranium ou le Thorium, tout en produisant des déchets radioactifs à vie longue qui doivent être gérés.

Les Réacteurs à Sels Fondus (RSF) sont une filière de réacteurs de nouvelle génération avec un fort potentiel de production sûre d'énergie durable grâce à leur utilisation d'un combustible liquide sous la forme de sels fondus. Cette thèse visait à passer en revue les concepts de RSF proposés dans le passé, examiner les possibilités alternatives de conception, et de proposer un concept capable d'éliminer les déchets existants de manière durable. Une possible voie est de concevoir un réacteur capable d'opérer dans un cycle régénérateur tout en utilisant les déchets existants sous la forme d'actinides comme inventaire initial, et c'est la route choisie dans cette thèse.

Pour ce faire, la procédure de calcul EQL0D dédiée au cycle du combustible des RSF a été développée en utilisant le code de transport neutronique Monte Carlo Serpent 2 et l'environnement de calcul MATLAB pour simuler le démarrage, la transition et l'équilibre des RSF.

La procédure fut ensuite appliquée à l'examen des performances de plusieurs sels combustibles et modérateurs potentiels dans un réseau infini et dans des cycles combustible Uranium-Plutonium et Thorium-Uranium fermés. Les résultats montrent que seul un cycle fermé et régénérateur Thorium-Uranium peut être obtenu en spectre thermique, alors que des cycles fermés et régénérateurs Uranium-Plutonium et Thorium-Uranium sont possibles en spectre rapide, ces derniers ayant une réserve de réactivité suffisamment grande pour leur permettre de fissionner des nucléides peu fissiles.

Le comportement en transition de sels à base fluorure et chlorure fût donc ensuite étudiée. Les cœurs à combustible fluorure utilisent tous un cycle Thorium-Uranium fermé et incluent deux concepts historiques modérés au graphite (les Molten Salt Breeder Reactors à un et deux fluides) et un concept moderne en spectre rapide (le Molten Salt Fast Reactor). Les cœurs à combustible chlorure furent proposés sur la base des résultats de l'étude de réseau. Les résultats indiquent que les capacités d'incinération de transuraniens des combustibles à base fluorure sont substantiellement limités par la faible solubilité des trifluorures de transuraniens dans les mélanges de sels de fluorures, alors qu'il n'existe pas de telle limite dans les sels chlorures. Les cœurs à combustibles chlorure nécessitent par contre de très larges dimensions et inventaires fissiles.

Acknowledgements

Finalement, la possibilité d'opérer des RSFs en deux types de cycles ouverts sans retraitement du combustible, d'un côté le Breed-and-Burn et de l'autre le passage unique en cœur, furent examinés pour répondre aux incertitudes liées à la faisabilité technique et économique du retraitement du combustible en cycle fermé. Les résultats obtenus indiquent qu'il est possible d'opérer des RSFs à combustible chlorures dans un cycle Breed-and-Burn durable ainsi que dans un cycle ouvert tout en atteignant des taux de combustion élevés.

Mots-clés : Réacteurs à Sels Fondus, Cycle du combustible nucléaire, Breed-and-Burn

Contents

Acknowledgements	iii
Abstract/Résumé	v
List of Figures	xi
List of Tables	xiv
List of Symbols	xvii
1 Introduction	1
1.1 Climate Change	2
1.2 Challenges Faced by Nuclear Power	4
1.2.1 Safety of Nuclear Power Plants	4
1.2.2 Sustainability of the Nuclear Fuel Cycle	5
1.2.3 Economic Performance	7
1.2.4 Proliferation	8
1.3 Advanced Nuclear Power Plants	8
1.3.1 Small Modular Reactors	8
1.3.2 Generation IV Reactors	9
1.3.3 Liquid fuel reactors	10
1.3.4 Other Advanced Reactors	11
1.4 Aim and Structure of this Thesis	12
1.4.1 Aim of the Thesis	12
1.4.2 Structure of the Thesis	12
2 Molten Salt Reactors	15
2.1 Background and Definitions	15
2.2 History of Molten Salt Reactors	17
2.2.1 Early Military Debuts	17
2.2.2 Continuation as a Civilian Program	18
2.2.3 The Molten Salt Reactor Experiment	21
2.2.4 The End of the Pioneering Era	25
2.2.5 Research Outside of the United States	26
2.3 Molten Salt Reactor Concepts	32

Contents

2.3.1	Graphite-moderated Fluoride Reactors	33
2.3.2	Fast-spectrum Homogenous Fluoride Reactors	33
2.3.3	Fast-spectrum Homogeneous Chloride Reactors	34
2.3.4	Heterogeneous Fast-spectrum Reactors	34
2.3.5	Other Concepts	36
2.4	Fuel Salts and Materials	38
2.4.1	Fuel Salts	38
2.4.2	Strutural Materials	43
3	Methods and Tools	49
3.1	Tools	49
3.1.1	Serpent	49
3.1.2	MATLAB	50
3.2	Applied Methods	50
3.2.1	Core Dimensions Estimation	50
3.2.2	Equilibrium reactivity break-down	53
3.2.3	Density of salt mixtures estimation	54
3.2.4	Nuclides removal	54
3.2.5	Burn-up in Molten Salt Reactors	57
3.2.6	Model of Breed-and-Burn in Molten Salt Reactors	58
3.3	The EQL0D Procedure	62
3.3.1	Bateman equations	63
3.3.2	Coupled Bateman equations	64
3.3.3	Nuclide addition operations	65
3.3.4	Verification	70
4	Equilibrium Closed Fuel Cycle Performance in an Infinite Lattice	75
4.1	Introduction	75
4.2	Assumptions	76
4.2.1	Lattice geometry	76
4.2.2	Closed fuel cycle	76
4.3	Results	78
4.3.1	Uranium-Plutonium cycle	78
4.3.2	Thorium-Uranium cycle	80
4.4	Separate Effects	84
4.4.1	Effect of cladding material	84
4.4.2	Effect of Protactinium capture	85
4.4.3	Effect of reprocessing cycle time	86
4.5	Conclusions	88

5	Transition to Equilibrium in a Closed Fuel Cycle	89
5.1	Introduction	89
5.2	Fluoride-fueled Reactors	89
5.2.1	Initial inventory	94
5.2.2	Equilibrium properties	95
5.2.3	Transition to equilibrium state	99
5.3	Chloride-fueled Reactors	109
5.3.1	Initial inventory	109
5.3.2	Equilibrium	110
5.3.3	Transition to equilibrium state	111
5.4	Conclusions	115
6	Open Fuel Cycles	119
6.1	Introduction	119
6.2	Breed-and-Burn Fuel Cycle	119
6.2.1	Lattice-level calculations	122
6.2.2	Full-core calculations	125
6.3	Once-through Cycle	129
6.4	Conclusions	130
7	Conclusions	133
7.1	Summary	133
7.2	Future work	135
	Bibliography	145
	List of Abbreviations	147
	Curriculum Vitae	151

List of Figures

1.1	Global average temperature and GHG emissions	3
1.2	Radiotoxicity of LWR Spent Nuclear Fuel	6
2.1	Aircraft Reactor Experiment	19
2.2	Aircraft Reactor Test	20
2.3	Two-fluid Molten Salt Breeder Reactor	22
2.4	Single-fluid Molten Salt Breeder Reactor	23
2.5	Molten Salt Reactor Experiment	24
2.6	Direct lead-cooling Graphite-Moderated Molten Salt Reactor	27
2.7	Indirect Lead Cooling Molten Salt Reactor	28
2.8	Single-fluid Chloride-fueled Molten Salt Reactor	29
2.9	Accelerator-driven Molten Salt Reactor for Transmutation	31
2.10	Classification of proposed Molten Salt Reactor Designs	33
2.11	Fast-spectrum Fluoride-fueled Molten Salt Reactors	35
2.12	Illustration of the Terrapower concept.	36
2.13	Illustrations of two Converter concepts.	37
2.14	Candidate elements for a molten salt fuel mixture	39
2.15	Microscopic capture cross-section of salt elements	40
3.1	Fission Product behavior in molten salt fuels	55
3.2	Illustration of Residence Time Distributions	59
3.3	Illustration of the neutron excess concept	61
3.4	Comparison of neutron excess predictions and direct calculation results	62
3.5	Flowchart of the EQL0D procedure	69
3.6	Comparison of EVOL benchmark results to EQL0D	71
4.1	Illustration of lattice heterogeneity	77
4.2	Maximum reactivity in fluoride salts in U-Pu cycle as function of moderator	78
4.3	Reactivity decomposition of $\text{LiF}-\text{UF}_4$ in a graphite lattice and closed U-Pu cycle	79
4.4	Reactivity decomposition of salts in fast spectrum and U-Pu cycle	79
4.5	Equilibrium reactivity as function of salt and moderator in closed Th-U cycle	81
4.6	Maximum reactivity in fluoride salts in Th-U cycle as function of moderator	82
4.7	Reactivity decomposition of salts in fast spectrum and Th-U cycle	82
4.8	Neutron spectrum of unmoderated fluoride salts	83

List of Figures

4.9	Neutron spectrum of unmoderated chloride salts	84
4.10	Effect of cladding materials on equilibrium reactivity	85
4.11	Effect of power density on isobreeding fuel volume	86
4.12	Effect of reprocessing cycle time on isobreeding fuel volume	87
4.13	Effect of cycle time on reprocessing rate	88
5.1	Core model of fluoride-fueled reactors	90
5.2	Comparison of the fuel cycle of MSBR(2f), MSBR and MSFR.	92
5.3	Comparison of initial critical load per thermal power.	96
5.4	Equilibrium nuclide masses in MSBR(2f), MSBR and MSFR	97
5.5	Comparison of ^{232}U content in fuel and feed materials at equilibrium.	98
5.6	Cumulative mass of fuel necessary to reach excess ^{233}U production	100
5.7	Neutrons balance of fluoride-fueled reactors during ^{233}U transition	102
5.8	Neutrons balance of fluoride-fueled reactors during HEU and LEU transition	103
5.9	Neutrons balance of fluoride-fueled reactors during Pu transition	104
5.10	Conversion ratio of fluoride-fueled reactors during transition	105
5.11	Net ^{233}U mass produced during transition to equilibrium	106
5.12	Concentration of trifluorides during transition to equilibrium	108
5.13	Core model of chloride-fueled reactors	110
5.14	Equilibrium nuclide masses in chloride-fueled reactors	111
5.15	Conversion ratio of chloride-fueled reactors during transition	112
5.16	Neutrons balance of chloride-fueled reactors during transition	113
5.17	Excess fissile material generated in chloride-fueled reactors	114
5.18	Sulfur production in chloride reactors	115
5.19	Radiotoxicity production in closed fuel cycle	117
6.1	Comparison of B&B reactors with converters and breeders	120
6.2	Comparison of the evolution burn-up of liquid and solid fuels	121
6.3	Achievable k_{∞} in B&B for fluorides	123
6.4	Achievable k_{∞} in B&B for chlorides	124
6.5	Equilibrium core dimensions in B&B	126
6.6	Cumulative volume of fuel salt discharged in B&B	127
6.7	Reactivity evolution of chloride-fueled reactors in an open cycle	130
6.8	Radiotoxicity production in open fuel cycle	132

List of Tables

1.1	Comparison of the six Generation IV systems	10
2.1	Fluoride salt compositions and characteristics	43
2.2	Chloride salt compositions and characteristics	44
2.3	Materials and characteristics	46
2.4	Isotopic composition of start-up fuels	47
3.1	Comparison of legacy ORNL and EQL0D results	72
5.1	Reference characteristics of MSBR(2f), MSBR and MSFR	91
5.2	Cycle times of FPs in MSBR(2f), MSBR and MSFR	93
5.3	Initial inventories of MSBR(2f), MSBR and MSFR using reference salts	94
5.4	Initial inventories of MSBR(2f) and MSBR using alternative salts	95
5.5	Breeding characteristics of MSBR(2f), MSBR and MSFR	97
5.6	Characteristics of the chloride-fueled configurations	109
5.7	Initial inventories of chloride-fueled configurations	110
6.1	Estimates of burn-ups achievable in B&B	125
6.2	Initial LEU and LWRPu fractions in B&B cores	127
6.3	First doubling times in B&B	128
6.4	Reactivity coefficients in B&B	128
6.5	Achievable burn-ups in a once-through cycle	129

List of Symbols

Symbol	Description	Page
A	Absorption rate	52
B	Burn-up	6
B_g	Geometrical buckling	45
B_m	Material buckling	45
C	Neutron capture rate	47
D	Diffusion coefficient	44
d	Density	48
Δt	Time step	51
E_f	Energy per fission	6
F	Fission rate	6
γ	Branching ratio or fission yield	57
H	Core height	45
k_{eff}	Effective multiplication factor	44
k_{∞}	Infinite multiplication factor	45
L	Neutron leakage rate	47
λ	Per-atom reprocessing or decay rate	50
\mathcal{L}	Neutron diffusion length	45
M	Mass	6
m	Molar or atomic mass	48
N	Number of atoms of nuclide	7
n	Atomic density of nuclide	50
N_A	Avogadro constant	6
$\bar{\nu}$	Average neutrons per fission	44
P	Neutron production rate	47

List of Symbols

Symbol	Description	Page
p	Volumetric power density	51
ϕ	Neutron flux	44
R	Core radius	45
r	Salt channel radius	68
ρ	Reactivity	47
s	Salt volume fraction	68
Σ	Macroscopic cross-section	44
σ	Microscopic cross-section	57
T	Reprocessing cycle time	51
$T_{1/2}$	Half-life	7
V	Volume	45
x	Molar fraction	48

1 Introduction

There is always a strong case for doing nothing,
especially for doing nothing yourself.

WINSTON CHURCHILL

The high level of development and standards of living achieved by humanity to this day rely extensively on the availability of affordable and abundant sources of energy. However, a large fraction of the currently used energy contributes to changing the Earth's climate via the emissions of Greenhouse Gases (GHG). Mankind is thus faced with the twofold challenge of increasing the availability of energy to further lift itself out of poverty while substantially diminishing its impact on the climate and Nature in general. To this end, sources of low-carbon energy such as hydropower, nuclear power, as well as wind and solar power must be further developed to meet Humanity's needs and replace essentially all high-carbon energies in use today: in 2014, the World's energy consumption amounted to 13'699 Mtoe (IEA, 2016), of which 28.6% were produced with coal, 31.3% with oil, and 21.2% with natural gas. Only 4.8% were produced using nuclear power, 2.4% using hydro power, and 1.4% of other renewables such as wind and solar.

However, civilian nuclear power, in its current implementation represented mostly by Light Water Reactors (LWRs), faces challenges. Notably, LWRs have low fuel resources utilization because of their low conversion ratios, thus they both necessitate enriched uranium and are unable to run in a closed fuel cycle, producing long-lived radiotoxic waste. Additionally, major accidents such as Three Mile Island (1979), Chernobyl (1986) and Fukushima (2011) have continuously eroded public trust in the safety of nuclear energy. Finally, existing power plants suffer from economic conditions combining low fossil fuel prices and the relative inflexibility of their production combined to the near-zero marginal cost of many new renewable energies such as wind and solar. Further deployment and renewal of nuclear capacity is also challenged by the high upfront cost of what is currently mature technology and the financial risk attached to it. Hence, a novel way to design, build and operate reactors was conceived in the form of Small Modular Reactors (SMRs); but as such this category of reactor only provides answers to

economic constraints: most SMR concepts are based on LWR technology and therefore have the same disadvantages in terms of sustainability. Therefore, a new generation of Nuclear Power Plants (NPPs) with answers to the other challenges is necessary for nuclear energy to contribute in the long term to the fight against climate change. This new generation is often called “Generation IV” and consists in six reactor concepts, amongst which Molten Salt Reactor (MSR) are possibly both the most promising and the most challenging. In this thesis, results of investigations pertaining to the ability of several potential MSR designs to operate while burning existing waste and not producing substantial amounts of own wastes are reported.

1.1 Climate Change

Since the middle of the 19th century and the industrial revolution, increasing amounts of GHGs have been released, including carbon dioxide (CO₂), methane (CH₄), and nitrous oxide (N₂O) into the Earth's atmosphere, of which CO₂ is the biggest contributor to total emissions (Pachauri et al., 2014).

Meanwhile, the average global surface and sea temperature, as well as the average sea level, have increased since the beginning of the 20th century and even more so since the 1970s (see Figure 1.1). GHG emissions are responsible for most of the forcing likely to be responsible for most of the surface temperature change over the second half the 20th century (Pachauri et al., 2014). It is projected that climate change will lead to an increase in extreme weather events, ocean acidification threatening marine ecosystems, have substantial impacts on agricultural productivity potentially leading to an increase in food scarcity in affected regions, as well as modify the cryosphere (parts of the Earth covered in ice such as the Arctic sea, glaciers, etc.) to the point of potentially leading to water scarcity in affected regions.

While there are available potential adaptation solutions to the consequences of global warming such as sea level rise and extreme weather events by locally reducing the vulnerability of affected regions, mitigation solutions are necessary to stabilize and reduce GHG emissions to limit the average temperature increase to acceptable levels.

Mitigation options include:

- Shift energy production to low-carbon sources such as hydropower, nuclear, wind, solar, biomass and geothermal
- Energy efficiency and conservation measures to limit consumption,
- Add carbon capture and storage to fossil fuel-powered (coal, oil and gas) energy sources,
- Use alternative mobile energy forms for transportation, such as hydrogen for combustion or fuel cells, and high-efficiency batteries.

It is likely that only a mixture of these solutions will permit to limit the temperature increase to acceptable levels while answering energy demand in the most economical way around the

globe. At the most recent United Nations Conference on Climate Change in Paris in December 2015, 175 parties agreed to implement measures to limit the said temperature increase to 2 °C and, if possible, 1.5 °C, both of which necessitate rapid and drastic measures to reduce GHG emissions.

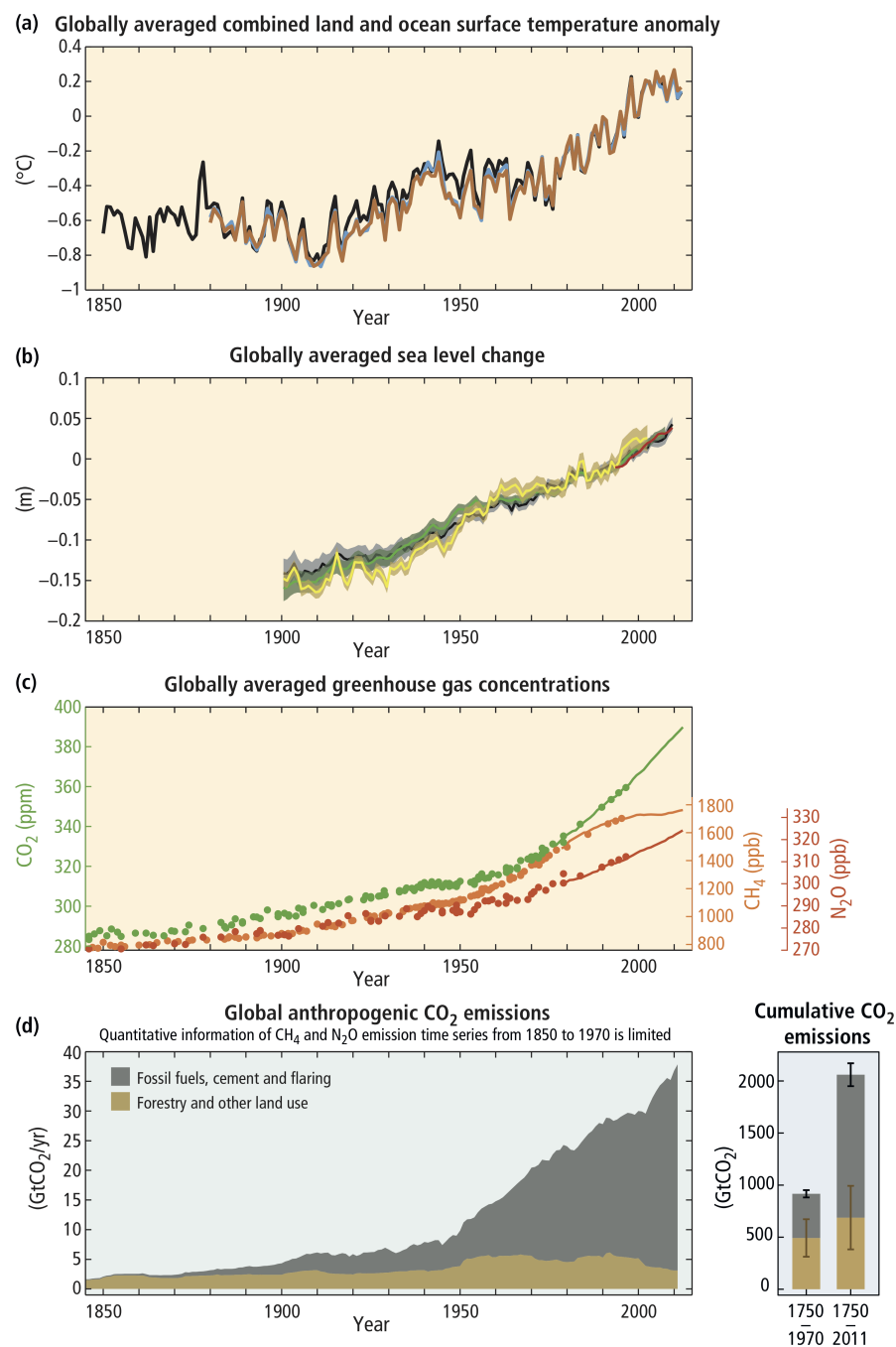


Figure 1.1 – Global average temperature and sea level change over time and GHG emissions and concentrations in the atmosphere (Pachauri et al., 2014).

1.2 Challenges Faced by Nuclear Power

As of March 2018, there were 450 power reactors in operation in the World (IAEA), totaling 393.8 GW_e of net installed capacity, most of which are LWRs, with 75 Boiling Water Reactors (BWRs) and 294 Pressurized Water Reactors (PWRs). Additionally, there were 55 reactors under construction.

Nuclear energy is generally recognized as a low-carbon source, having nearly no GHG emissions resulting from energy production (Bauer et al., 2012; Treyer et al., 2014). Most of the life cycle emissions originate from the front-end (uranium mining, plant construction, fuel fabrication) and back-end (eventual fuel reprocessing, plant decommissioning, disposal of spent fuel) of the nuclear life cycle, and these are averaged over a large energy production throughout the plants' lifetime. Research shows that the lifecycle GHG emissions of NPPs vary substantially depending on assumptions made, but generally remain comparable to most renewable energies. Moreover, other life cycle indicators are favorable as well: land use, production of fine particles, etc., making nuclear power a generally attractive, low-environmental impact power generation technology.

However, nuclear power faces both technological and economical challenges. Technologically, nuclear faces safety, sustainability, and proliferation concerns. While efforts have been made consistently to improve safety of existing and new NPPs over the years, most reactors today have a resource utilization that is substantially below the full potential of nuclear fission. Moreover, the same reactors produce long lived actinide waste because of their open, or partially open cycle for reactors using Mixed Oxide (MOX).

1.2.1 Safety of Nuclear Power Plants

Because there have been several large-scale nuclear accidents such as the Three Mile Island accident (1979), the Chernobyl accident (1986) and Fukushima accident (2011), the safety of civilian nuclear power is regularly at the center of the political debate.

After the Three Mile Island accident, many Western European countries, including Switzerland, have taken measures to extend both Design-Basis (DBA) and Beyond Design-Basis Accident (BDBA) management measures. Regarding Design-Basis Accidents, which are accidents the plant is required to weather with minimum off-site releases of radioactivity, plants have been outfitted with additional bunkered, flooding-resistant safety systems covering all necessary safety functions (reactivity control, core cooling, and retention of radionuclides).

For beyond-design-basis accidents, NPPs have been outfitted with accident management measures dedicated to minimizing radioactive releases in the case of a partial or full core meltdown. Amongst those systems are hydrogen recombiners able to cope with the hydrogen released during the oxidation of the zirconium-based cladding tubes of nuclear fuel, with the aim of preventing a detonation that would damage the containment. Another such system is

the Filtered Containment Venting System (FCVS) designed to retain a maximum of the volatile fission products released in the containment atmosphere in case of a core meltdown, once again with the aim of preserving the integrity of the containment if it were to be threatened by increased pressure. These measures have brought the probability of core damage below the threshold of $1\text{E} - 5$ per reactor-year for Swiss reactors (Hirschberg et al., 2004).

Despite major accidents the safety record of nuclear energy can be considered as good. Notably, the risk of casualties in an accident is comparable to other low-carbon energy technologies (Hirschberg et al., 2004). Nevertheless, the risk of long-term radioactive contamination necessitating the evacuation of the local population is a remaining concern which is to be addressed by newer technologies. The Generation IV International Forum (GIF) has included the goal of limiting the need for such measures as a Generation IV criterion.

1.2.2 Sustainability of the Nuclear Fuel Cycle

The mass of natural Uranium M_{nat} with a natural ^{235}U abundance e_{nat} necessary to produce a given mass of enriched fuel M_{enr} with an enrichment e_{fuel} while leaving tailings with an enrichment e_{tail} is giving by a simple conservation equation:

$$e_{\text{nat}}M_{\text{nat}} = e_{\text{fuel}}M_{\text{enr}} + e_{\text{tail}}(M_{\text{nat}} - M_{\text{enr}}) \Rightarrow \frac{M_{\text{enr}}}{M_{\text{nat}}} = \frac{e_{\text{nat}} - e_{\text{tail}}}{e_{\text{fuel}} - e_{\text{tail}}}$$

Assuming a natural abundance of 0.72 %, tailings of 0.3 % and an enrichment of 4.4 %, one gets a ratio of 10 % of enriched Uranium to mined Uranium. Moreover, the fraction of initial fuel used F can be deduced from the discharge burn-up B , the energy released per fission E_f and the molar mass of uranium m_{U} :

$$\frac{\text{Fission energy released}}{\text{Fission energy potential}} = \frac{B m_{\text{U}}}{E_f N_{\text{A}}} \quad (1.1)$$

Assuming a burn-up of 55 GWd/t and an energy per fission of 200 MeV, the fraction of energy released to the total fission energy available in fuel is 5.9 %. Thus 5.9 % of the energy potential of enriched Uranium is released during its time in core, enriched Uranium itself being 10 % of the natural Uranium mined, which means that only 0.59 % of the energy potential of mined Uranium is currently used.

The generation of long-lived high-level radioactive waste has been another contentious point. Indeed, most reactors operating to this day have a once-through open fuel cycle in which the spent fuel is discarded after a few years in the core and not recycled. This spent fuel contains long-lived radioactive isotopes that are dangerous to the biosphere, necessitating its long-term separation from the latter. The danger represented by radioactive nuclides is usually quantified using the radiotoxicity which is a function of their activity and of a dose

Chapter 1. Introduction

coefficient δ expressed in Sievert per Becquerel of activity:

$$\text{Radiotoxicity} = \sum_i \delta_i \frac{\ln 2}{T_{1/2}} N_i \quad (1.2)$$

The dose coefficient depends mostly on the mode of incorporation (ingestion or inhalation) and represents the biological damage due to radiation emitted by the nuclide of interest when it has been incorporated by an adult.

A potential solution is that of a so-called closed fuel cycle, by opposition to an open fuel cycle. Ideally, it is a fuel cycle in which all actinides discharged from the spent fuel of a reactor are returned to that reactor to be fissioned or transmuted. While Fission Products (FPs) could be recycled and transmuted as well, they cannot undergo fission and thus do not release substantial amounts of energy, which is likely to make their transmutation economically unattractive. In reality the processes necessary to separate FPs from the actinides to be recycled have a finite efficiency and thus small amounts of actinides must be expected to be left in the waste produced, along with FPs. The radiotoxicity production of closed fuel cycles is thus mainly driven by losses incurred during chemical processing.

While the production of Spent Nuclear Fuel (SNF) both in mass and volume is small enough not to be a substantial challenge, the large amount of radiotoxicity it carries over a long period is problematic. Nevertheless, this radiotoxicity is dominated by short-lived fission products in the short-term and mostly to transuranics (TRUs) on the long-term, as can be seen on Figure 1.2 below.

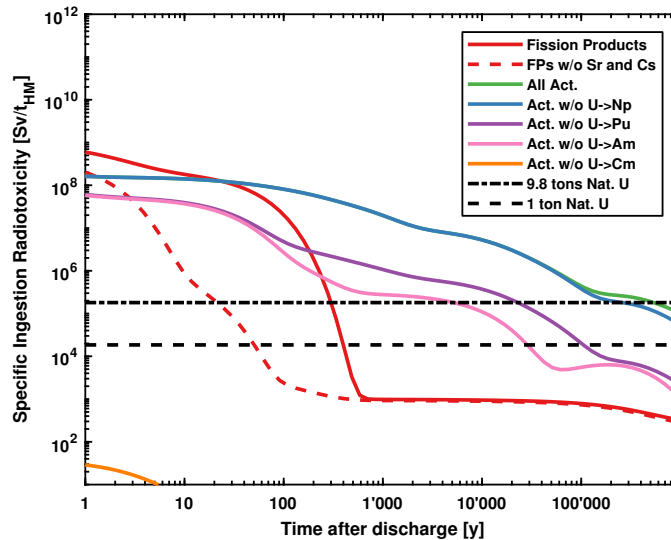


Figure 1.2 – Influence of the various actinides on the specific ingestion radiotoxicity of PWR spent fuel after discharge at a burn-up of 55 MWd/t.

The radiotoxicity level of a ton of uranium ore in equilibrium, approximately 10 kSv/t is often

considered a good threshold for determining how harmful human-made radionuclides are in comparison to those found in nature.

As can be seen on figure 1.2, the threshold is reached after a little over 300 y for FP taken separately, which can be considered representative of an ideal closed fuel cycle without actinides losses during reprocessing. The removal of high-heat contributors such as Cesium and Strontium which could be transmuted, used in radioisotope batteries or stored separately decreases this time to 22 y only.

The time needed for the once-through actinides is approximately 600 000 y. Removal of Uranium and Neptunium isotopes has a very limited impact on this limit. Additional removal of Plutonium isotopes decreases the time needed to reach the threshold down to 21 000 y, while also removing Americium isotopes brings this time to 5000 y. Finally, removal of all isotopes up to Curium results in the radiotoxicity being lower than the reference level already immediately after discharge.

This observation combined with the fact that actinides can be fissioned leads to the conclusion that a closed fuel cycle in which all actinides are recycled into new fuel and the only waste produces are fission products allows to reduce the long-term radiotoxicity production of the nuclear fuel cycle. Partial fuel cycle closure is already technically achieved today with the use of MOX fuel made with reprocessed Plutonium from LWRs and used in the same reactors. However, multiple or infinite recycling of that plutonium is technically challenging using current LWRs, and thus further fuel cycle closure necessitates the use of a different reactor technology.

1.2.3 Economic Performance

Economically, nuclear power has essentially been used for so-called baseload generation and sometimes for some form of load-following production, due to the large fixed costs and the very low variable costs of the technology, compared to fossil fuels such as coal or gas which have both low fixed costs but relatively high variable costs in the case of gas, which is therefore traditionally used as a peaking power generation method. However, the increased penetration of renewable technologies such as on- and off-shore wind power, as well as solar photovoltaic, have changed the landscape of electricity grids and markets, and the usual roles of some forms of power generation have changed. Notably, the intermittency of some renewable energies combined with their ever-increasing installed capacity have led to the appearance of negative temporary electricity prices on several electricity markets due to supply largely exceeding the demand for electricity. It is therefore necessary for new NPPs to offer increased cost-competitiveness if they are to contribute substantially to the World's energy production.

1.2.4 Proliferation

A fourth and final concern linked to the civilian use of nuclear power for energy is the risk of nuclear proliferation, that is, the possibility for non-nuclear-weapons states or non-state actors to obtain both fissile material and technology that could be used in a nuclear weapon. Because of this possibility, all fissile material in the nuclear fuel cycle should be carefully accounted for and tracked along the cycle. It is obvious that the proliferation risk increases with higher accessibility, higher isotopic purity, or higher quantity of the nuclear material. Therefore, it is important to limit enrichment of fissile material, limit the separation of fissile material in fuel reprocessing, and if possible leave the material in an unattractive form.

Current reactors are relatively proliferation resistant because of their use of low-enriched uranium fuel, the low attractiveness of the fissile material they contain (Uranium and Plutonium with unfavorable isotopic compositions). Additionally, in most nuclear countries, International Atomic Energy Agency (IAEA) surveillance and safeguards further facilitate the accountability of the nuclear materials in NPPs.

1.3 Advanced Nuclear Power Plants

Various solutions have been proposed to the previously mentioned challenges, including modular reactors, novel reactor types, and so on. Some of these solutions are mutually exclusive, while some are complementary, e.g. advanced reactors can be built as modular reactors. In this section, the most relevant options are outlined.

1.3.1 Small Modular Reactors

SMR are a category of reactors defined by their electrical power range (up to 300 MW_e) and modular nature, that is, the fact that they should be mainly factory-built rather than assembled on site like most power reactors have been to this day.

Some of the first commercial power reactors such as Shippingport could fit the definition, but their small power rating was largely due to their experimental or prototypical status. The size of subsequent commercial reactors quickly increased in the hope of achieving economies of scale and very inexpensive power (Weinberg, 1994). However, the cost of reactors generally escalated with time (Koomey and Hultman, 2007; Lovering et al., 2016) rather than decreasing as originally expected. A major challenge faced by new reactors is the combination of high capital costs and long construction times. Indeed, most utilities must take a loan to finance construction, which, combined with the substantial construction times, increases costs. These large fixed costs represent a high financial risk compared to other generation technologies, making nuclear comparatively less attractive. The rationale behind SMRs is threefold:

- By building several smaller units instead of a single large one, the investment can be better distributed over the total construction time of the plant, thereby decreasing the

up-front cost and financial risk.

- By maximizing the factory-building of the reactor, economies of numbers can potentially be reached and the construction times lowered.
- Smaller units are better suited to smaller grids or off-grid applications. Additionally, a crude form of load-following can be achieved by bringing single units on- or off-line.

However, the success of this business model will depend on several factors, such as the final cost per installed capacity, which can be expected to rise compared to large units, or the regulatory environment, which can have a strong influence on construction times.

1.3.2 Generation IV Reactors

In 2001, major nuclear countries convened at the behest of the Department of Energy (DOE) to found what would become the GIF with the aim of establishing a platform to exchange and coordinate research into advanced reactors of the so-called fourth generation. A list of requirements that would have to be fulfilled by the said advanced reactors was drawn which included:

Sustainability

use resources substantially more efficiently and produce substantially less waste,

Economics

be competitive against other power sources and have a level of financial risk comparable to other energy projects,

Safety and Reliability

have a very low probability of core damage, and eliminate the need for off-site emergency response,

Proliferation Resistance and Physical Protection

remain unattractive both as sources of weapon-usable materials and as potential terrorist targets,

The most substantial gain that can be acquired over the current generation of NPPs is arguably that of sustainability. Several of these goals reinforce each other, while others can be in conflict with each other:

- Sustainability can come at the cost of economics, as it may necessitate fuel reprocessing, increasing fuel cycle costs;
- Sustainability can contradict proliferation resistance, since breeding produces more fissile material which can be separated and potentially diverted;
- Sustainability can threaten safety, as breeding can be detrimental to safety parameters such as the void coefficient in fast reactors.
- Economics can conflict with safety, since additional safety measures may increase costs.

Balancing each of these goals is the challenge of modern reactor design. The fact that some of these goals potentially contradict each other makes any choice of technology non-obvious.

Chapter 1. Introduction

Nonetheless, in 2002, six reactor types (called *systems* by the GIF) were selected:

- the Gas-cooled Fast Reactor (GFR),
- the Lead-cooled Fast Reactor (LFR),
- the MSR,
- the Sodium-cooled Fast Reactor (SFR),
- the Supercritical Water Reactor (SCWR), and
- the Very High Temperature Reactor (VHTR),

A comparison of the main characteristics of these six reactors types is given on the following table:

Table 1.1 – Comparison of the six Generation IV systems.

Reactor	SFR	LFR	GFR	HTR	SCWR	MSR
Coolant	Na	Pb, Pb-Bi	He	He	H ₂ O	Fluorides, Chlorides
Pressure	1 bar	1 bar	90 bar	80 bar	220 bar	1 bar
Temperature	550 °C	500 °C	850 °C	950 °C	600 °C	700 °C
Spectrum	Fast	Fast	Fast	Thermal	Thermal Fast	Thermal Fast
Fuel Type	Oxide, Carbide, Metal	Oxide, Nitride	Oxide, Carbide	Oxide, Oxycarbide	Oxide	Fluorides, Chlorides
Fuel Cycle	Closed, Open	Closed, Open	Closed, Open	Open	Closed, Open	Closed, Open

This thesis only deals with a single type of Generation IV reactor: MSRs, arguably one of the most peculiar due to its use of a liquid fuel. Nonetheless, the promising safety and fuel cycle characteristics of the concept make it attractive.

1.3.3 Liquid fuel reactors

While most of the reactor concepts that have been proposed to this day are based on a nuclear fuel in solid form, usually cooled by a gas or a liquid, other concepts based on liquid nuclear fuel have been studied. There are two main advantages to using a fuel in liquid form:

1. Liquids do not lose their structural integrity under irradiation, while most solids swell, are embrittled or creep at high fluences, and
2. Liquids can be cooled by their own convective heat transfer, whereas solids can only be cooled by conductive and radiative heat transfer.

The first advantage means that, assuming that the other properties of the liquid can be kept between reasonable boundaries, the fuel can remain indefinitely exposed to the neutron flux of the core. In the case of solid fuels, high neutron fluences can only be reached using specially engineered fuels and cladding materials. After fuel in solid form has reached its maximum fluence, it must be discarded (at the cost of sustainability because of the unburnt actinides it may contain) or reprocessed. The latter can generally only be achieved by changing the form of the fuel to a gas (as in the case of voloxidation, fluoride volatility, etc.) or a liquid (as in the case of Plutonium-Uranium Redox Extraction (PUREX), electrodeposition, etc.).

The second advantage implies that the fuel itself can be used as a coolant, which removes one major constraint of core design: heat transfer between fuel, cladding, and coolant and its usual temperature limits during both normal operation and transients. This possibility comes at the cost of a higher fuel inventory, because the volume of coolant needed to cool a reactor is necessarily higher than its core volume. An alternative choice is the use of a liquid fuel with a separate coolant, which can exist in two distinct implementations: one where the coolant and fuel are not miscible (neither is soluble in the other) and will therefore remain separated, and another where they are separated by some cladding material as in the case of solid fuel. The former is called direct cooling and the latter indirect cooling. These design choices are further explained in the next chapter.

Historically, three types of liquid fuel reactors have been investigated: Aqueous Homogeneous Reactors (AHRs), using fuel dissolved in water, the Liquid Metal Fuel Reactor (LMFR), using liquid metallic fuel in pure form or dissolved in other metals, and the MSR, which use fuel dissolved in molten salts. AHRs proved troublesome at high power density because the thermophysical properties of water are unfavorable (high vapor pressure) and because of solubility problems. They remain of interest for medical radioisotopes in dedicated low-power reactors, however. LMFRs have been plagued with corrosion problems not unlike those affecting lead-cooled reactors, with the dissolution of metallic actinides further enhancing the corrosion. In 1957, MSR were already considered to be the liquid fuel reactors with the highest chances of achieving technical feasibility (Alexander, 1958).

1.3.4 Other Advanced Reactors

Other reactors not covered in the six Generation IV systems exist: for example, Accelerator-Driven System (ADS) or Nuclear Fusion.

The ADS concept is based on subcritical reactors in which the missing neutrons to provided constant power and thus constant fission rate are provided by a particle accelerator (usually using protons) and a spallation source using heavy atoms. Spallation is a process in which a heavy nucleus bombarded with high energy protons is “evaporated”, releasing approximately 20 neutrons in the process. Since the reactor is subcritical, an interruption of the beam leads to a decrease of power in the reactor, eventually reaching zero. The concept gained in popularity in the 1990s after the Chernobyl accident, which was a reactivity-initiated accident.

Nevertheless, subcriticality must always be guaranteed, which remains challenging as the core of the reactor is still subject to variations of reactivity (e.g. from hot to cold fuel conditions). Moreover, the necessity to maintain cooling of the core after shutdown remains. Finally, the reliability requirements on the accelerator remain technically challenging to this day. The use of ADS may be justified on grounds of their good transmutation capability, but it may be possible to obtain similar performance with critical reactors.

Nuclear fusion on the other hand relies on different nuclear reactions than fission reactors. In this case, energy is produced by fusing light nuclei such as deuterium and tritium at very high temperatures at which matter is in the form of a plasma. To achieved useful power production, the plasma must be confined sufficiently long for enough fusion reactions to take place and provide a positive net energy output, which has not yet been achieved to this day. Advantages of fusion reactors are the very high energy density, abundant fuel in the case of Deuterium, low volume of radioactive waste produced (essentially limited to activated reactor structural materials) and the low probability of substantial releases of radioactivity since the system neither relies on a chain reaction (as in the case of fission) nor produces substantial decay heat after the fusion reactions have

1.4 Aim and Structure of this Thesis

In this section, the aim and subsequently the structure of the thesis are described.

1.4.1 Aim of the Thesis

The aim of this thesis can be described in three steps, which each following a common thread, that is, sustainability and waste-burning potential.

1. Review existing MSR concepts: a large body of literature exists about molten salt reactor designs, with sometimes very strong variations between concepts. At the same time, several designs are variations of the same concept. These concepts should be reviewed from the perspective of sustainability potential of the fuel cycle and potential for waste burning.
2. Investigate novel MSR concepts: from the previously mentioned investigations, it should be possible to identify gaps in the literature and thus reactor concepts that have not been thoroughly investigated and could therefore be proposed.
3. Propose a MSR concept for waste burning: following the previous results, a sustainable MSR design for waste-burning should be identified and proposed.

1.4.2 Structure of the Thesis

This thesis is structured in the following way:

- Chapter 1** introduces the reader to the topic and discusses the need for a new generation of NPPs with increased sustainability both in the sense of better utilization of natural resources and in the sense of minimized long-lived waste production.
- Chapter 2** reviews the history and explains the nature of molten salt reactors in more details, as well as introduces the fuel salt candidates used in this thesis.
- Chapter 3** outlines the mathematical methods and computational tools used in this work, including the EQL0D procedure which was developed during this thesis for the purpose of fuel cycle simulation of MSRs.
- Chapter 4** deals with the evaluation of the sustainability of an ideal closed Thorium-Uranium and Uranium-Plutonium fuel cycle in molten salt reactors using several possible fuel salts and moderators in an infinite lattice. The influence of various parameters such as the power density and reprocessing rates, and reprocessing losses on the results is studied separately.
- Chapter 5** studies the transition behavior of selected fluoride and chloride-fueled concepts from an initial critical state using several potential fuels, including actinides from spent nuclear fuel, to a closed fuel cycle equilibrium.
- Chapter 6** treats the possibility of operation in two types of open fuel cycles without fuel processing, one being the Breed-and-Burn fuel cycle in which fuel is discharged to be reused in other reactors, and the other being a once-through fuel cycle in which the fuel is not returned to the core but may be reprocessed off-site.
- Chapter 7** provides the conclusion of this thesis, including an outlook and proposals for further work on this subject.

2 Molten Salt Reactors

I hope that after I am gone people will look at the dusty books that were written on molten salts and will say *hey, these guys had a pretty good idea, let us go back to it!*

ALVIN WEINBERG

MSRs are defined in a broad sense as reactors using molten salts as coolants. Historically, the term referred only to molten salt-fueled reactors, in which the fuel is dissolved in the coolant salt. More recently however, a novel concept employing solid fuel based on high-temperature gas-cooled technology have been proposed in the United States, and have been termed Fluoride-cooled High temperature Reactors (FHRs), but are also included under the MSR umbrella, including within the framework of the GIF. In this thesis, the term MSRs will be exclusively used to refer to liquid fuel reactors using molten salts.

2.1 Background and Definitions

Two major categories of MSRs have been proposed: those using fluoride salts and those using chloride salts, of which the former have been far more studied. While using higher halides such as bromides and iodides is theoretically possible, their chemical stability seems too low in the temperature range of interest for power production.

MSRs have many potential configurations, as mixtures with low enough neutron absorption exist, making them capable to operate both in thermal, moderated, and fast spectrum. Moreover, many possible fluorides can be mixed to obtain a potential salt mixture for a reactor. In the early days of the work at Oak Ridge National Laboratory (ORNL), Grimes (1970) listed criteria for the selection of potential salt mixtures:

- Exhibit chemical stability at temperatures above 800 °C,
- Be stable under intense radiation,
- Melt at useful temperatures and not be volatile,

Chapter 2. Molten Salt Reactors

- Be compatible with high-temperature alloys and graphite, and
- Dissolve useful quantities of fertile and fissile material.

This list explains the exclusion of other types of molten salts that are routinely used as coolants in other industries, such as nitrides, which have been excluded for thermal stability reasons. The list also implies the exclusion of some fluorides of elements that are not compatible with alloys typically used with fluoride salts, such as Pb or Bi, because of their tendency to be reduced. Other constraints imposed by the chemistry can be limiting the content of a given fluoride within a mixture, such as Zr, due to the relatively high volatility of its tetrafluoride, or Be, due to both its effect on limiting the solubility of PuF_3 , and its tendency to form glass-like clusters rendering the salt mixture extremely viscous and thus difficult to pump. Finally, the most common criterion is of course the melting point of the mixture, which is paramount.

Historically, the upper limit of 500 °C for the melting point has been used because the allowable upper limit on the salt temperature was set to 704 °C, the point until which Hastelloy N was tested in the Molten Salt Reactor Experiment (MSRE). Allowing a margin to freeze of circa 50 °C for transients, one is left with a salt heat up of 100 °C in the core. In some cases, with the use of novel materials, a higher core outlet temperature could be allowable and thus a higher melting point as well. The ability of materials to retain their mechanical properties at high temperature, under irradiation and submitted to salt corrosion is thus the only obstacle to higher outlet temperatures, which makes MSRs quite promising for process heat applications, along with High Temperature Reactors (HTRs). Using molten salts as coolants and fuel for nuclear reactors provides several advantages, amongst which:

- the absence of radiation damage on the salt, compared to solid fuels which are limited both by the life of the cladding they are surrounded by, and their own evolution,
- the ability to remove or add salt simply, as well as the ease of processing the salt. Most processing steps on nuclear fuel include their conversion to a liquid and back into a solid, often using dusty powder-based processes, both of which can be avoided in the case of liquid fuel,
- the ability to operate the reactor at low, near-atmospheric pressures in the useful temperature range 600 °C to 700 °C for power production,
- the relatively high heat capacity compared to liquid metals and gas coolants,
- the continuous removal of insoluble fission products from the salt mixture, which lowers the source term in the reactor and some of the parasitic absorptions on fission products.
- a favorable situation concerning feedback coefficients, since a higher temperature lowers the salt density and expulses salt from the core.

However, MSRs also have disadvantages that must be mentioned, including:

- the strong corrosiveness of the molten salt fuels, especially in the presence of moisture, which necessitate their proper handling and treatment
- the lack of usual barriers to nuclide released such as the claddings of fuel rods, which necessitate a very different safety approach and substantial amounts of research to

understand the behavior of nuclides released during both operating and accidental conditions

- the high fluence on structural materials used in the core due to the presence of fissions extremely close to the wall, unlike most solid fuel reactors in which the coolant partially shields the vessel from irradiation,
- the larger fuel inventories needed to operate the reactor due to the volume of coolant circulating in the cooling loops (piping, heat exchanger) in the case of externally-cooled MSRs,
- the partial loss of delayed neutron precursors due to the circulation of the fuel, decreasing the reactivity margin to prompt criticality,
- the comparatively low heat conductivity of salts that complicates heat transfer away from the fuel salt,
- the comparatively high melting point of salt mixtures that necessitate high temperatures to guarantee that it does not freeze unexpectedly,
- the low and sometimes unknown solubility of many compounds that could be formed during operation whose precipitation could be detrimental to safety.

2.2 History of Molten Salt Reactors

Most of the past research lead about MSRs was performed at ORNL, in Oak Ridge, Tennessee, in the United States. This work was performed during a period lasting from 1946, when focus in the Aircraft Nuclear Propulsion Program (ANP) program changed to MSRs, to 1976, when the Molten Salt Reactor Program (MSRP) was officially canceled and defunded.

2.2.1 Early Military Debuts

From 1946 to 1961, the U.S. investigated the possibility of building nuclear-powered aircraft for military purposes. The advantage was obvious: nuclear-capable bombers would gain the ability to stay in the air for very long periods of time, similarly to nuclear-powered submarines. The major problem was the difficulty of shielding the crew from the radiation coming from the reactor without making the aircraft too heavy. Ultimately, the program was canceled after the advent of Intercontinental Ballistic Missiles (ICBM) which rendered this kind of technology obsolete.

The ANP however highlighted the attractiveness of MSR for power production. Originally, the ANP reactor was designed as a BeO-moderated Na-cooled solid fuel reactor, due to the attractive features of metallic Na as a coolant. Soon after however, the combined needs for a reactor with high power density, high specific power, and high enough temperature to efficiently drive a gas turbine revealed some problems with solid-fueled designs: Xe could cause a positive feedback coefficient at high temperature, and the reliability of fuel pins at high temperature was questionable. This lead to the idea of using a liquid fuel, which would have a higher expansion coefficient than solid fuel, and potentially the ability to remove Xe

Chapter 2. Molten Salt Reactors

from the fuel, which would guarantee a negative feedback coefficient. For reasons of stability at high temperature, molten salts were chosen as liquid fuel matrix.

BeO remained the moderator for the second design because the blocks had already been manufactured at that time. A mixture of $\text{NaF}-\text{ZrF}_4-\text{UF}_4$ with 93%-enriched U was chosen as the fuel salt, having a satisfyingly low melting point and being relatively simple to acquire compared to the later Li-based salts used in breeder designs. Inconel 600 was used as cladding material to separate the BeO from the salt, due to it being a Ni alloy and the known compatibility of fluoride salts with Ni. The reflector cooling loop used liquid Na as a coolant. Operating at a thermal power of $2.5 \text{ MW}_{\text{th}}$, the inlet temperature was 660°C and the outlet temperature was 860°C (and even went up to 880°C for some time), one of the highest reached by a reactor at the time.

The experiment ran smoothly for ten days in November 1954 (Bettis et al., 1957b,a; Ergen et al., 1957). The experimenters noticed the near absence of Xe reactivity effect and the generally high stability of the reactor. One of the tubes leaked radioactive fission gases during the experiments, but unlike most modern designs the reactor was not designed to be drained from its fuel, preventing the full repair of the leak. The program was however considered successful, and established the practicability of MSR for power production.

At the end of the experiment, corrosion in the Inconel tubes lead to investigations of the corrosion of molten fluoride salts and thus to their specific tendency to leach chromium from the alloy matrix. To alleviate this problem, a tailored alloy, Hastelloy N (also called INOR-8) was designed at ORNL and commercialized.

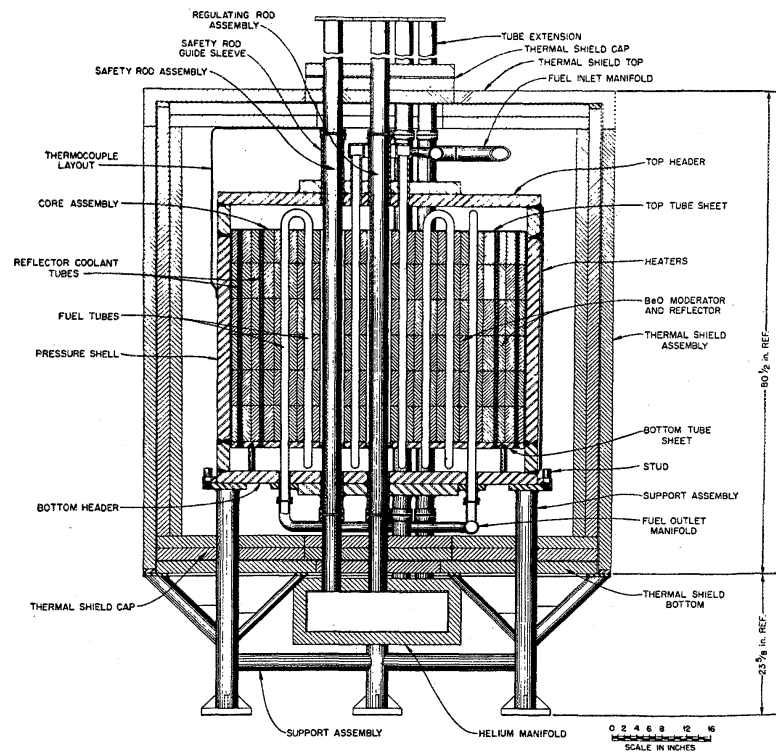
Meanwhile, a full-size aircraft reactor based on a MSR was designed: the Aircraft Reactor Test (ART). It was a $60 \text{ MW}_{\text{th}}$ Be reflector-moderated spherical reactor design cooled by a NaK eutectic coolant.

When the ANP program was hurriedly canceled due to the advent of Intercontinental Ballistic Missiles (ICBMs), the ART was shelved, even though it was already under construction at the time. The scientists working in the program were skeptical with respect to the actual feasibility of a nuclear-powered aircraft from the beginning, even calling the idea “daft” (Weinberg, 1994), but were however convinced that the MSR technology was very suitable to civilian power production. This lead to the MSRP that largely built on the experience acquired during the ANP.

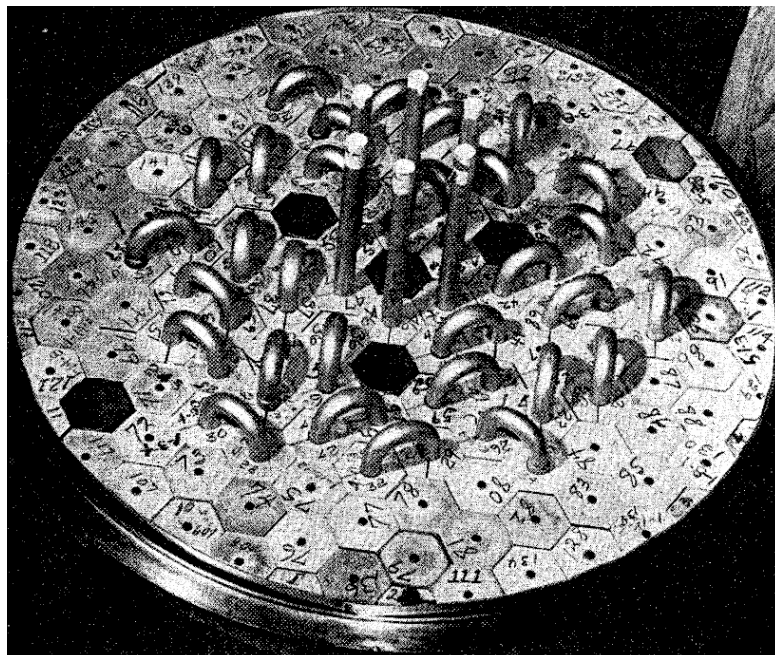
2.2.2 Continuation as a Civilian Program

After the cancellation of the ANP program, the focus in the ORNL work shifted toward civilian power production. At the time, the emphasis in advanced reactor research was on breeder reactors, due to the low U resources known at the time, and the thus projected rapid increase in U price. MSR using fluoride salts being particularly well suited for the Th cycle, and the thermal breeders being possible in the Th cycle, the MSRP focused early on a moderated Th

2.2. History of Molten Salt Reactors



(a) ARE, side view



(b) ARE, top view

Figure 2.1 – The Aircraft Reactor Experiment (ARE).

Chapter 2. Molten Salt Reactors

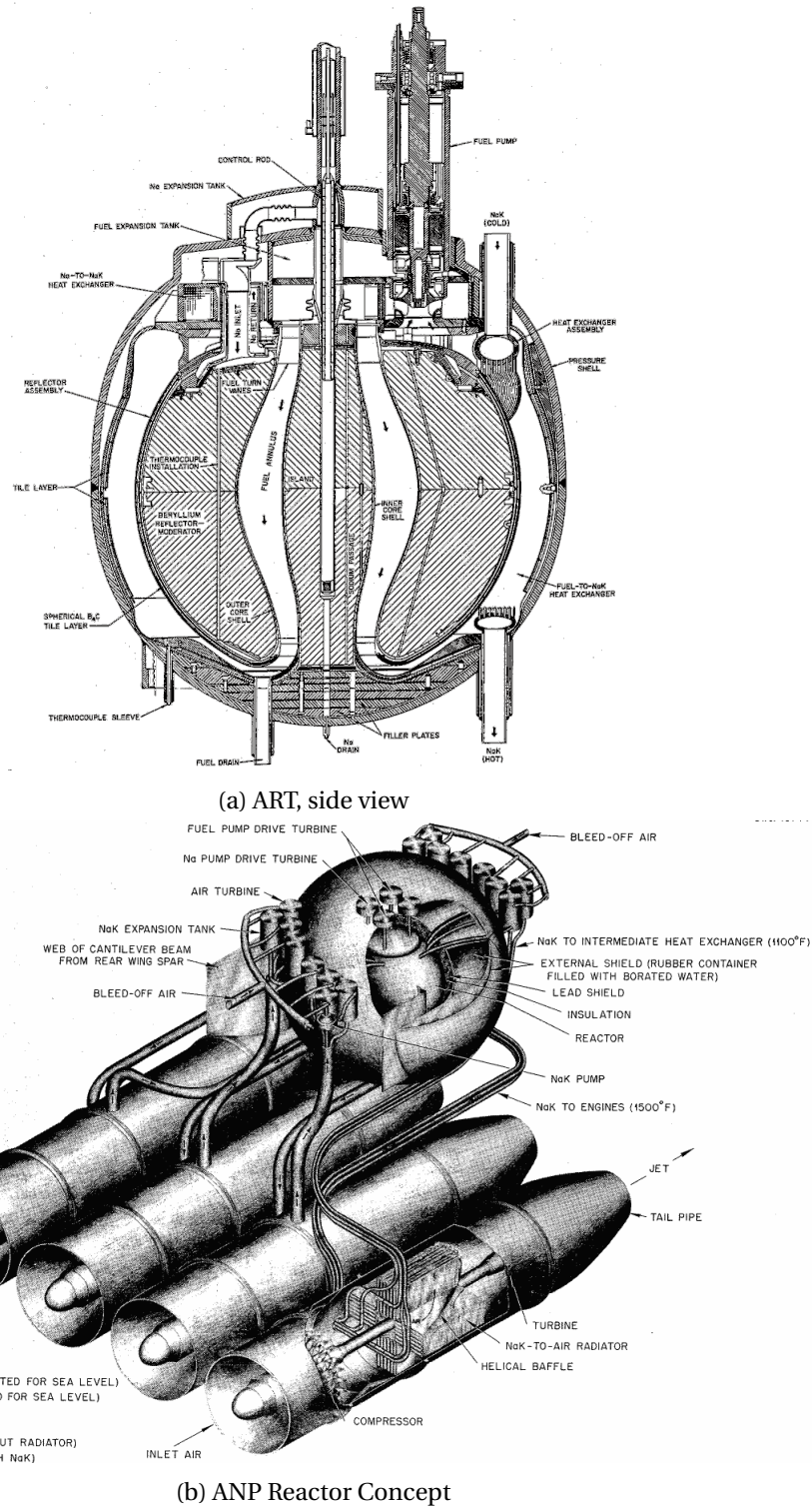


Figure 2.2 – The Aircraft Reactor Test (ART) reactor and its related aircraft power plant concept (Fraas and Savolainen, 1956).

breeder. It was discovered that graphite was compatible with salts and thus did not need to be clad. Also, it was not wetted by the salts, diminishing the accumulation of FPs in its pores.

Early on, the attractiveness of two-fluid breeders was clear: one can have a very low inventory thanks to the thermal spectrum and purely fissile content of the fuel salt, while breeding in a Th-bearing blanket salt. This led to the development of the two-fluid versions of the Molten Salt Breeder Reactor (MSBR) concept. Additionally, the reprocessing scheme was very simple: U would be fluorinated out of the Th blanket and transferred to the fuel; U would be fluorinated out of the fuel salt and separated from the volatile fission products, and then the fuel salt would be distilled under vacuum, resulting in most of the FPs being left at the bottom of the still and the salt being cleaned, filled with U again, and returned to the core. Extraction of Pa via reductive extraction from the blanket was considered to improve breeding performance, but was not necessary to have a positive breeding gain.

However, the problems inherent to joining graphite moderator blocks to metallic tubing, including the graphite volumetric changes during irradiation, pressed the search for another solution. In the end of 1967, it was discovered that reprocessing of salts containing Th by liquid-liquid reductive extraction in molten bismuth containing Li or Th was feasible, including the separation of Pa.

This discovery led to the design of a single-fluid MSBR, which remained the reference until the end of the MSRP (Bettis and Robertson, 1970; Robertson, 1971). In this design, the fertile material is dissolved in the same salt as the fissile material. This simplifies the core design substantially but also complicates the reprocessing scheme compared to the two-fluid version. The breeding requirements at the time also implied a quite large reactor with low power density to both minimize neutron leakage and increase the moderator lifetime.

2.2.3 The Molten Salt Reactor Experiment

The MSRE was designed and built from 1960 to 1964 (Robertson, 1965) and was run from 1965 to 1969, lasting two times longer than its design lifetime (Haubenreich and Engel, 1970). It was a 7.3 MW_{th} graphite-moderated reactor fueled by the mixture LiF–BeF₂–ZrF₄–UF₄, with ZrF₄ added to prevent precipitation of U in case of air ingress in the salt.

To this day, it is the reference experiment and the main source of operating experience and experimental data in MSR. Toward the end of the experiment, the original 33%-enriched U fuel was wholly fluorinated out of the carrier salt, to be replaced by ²³³U bred elsewhere to run some experiments on the physics of that fissile element. Finally, some plutonium was also added to the carrier salt, making the MSRE one of the few reactors to have run on the three main fissile isotopes.

The MSRE provided valuable information on the physics of MSR (Kerlin et al., 1971), as well as corrosion of structural materials in a molten salt environment with fission products (Compere et al., 1975). It was discovered that Te was attacking grain boundaries of Hastelloy N and

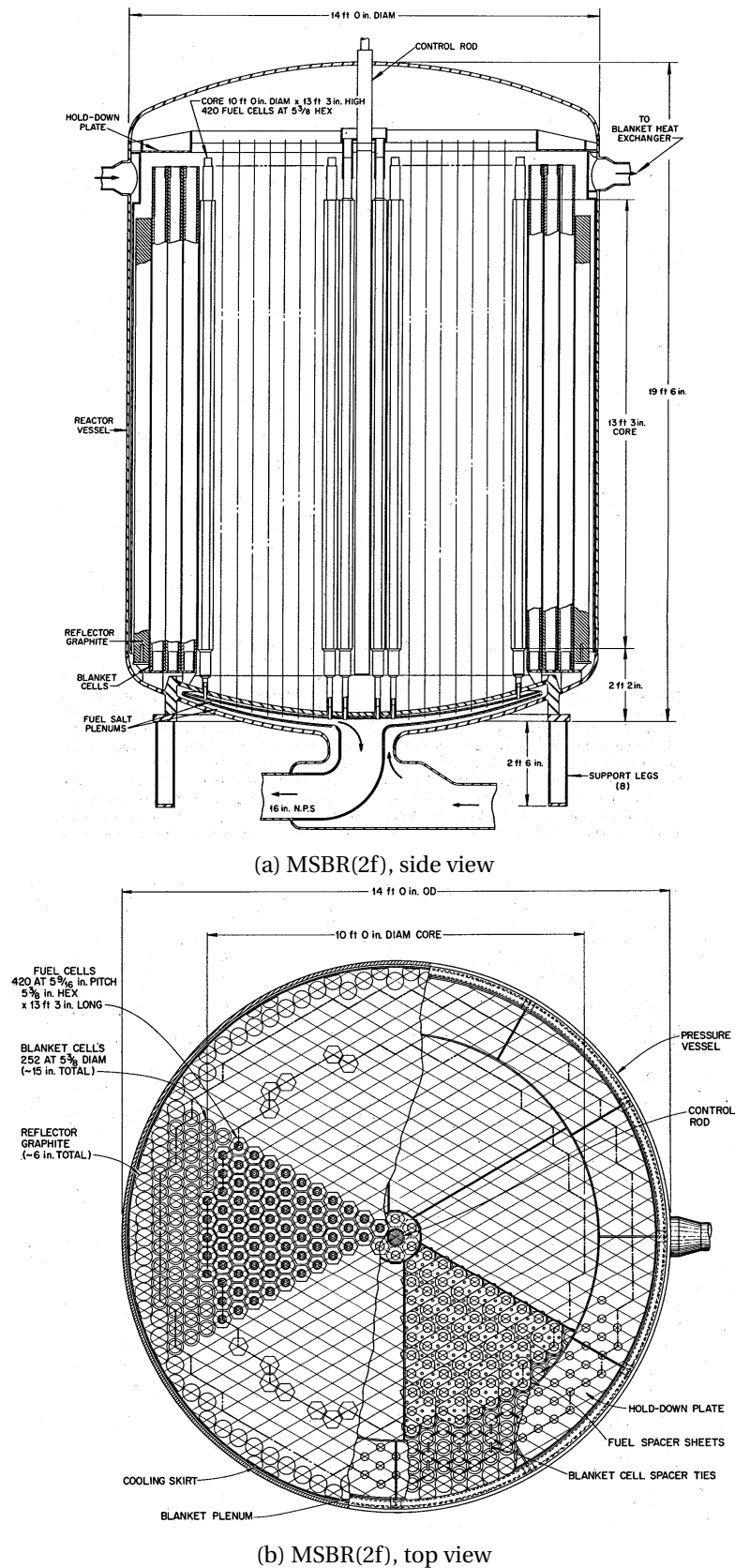
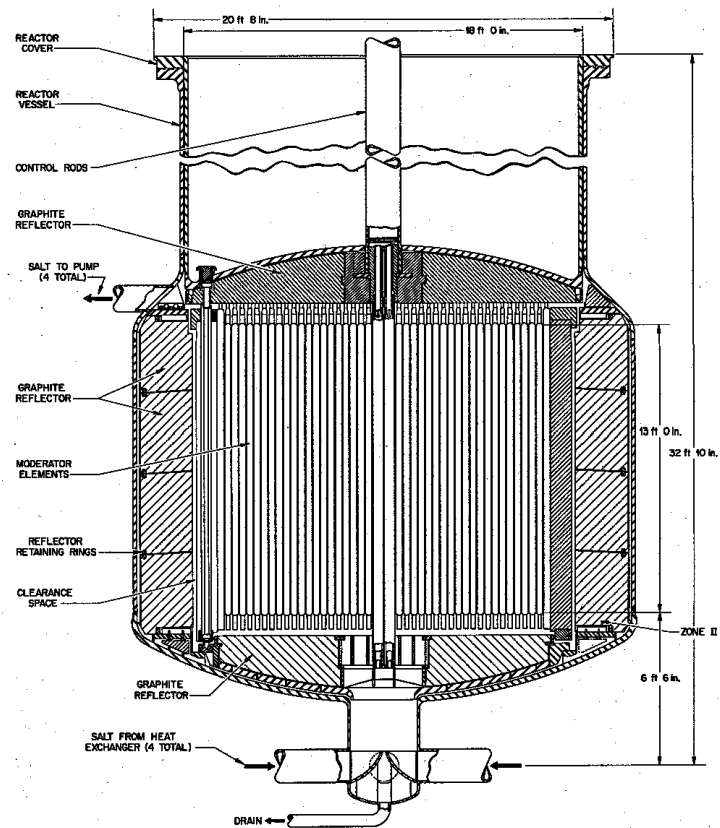
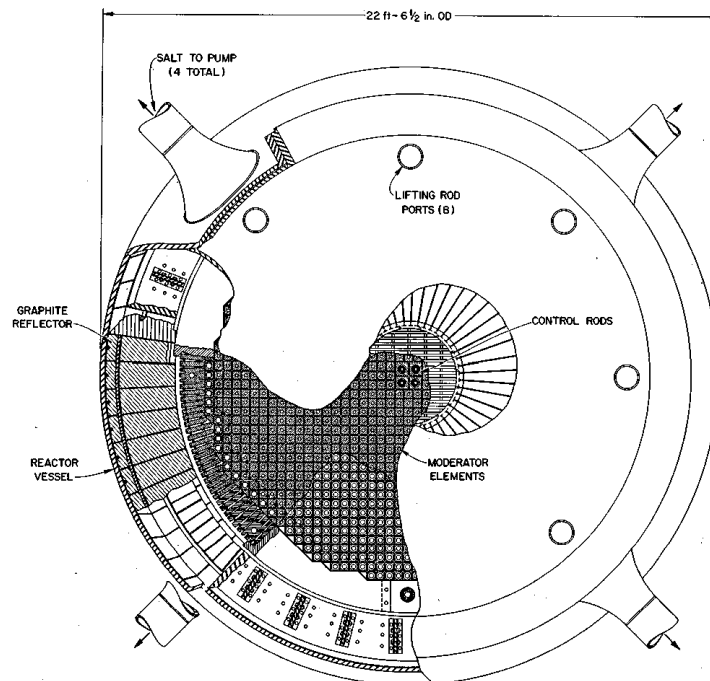


Figure 2.3 – Side and top cut view of the two-fluid MSBR (Robertson et al., 1970).

2.2. History of Molten Salt Reactors

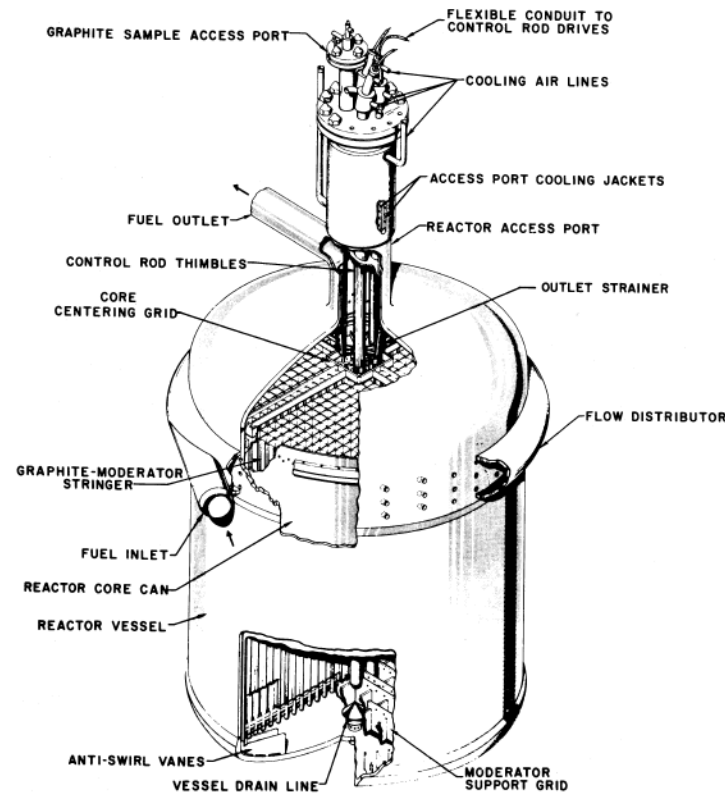


(a) MSBR, side view

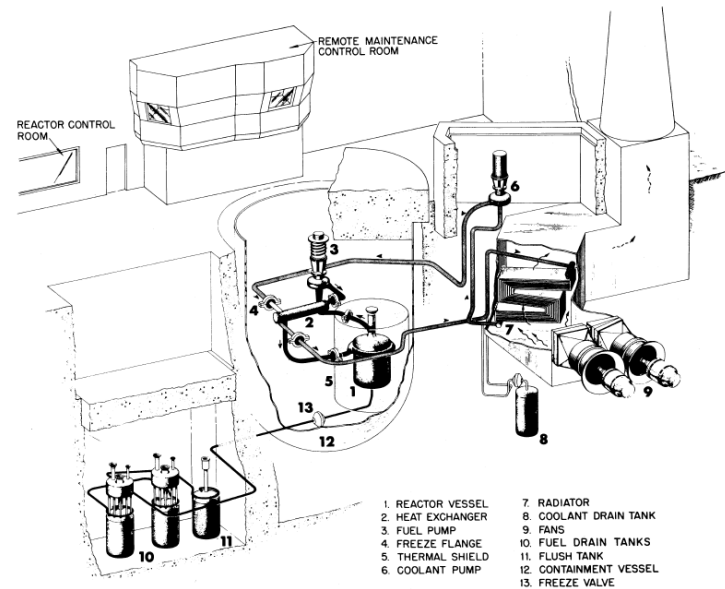


(b) MSBR, top view

Figure 2.4 – Side and top cut views of the single-fluid MSBR (Rosenthal, 1969).



(a) MSRE reactor



(b) MSRE facility

Figure 2.5 – Reactor and facility of the MSRE (Haubenreich and Engel, 1970).

embrittling it, additionally to the neutron-induced embrittlement typical of Ni-base alloys such as Hastelloy N.

2.2.4 The End of the Pioneering Era

After the end of the MSRE, the MSRP focused on improving the feasibility of the MSBR concept by further developing fixes to the remaining problems, that is, salt chemistry, and irradiation & corrosion embrittlement of Hastelloy N (Keiser, 1977a,b). Some changes to the alloy composition to prevent the fission product Te from attacking grain boundaries were tested at a laboratory scale. They would later be implemented and refined in Russia.

A few studies were carried out in the frame of President Carter's new focus on non-proliferation and to provide a design option answering to concerns with the MSBR that were raised at the end of the MSRP: the short graphite lifetime, the proliferation risk associated with a breeder reactor which extracted U and Pa on a regular basis, and the complexity of the fuel reprocessing plant. This led to the design of the Denatured Molten Salt Reactor (DMSR) (Engel et al., 1980), which is a graphite-moderated high-conversion ratio (ca. 0.8) Th converter refueled at regular intervals with 20%-enriched U. The concept did not use a fuel reprocessing plant and the sole extraction process was He bubbling to remove insoluble fission products. Combined with the constraint of not extracting Pa from the fuel to let it decay out of the neutron flux, this implies a penalty on breeding. To limit these losses, the reactor core was very large (10 m height and diameter) to decrease neutron leakage and the power density was lowered to limit parasitic captures on Pa. This however allowed for some margin to flatten the neutron flux profile and thus optimize the lifetime of the graphite moderator, which increased from 4 years (MSBR) to 30 years (DMSR). Being refueled with enriched U, the ^{233}U bred from Th would systematically remain "denatured", that is, considered to be of "low enrichment" (^{233}U less than 12% of the total U by weight), reducing the proliferation concerns. The balance of plant remained the same as the MSBR, a Water Rankine cycle being used for power conversion.

After the end of the MSRP, interest in MSR remained low and confined to essentially academic studies for two decades, before Bowman suggested using a molten salt-fueled accelerator-drive waste transmutation system (Bowman, 1998). In the beginning of the 2000s, a molten-salt cooled, solid-fuel concept based on both MSR (salt coolant and materials) and HTR (TRISO particle-based fuels) technologies was brought forth (Forsberg et al., 2003) with designs spanning several power ranges and fuel types (both pebble-bed and pin-type hexagonal fuel elements). Such reactors are recognized as MSR but typically are referred to as FHR. Three major designs have been established: the Advanced High Temperature Reactor (AHTR) (Varma et al., 2012) and the SmaHTR (Greene et al., 2010), a SMR variant of the much larger AHTR, and the PB-FHR (Allen et al., 2013b,a; Facilitators and Facilitators, 2013a,b), a pebble-bed variant designed in a collaboration between the University of California, Berkeley (UCB), the University of Wisconsin, Madison (UWM), and the Massachusetts Institute of Technology (MIT)

2.2.5 Research Outside of the United States

A relatively short time after the beginning of the MSR-related investigations at ORNL, other research institutions learned about the attractiveness of MSR technology and started smaller research programs of their own, including the U.K., France and the USSR. The involvement of several individuals also contributed to research being carried out in countries such as Japan or Poland and Switzerland.

France

French research in the domain of MSR started in 1973 at the behest of Électricité de France (EDF) and Commissariat à l'Énergie Atomique (CEA) after exchanges with ORNL, although the interest can be traced back to at least the late 1950s (Dirian and Saint-James, 1959). It first focused on re-evaluating the design choices made for the MSBR, after which the French focused on developing their own design to alleviate the shortcomings identified prior. The program received some industrial support through Péciney Ugine Kuhlman, an industrial consortium involved in electrometallurgy, nuclear fuels and chemistry.

The French developed a graphite-moderated reactor concept fueled with fluoride salts and directly cooled by molten Pb (Hery and Lecocq, 1983), as they saw the indirect cooling method as too detrimental to the reactor inventory due to the additional volume of salt needed for cooling. The direct Pb cooling method proved difficult to implement: separating it from the molten salt is challenging, and a certain amount of salt would follow the coolant into the cooling circuit. Moreover, the lead can reduce and dissolve some FPs from the salt, thereby contaminating the coolant. The French went as far as running several large-scale experiments such as material testing and molten salt loops as well as to specifically study direct cooling through experiments with water. Efforts continued until 1983, when the program was shut down.

Revival of the interest in MSR in France came in the 1990s. Several concepts were put forth, such as the thermal waste incinerator AMSTER (Actinides Molten Salt TransmutER) by EDF (Vergnes and Lecarpentier, 2002), the accelerator-driven system Thorium-based Accelerator-driven System with Simplified fuel cycle for long-term Energy production (TASSE) by the CEA (Berthou et al., 2001), or the chloride-based REBUS reactor (Mourogov and Bokov, 2006) by EDF. Parallel re-evaluation of the MSBR concept at the Centre National de la Recherche Scientifique (CNRS) led to a renewed interest in fast-spectrum fluoride-fueled MSR, giving birth to the Molten Salt Fast Reactor (MSFR), originally named Thorium Molten Salt Reactor-Non Moderated (TMSR-NM) (Heuer et al., 2014).

Research has since the late 2000s thus focused on the MSFR, to the point that it is now the reference system for both European projects and the GIF. The French contribute to European programs, but also have had several national programs such as GEDEPEON and PACEN which both focus on the back-end of the fuel cycle and waste management. Notable contributions

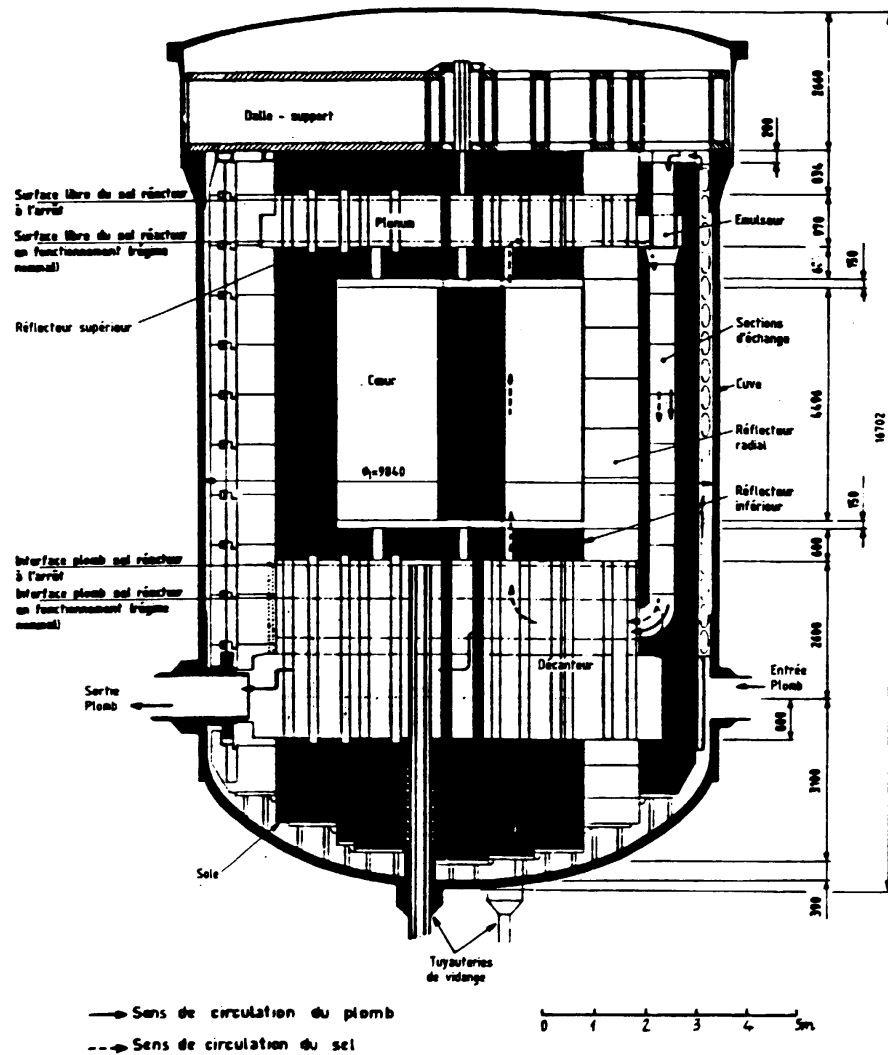


Figure 2.6 – Reactor layout of one of the reference CEA-EDF directly lead-cooled molten salt reactor concept from the 1980s (Groupe de Travail CEA-EDF "Concept RSF", 1983).

include the chemistry of the reprocessing of salts (Delpech et al., 2009) and alloy development (Cury, 2007). Indeed, two variants of a novel Ni-Cr-W alloy called EM-721 and EM-722 were produced and investigated in a corrosive salt environment with the help of the Russian facilities (Ignatiev et al., 2013).

United Kingdom

In the UK, starting in 1964, research on MSR was essentially lead by the Atomic Energy Research Establishment (AERE), part of the United Kingdom Atomic Energy Authority (UKAEA) at Winfirth and focused on chloride-based fast-spectrum MSR using the U-Pu cycle early on. Several designs were proposed, culminating in various versions of a 2500 MW_e reactor with

Chapter 2. Molten Salt Reactors

either direct lead cooling, He cooling or indirect salt cooling (Smith and Simmons, 1974). Like other programs around the World, efforts declined quickly after the end of the ORNL program in 1976.

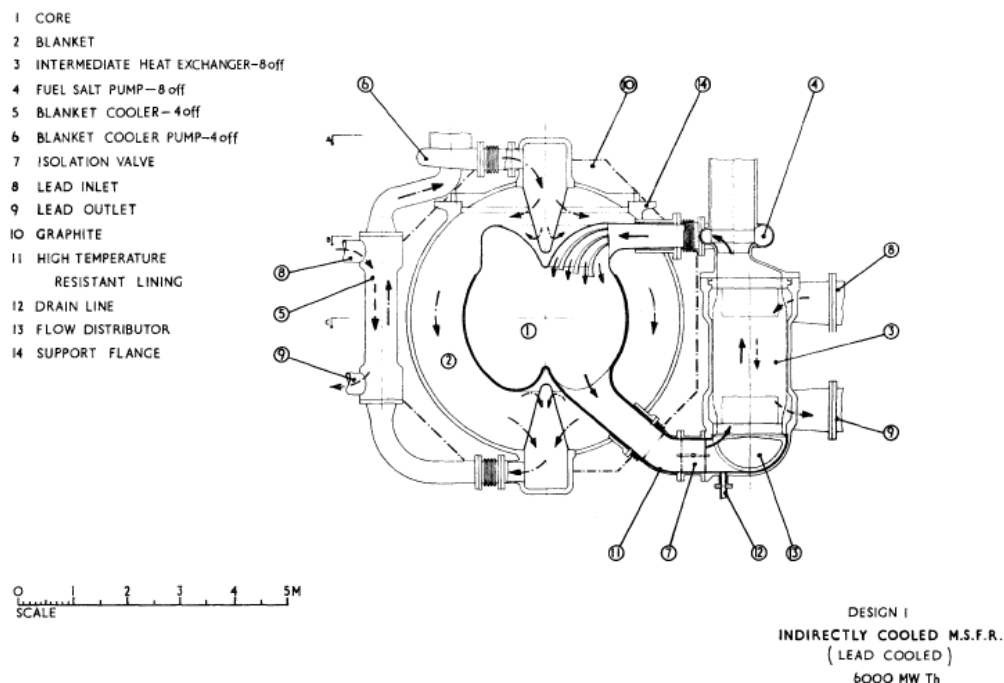


Figure 2.7 – Depiction of one of the AERE concepts: an indirect, lead-cooled chloride-fueled MSR (Smith and Simmons, 1974).

Switzerland

An extensive body of design studies lead by M. Taube essentially on chloride-fueled MSR started in Poland at the Institute for Nuclear Research (INR) in Warsaw in the early 1960s (Taube et al., 1967) and continued at the Eidgenössisches Institut für Reaktorforschung (EIR) after Taube's move to Switzerland in the late 1960s. Research lasted until the late 1970s (Taube, 1978), developing concepts such as coupled systems of thermal and fast MSR (Taube, 1974), several concepts of fast-spectrum MSR including some cooled by boiling salt, and the incineration of troublesome FPs in the neutron flux of a fast MSR (Taube et al., 1975).

More recently, in 2015, Switzerland joined the MSR Memorandum Of Understanding (MOU) within the GIF Framework.

Japan

Japan has a sizeable body of experience with molten chloride salts due to their pyro-processing research program. Like in other countries, research activities in Japan started after exchanges with ORNL. In 1968, Dr. Furukawa of Japanese Atomic Energy Research Institute (JAERI) visited

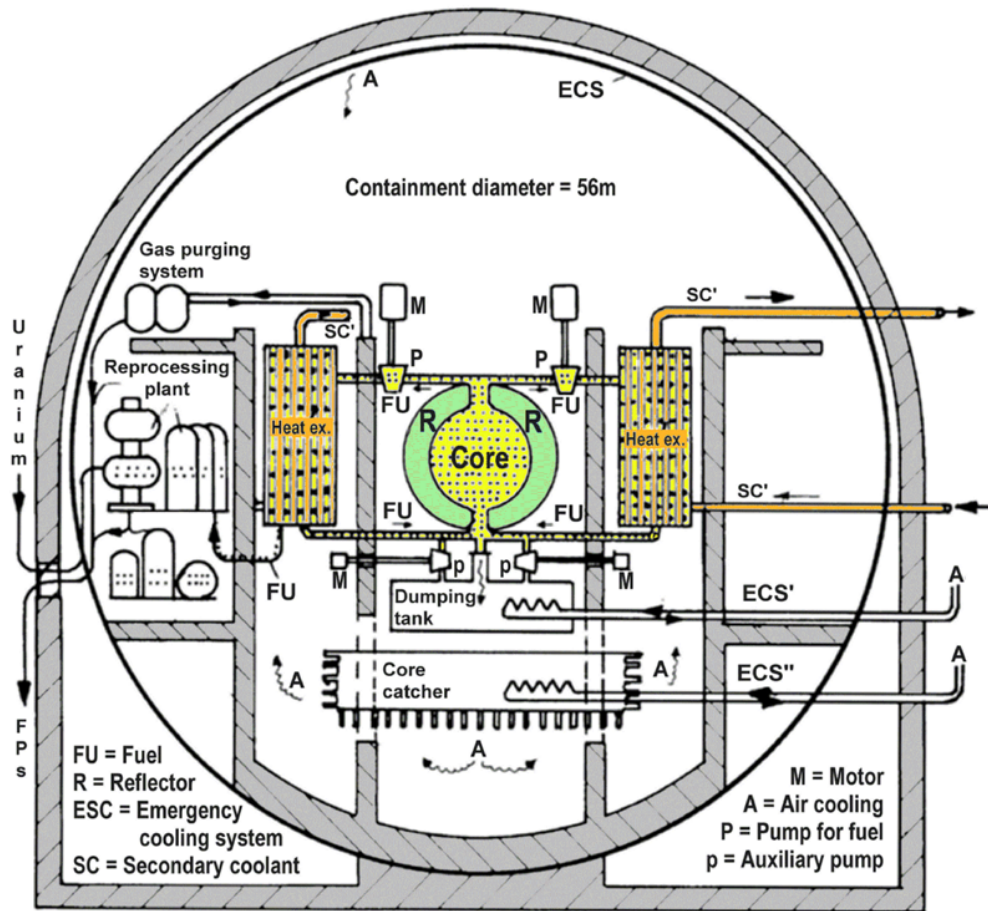


Figure 2.8 – The single-fluid chloride-fuelled SOFT reactor concept of EIR, with a containment building visibly inspired by German pre- and Konvoi reactors (Taube and Heer, 1980).

ORNL at the time of the operation of the MSRE and was impressed by the technology. As he came back to Japan, he dedicated much of his later work to MSR technology, and developed several concepts, amongst which are the FUJI reactor series and the Accelerator Molten Salt Breeder (AMSB) joined in a system named Th Molten-Salt Nuclear Energy Synergetic System (THORIM-NES) (Furukawa et al., 1990, 1992).

The FUJI series is essentially based on the MSBR, but the choice was made to renounce net breeding in favor of simpler design choices. To achieve a longer graphite lifetime, the layout of the core and power density were changed to flatten the neutron flux. The on-site continuous processing of fuel was abandoned in favor of an off-site, batch processing scheme. These two choices came at a cost for the breeding gain, which became slightly negative. To alleviate this, the role of breeding the needed make-up fuel was given to a non-critical facility such as a fusion neutron source or an ADS. It was foreseen to start the first few FUJI reactors using LWR Pu (FUJI-Pu), thereby disposing of a sizeable portion of the world's stockpiles of plutonium. After the production of ^{233}U was sufficient to start new reactors, the FUJI-U233 would be built

Chapter 2. Molten Salt Reactors

directly. A smaller version of the FUJI concept was also designed essentially to play the role of a prototype and was named miniFUJI.

Soviet Union and Russia

It is known that some research on MSR was conducted in the Soviet Union, probably shortly after the start of the MSRP at ORNL. Before that, an extensive body of research was conducted on fundamental salt properties, essentially due to the dual use of molten salts as reactor fuels and reprocessing medium for fast reactors fuel. The Soviet program is likely the forerunner of the modern Russian program.

The Russian program was at the beginning largely funded by several ISTC initiatives after the fall of the Soviet Union. It is likely a continuation of the Soviet program and consists in the development of a fast-spectrum, fluoride-based minor actinides burner named MOlten Salt Actinide Recycler and Transmuter (MOSART) (Ignatiev et al., 2007). It is mostly intended to be a waste burner for leftover actinides from LWRs not burnt in other conventional fast reactors. Variants including Th in blankets have also been studied (Ignatiev et al., 2014). Due to the many similarities with the French/European MSFR, the Russians have long been associated to the European research programs, such as the Russian program MARS (Minor Actinide Recycling in Salts) running in collaboration with Evaluation and Viability Of Liquid fuel fast reactor system (EVOL). Contributions of interest include numerous experimental studies on salt properties and salt corrosion and plutonium trifluoride solubility, tested in several molten salt loops. Work on materials also included the implementation of the recommendations for the modification of Hastelloy N that have been made at the end of the MSRP at ORNL (Ignatiev et al., 2008).

China

In the early 1970s, investigations were carried out at the then Shanghai Institute for Nuclear Research (SINR) to the point of a zero-power reactor with frozen salt being built in 1971 and operated until 1973. Research was likely inspired by efforts at ORNL and identified the Th-use potential of MSR as particularly relevant to China. The program was short-lived however since shortly after the institute was tasked with participating in the development of the first indigenous LWR, the Qinshan NPP. The Fukushima disaster in 2011 brought renewed interest in MSR technology at the Shanghai Institute of Applied Physics (SINAP) which is part of the Chinese Academy of Sciences (CAS). An ambitious research program was started which aims at the development of both solid-fuel FHR as a first step and liquid-fuel MSR as a longer-term option. The objectives are to utilize Th, to open the potential for non-electricity applications (e.g. Hydrogen production) and allow water-free cooling to provide power for the arid Western part of China.

Czechoslovakia/Czechia

Czechia benefits from its experience with fluoride chemistry, having pioneered the fluoride volatility process for reprocessing of spent solid fuel via flame fluorination. In the 1990s and 2000s, a Czech program focused on the development of the SPHINX reactor (Spent Hot Fuel Incinerator in neutron flux) (Hron, 2005), an accelerator-driven graphite-moderated fluoride-based LWR SNF incinerator. Meanwhile, they have been contributors of several European programs such as ALISIA or EVOL. Additionally, due to experimental needs, the Czech developed and tested a Ni-Cr-Mo alloy (named MONICR) based on Hastelloy N, in partnership with ŠKODA nuclear machinery.

More recently, Czechia established a bilateral collaboration with the United States and their own FHR program. The collaboration lead to the delivery of leftover salt from the MSRE secondary loop that has the property to have its Li enriched in ^7Li and thus can be investigated neutronically, which is the goal of the initiative. The salt is being used in the Czech Republic for experiments with the zero-power reactor LR-0 (Losa et al., 2015).

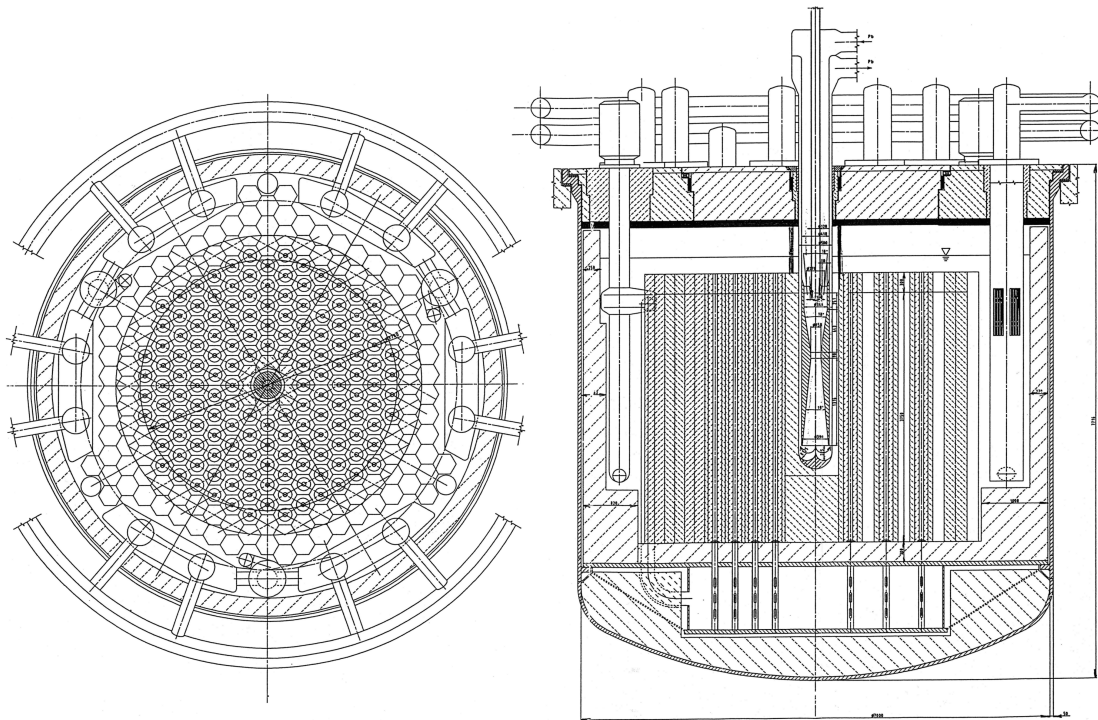


Figure 2.9 – One of the Czech designs for a graphite-moderated accelerator-driven Molten Salt Reactor for transmutation.

India

India's involvement in MSR research is old and very much linked to the country's ambitious three-tier Th use program, India having close to no U reserves but large Th ones. The plan is to combine Th breeding in heavy water-moderated reactors, fast Na-cooled reactors, and MSR, with the fast reactors contributing mostly indirectly through the breeding of Plutonium used subsequently to start a full-scale Th cycle.

European Programs

Recent research programs in Europe find their origins mostly in the end of the 1990s, in France, Russia, and the Czech Republic, which all had sizeable national research programs. Additionally, there have been European research programs dedicated to MSR in the 5th, 6th and 7th Framework Programs of the European Commission, as well as in the most recent Horizon 2020 program. Several joint European research programs have been carried out as part of the European Commission's Framework Programs: Review of Molten Salt Reactor Technology (MOST) , Assessment of LIquid Salts for Innovative Applications (ALISIA) , EVOL and most recently, Safety Assessment of the MOlten salt FAst Reactor (SAMOFAR):

- MOST (2001-2003, 5th Framework Programme) concentrated on re-evaluating the MSBR concept and on applying modern computational tools to the study of the behavior of MSR (MOST Project, 2005).
- ALISIA (2006-2008, 6th Framework Programme) focused on identifying needs for use of liquid salts in industrial applications, including nuclear, and produced several experimental studies on the properties of salts, as well as preliminary studies on a fast-spectrum MSR, which would lead to the next project.
- EVOL (2010-2013, 7th Framework Programme) further developed the originally French MSFR concept, a fast-spectrum (unmoderated) two-fluid Th breeder. Specific problems such as start-up fuel, the possibility of starting the reactor using LWR plutonium, and the core layout for optimal cooling and safety were studied.
- SAMOFAR (2015-2019, Horizon 2020) builds on the improvements brought by the EVOL project and aims at demonstrating and improving the safety characteristics of the MSFR.

2.3 Molten Salt Reactor Concepts

As is apparent in the previous sub-chapter, MSR are characterized by a wide array of concepts that have been put forth since their first inception. In this sub-chapter, we describe the most prominent of these concepts. They are organized in major categories which can be found also on the MSR classification of Figure 2.10.

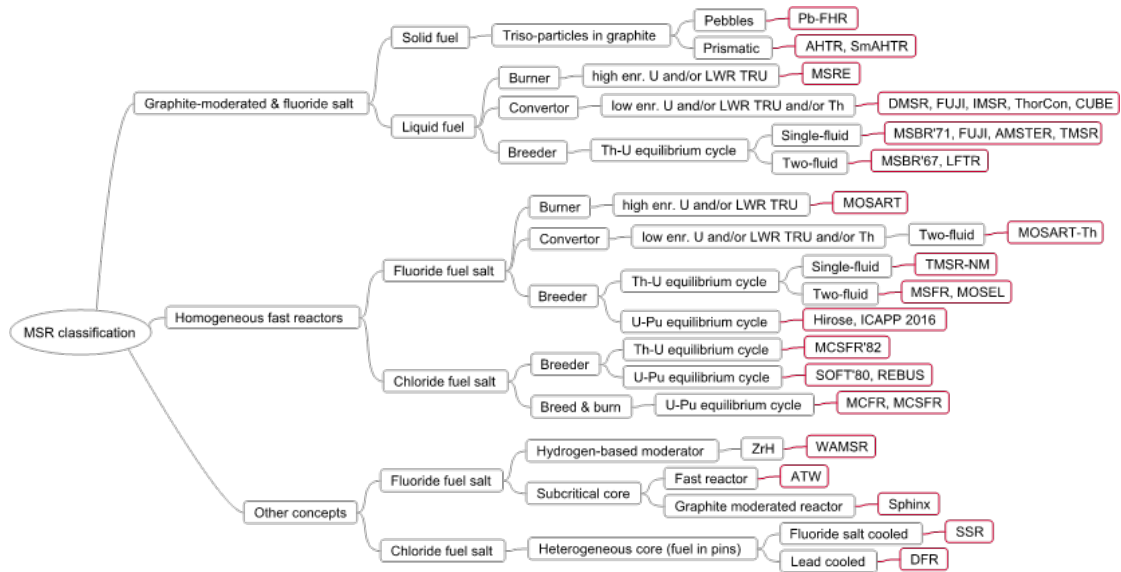


Figure 2.10 – A classification of MSR designs proposed to this day.

2.3.1 Graphite-moderated Fluoride Reactors

The MSBR is the name of several variants of the concept pursued by ORNL during the MSRP. ORNL focused early on a Th breeder; fast-spectrum systems were considered but thermal ones were preferred due to their lower inventories and the excellent properties of graphite used in conjunction with salts. Both single-fluid and two-fluid concepts were called MSBR, but the name nowadays mostly refer to the last version, a single-fluid graphite moderated Th breeder.

Numerous other variants of this concept have been proposed, amongst which are the several Fuji MSR designs, which are largely based on the work done at ORNL. A defining feature of FUJI MSRs are their slightly negative breeding gain when considering a single reactor (Kato et al., 2003) due to the minimization of fuel processing over the reactor's lifetime. It was foreseen to breed the necessary ^{233}U make-up fuel in accelerator-driven systems.

2.3.2 Fast-spectrum Homogenous Fluoride Reactors

Choosing an opposite way to their moderated counterpart, fluoride reactors can also be designed without a moderator, that is, in a fast-spectrum arrangement. These concepts trade the usual issues associated with the use of graphite (limited lifetime, power coefficient, core size, etc.) for other ones (higher inventory, complex core flow pattern, etc.). Their layouts are essentially similar due to the core being an open cavity filled with fuel salt.

The Molten Salt Fast Reactor

The MSFR was born from French investigations of graphite-moderated Th-cycle breeders which concluded that the best way to alleviate the drawbacks of a graphite moderator (limited lifetime, large core, huge reprocessing requirements, potentially positive feedback) were to not have any moderator at all. The MSFR was born: a two-fluid, unmoderated Th-cycle breeder. It has become the reference design of the European MSR projects (EVOL, SAMOFAR) and of the GIF.

The Molten Salt Actinide Recycler and Transmuter

The Russian program is dedicated to burning TRU waste, with their reference concept not using any fertile support nor any blanket, i.e. the fuel only contains transuranics to be burnt. It is embodied by a fast-spectrum fluoride-based graphite-reflected reactor, somewhat like the French-European MSFR. Major differences in design include the loop-type nature of MOSART versus the pool-type nature of MSFR, as well as different solutions to the problem of in-core recirculation of fuel in the form of a flow skirt at the bottom of the core for the Russian concept, whereas the modification of the core shape from a cylinder to a hyperboloid was preferred in the case of MSFR.

2.3.3 Fast-spectrum Homogeneous Chloride Reactors

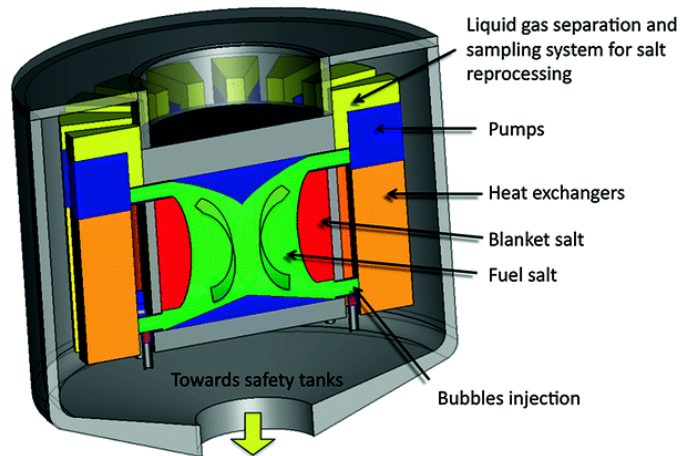
Other halide bases than fluorides were also investigated since they would chemically have similar properties as their fluoride counterparts, while having quite different nuclear properties: heavier halides would moderate neutrons much less, allowing for a harder neutron spectrum than unmoderated fluoride can ever achieve.

The first proposal of such a reactor seems to go back to Bullmer (1956) in which a core a chloride salt and a blanket of U oxide slurry in liquid Na was proposed. Several prominent design studies have been conducted by Nelson et al. (1967) and Taube (1978), in which both in-core and ex-core indirect-cooling by salt as well as direct-cooling using liquid lead or boiling Al chloride designs have been proposed. Ottewitte (1982) studied the possibility of running a chloride MSR on the Th cycle after his stay at EIR. Chloride-based MSR designs have resurfaced since then, as exemplified by the single-fluid REBUS concept (Mourogov and Bokov, 2006) as well as concepts by the privately financed TerraPower and Elysium Industries companies. Modern designs seem to favor the simplest options, that is, a single-fluid reactor with ex-core indirect cooling.

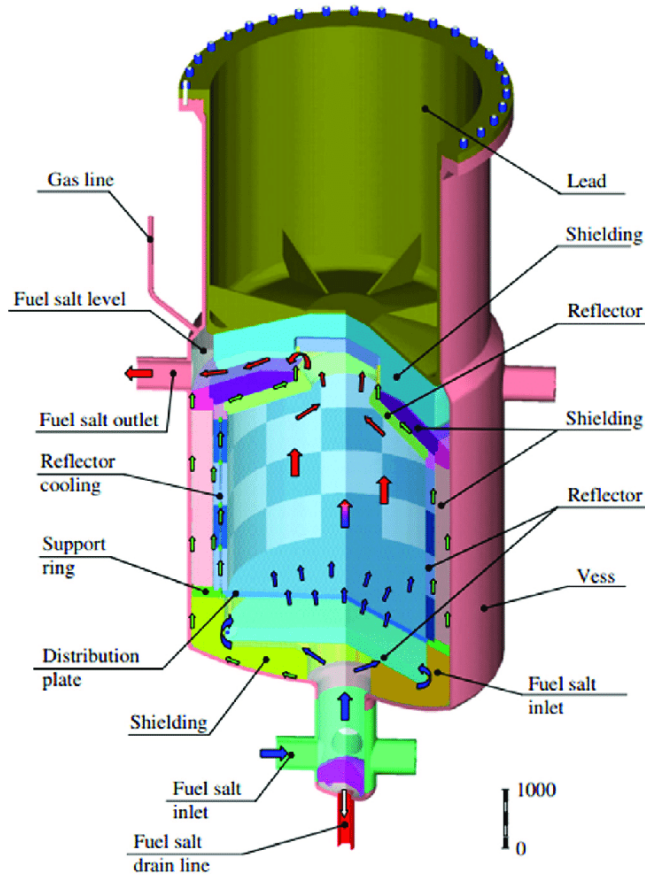
2.3.4 Heterogeneous Fast-spectrum Reactors

Alternatively to the homogeneous fast-spectrum reactors, one can conceive heterogeneous fast-spectrum reactors in which the fuel salt is cooled in the core by another coolant, with the

2.3. Molten Salt Reactor Concepts



(a) MSFR



(b) MOSART

Figure 2.11 – Illustrations of the fast-spectrum fluoride-fueled MSFR and MOSART concepts (not to scale).

heat exchange happening through fuel tubes, a method also termed internal indirect cooling.

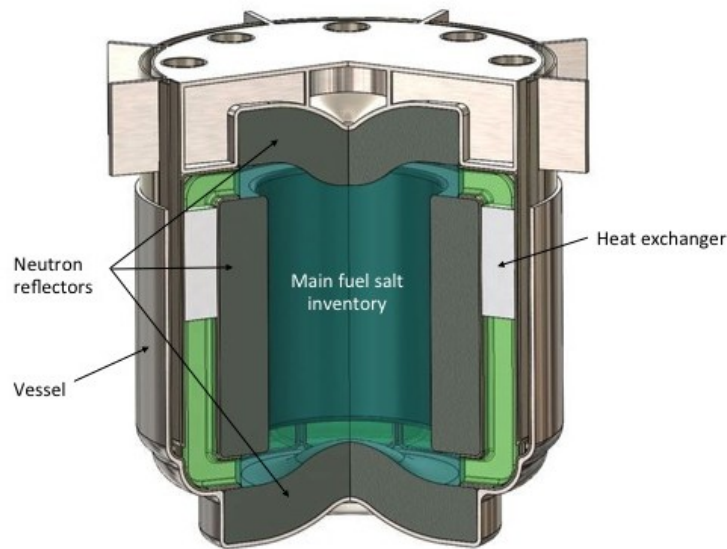


Figure 2.12 – Illustration of the Terrapower concept.

Advantages of this method is that one can decouple the coolant inventory from the fuel inventory and thus minimize the latter. Moreover, since the primary form of cooling is through circulation of the coolant and not the fuel salt itself, the temperature of the fuel salt will be substantially higher and thus fuel mixtures with higher melting points can be used.

The disadvantages of this method include the irradiation of the material separating the fuel salt from the coolant which will therefore have a more limited lifetime, the neutron losses due to parasitic captures on this material, and the potential for contamination of the coolant through leaks in the tubing containing the fuel salt.

Several variants of this concept have been proposed over the years, some of which foresee the use of coolant in the form of a salt acting as breeding blanket (Kasten et al., 1965; Taube and Ligou, 1974), in the form of an inert salt (Scott, 2017) or in the form of lead (Huke et al., 2017).

2.3.5 Other Concepts

Several other MSR concepts have been put forth but do not fit the classification above. In this section, a few of these designs are presented for comparison.

Graphite-moderated Converters

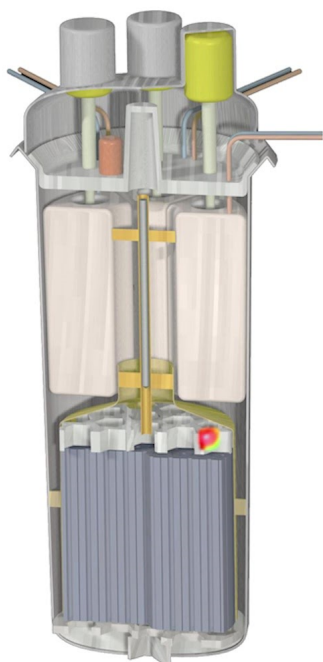
The most prominent concept in the category of graphite-moderated converters is arguably the above-mentioned DMSR designed by ORNL at the end of the MSRP. Some of the recent private companies proposing MSR designs have made near-term deployment capability their

priority, and have thus been inspired by the DMSR design. This implies using mostly proven technology, with as few novelties as possible, taking most of the design features from the MSRE. Therefore, they also renounce in-situ fuel recycling and have simple fuel cycles, at the cost of major sustainability gains.

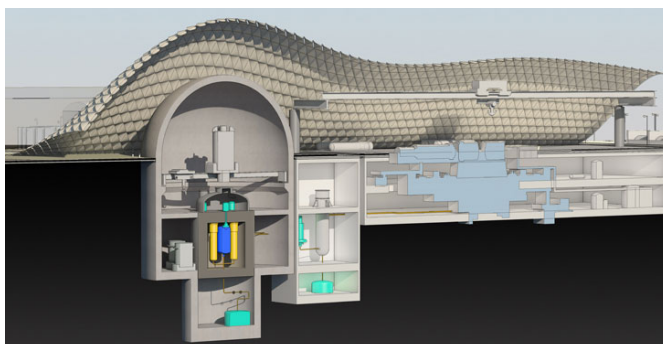
Amongst these companies are Terrestrial Energy and ThorCon. Terrestrial Energy focuses on a graphite-moderated Uranium converter using Low-Enriched Uranium (LEU) fuel (see figure 2.13a). The reactors are planned to be modules to be operated for approximately 7 y thanks to regular fuel additions. They would afterwards be swapped for another module. ThorCon on the other hand foresees to use Thorium in the start-up fuel to improve the conversion ratio, and focuses on shipyard-built reactor modules that could be shipped by barges to the plant site, requiring minimal on-site construction work.

Zirconium Hydride-moderated Converters

As proposed by Transatomic Power, a converter could be moderated using ZrH instead of graphite (see figure 2.13b). It contains approximately as many hydrogen atoms per unit volume as pressurized water, making it a more potent moderator than graphite, therefore reducing the amount of moderator needed and thus the size of the core. Additionally, ZrH is potentially beneficial when used with plutonium compared to graphite, hence the waste-burning orientation of the Transatomic Power design.



(a) Terrestrial Energy concept.



(b) Transatomic Power concept.

Figure 2.13 – Illustrations of two Converter concepts.

Accelerator-driven Molten Salt Reactors

In the 1990s, the concept of ADS gained popularity after the Chernobyl accident in the previous decade. ADS are subcritical reactors in which the missing neutrons are produced using a proton accelerator and a spallation source made of heavy atoms. Neutrons are produced by spallation, i.e. the ejection of numerous neutrons after the bombardment of a heavy nucleus with a proton. Since the reactor is subcritical, the chain reaction would die out after the proton beam has been cut off, which can be easily achieved, making reactivity-initiated accidents unlikely. However, this advantage comes at the cost of the addition of a complex and expensive accelerator.

Nonetheless, various molten-salt-based ADS concepts have been proposed. MSR-based ADS benefit of the advantages inherent to liquid fuels as well as from the sub-criticality of the accelerator-driven system. An additional benefit is the possibility of using the molten salt itself as a spallation target, since it contains heavy nuclides (actinides). Two main categories of concepts have been put forth: thermal- and fast-spectrum designs. Amongst the first are notably the Czech SPent Hot fuel Incinerator in Neutron fluX (SPHINX) project or the GEM*STAR of Bowman (1998). The latter include both the French TASSE concept Berthou et al. (2001), which uses fluoride salts, and the Japanese ADMSR concept of JAERI and the concept at Texas A&M University (Sooby et al., 2013).

2.4 Fuel Salts and Materials

In this thesis, several materials have been evaluated with regards to their use in a molten salt reactors; most notably, fuel salts have been used for calculations. In this section, the underlying assumptions in the selection and modelling of each material are detailed and explained.

2.4.1 Fuel Salts

This section described the assumptions made when candidate salts were selected for investigation. First, some general considerations on the selection of a salt mixture are given. Afterwards, the selected salts are outlined in two main parts, with fluoride salts on the one hand and chloride salts on the other. Higher halides were not considered due to their relatively lower chemical stability at higher temperatures.

Admissible elements in fuel salt mixture

Once the salt base (fluoride or chloride) has been chosen, the following step is to select the elements whose halides will make up the mixture. This choice has strong implications not only on the chemistry of the system, but also on the neutronics, and thus on the fuel cycle features of the resulting salt. For example, some elements may have a too large neutron

2.4. Fuel Salts and Materials

capture cross-section. Others may be incompatible with reprocessing techniques. On the other hand, given the technical constraints on the melting point of the fuel salt, it follows that not all elements are applicable following simple neutronics considerations.

In this section, the reasons for selecting or excluding specific elements are summarized on figure 2.14 and explained below.

Figure 2.14 is a periodic table of elements categorized by color. The legend indicates four categories: Major candidate components (dark green), Minor candidate components (light green), Actinides (blue), and Fission products (red hatched). The table shows the following elements categorized:

- Major candidate components:** Li, Be, Na, Mg, Al, Si, P, S, Cl, F, Ne, Ar, Kr, Xe, Rn.
- Minor candidate components:** K, Ca, Sc, Ti, V, Cr, Mn, Fe, Co, Ni, Cu, Zn, Ga, Ge, As, Se, Br, Kr, Xe, Rn.
- Actinides:** Ac, Th, Pa, U, Np, Pu, Am, Cm, Bk, Cf, Es, Fm, Md, No, Lr.
- Fission products:** H, He, B, C, N, O, Ne, Na, Mg, K, Rb, Cs, Fr, Ra, Ba, Sr, Y, Zr, Nb, Mo, Tc, Ru, Rh, Pd, Ag, Cd, In, Sn, Sb, Te, I, Xe, Rn, La, Ce, Pr, Nd, Pm, Sm, Eu, Gd, Tb, Dy, Ho, Er, Tm, Yb, Lu.

Figure 2.14 – Candidate elements for a molten salt fuel mixture.

As depicted on the periodic table of 2.14, mostly alkali and alkali-earth metals have been considered for use as salt components, with Li, Be, Na and potassium being the most prominent. These have mixtures with low enough melting points and low enough cross-sections for both thermal- and fast-spectrum MSR. Other components that have been considered include Al, Zr, and La, due to their properties of low capture cross-section and admissibly low melting points of their respective mixtures.

Magnesium has mostly been considered for chloride salts for $\text{NaCl}-\text{MgCl}_2-\text{AnCl}_{3,4}$ mixtures, however the gain in melting point does not seem to be substantial (Beneš and Konings, 2008a), therefore it was not considered.

Aluminium and Calcium have mostly been considered as elements for solvents for pyroprocessing of solid fuel, with typical mixtures being $\text{LiF}-\text{AlF}_3$ and $\text{LiF}-\text{CaF}_2$. Unfortunately, no ternary phase diagrams including actinides fluorides could be found in the open literature and consequently they were not further considered in the selected mixtures.

The capture cross-sections of elements in thermal and fast spectra is depicted on figure 2.15.

Moreover, using elements that also happen to be FPs will result in the gradual isotopic pollution of the fuel salt mixture. Since isotopic separation is unlikely to be feasible or economical,

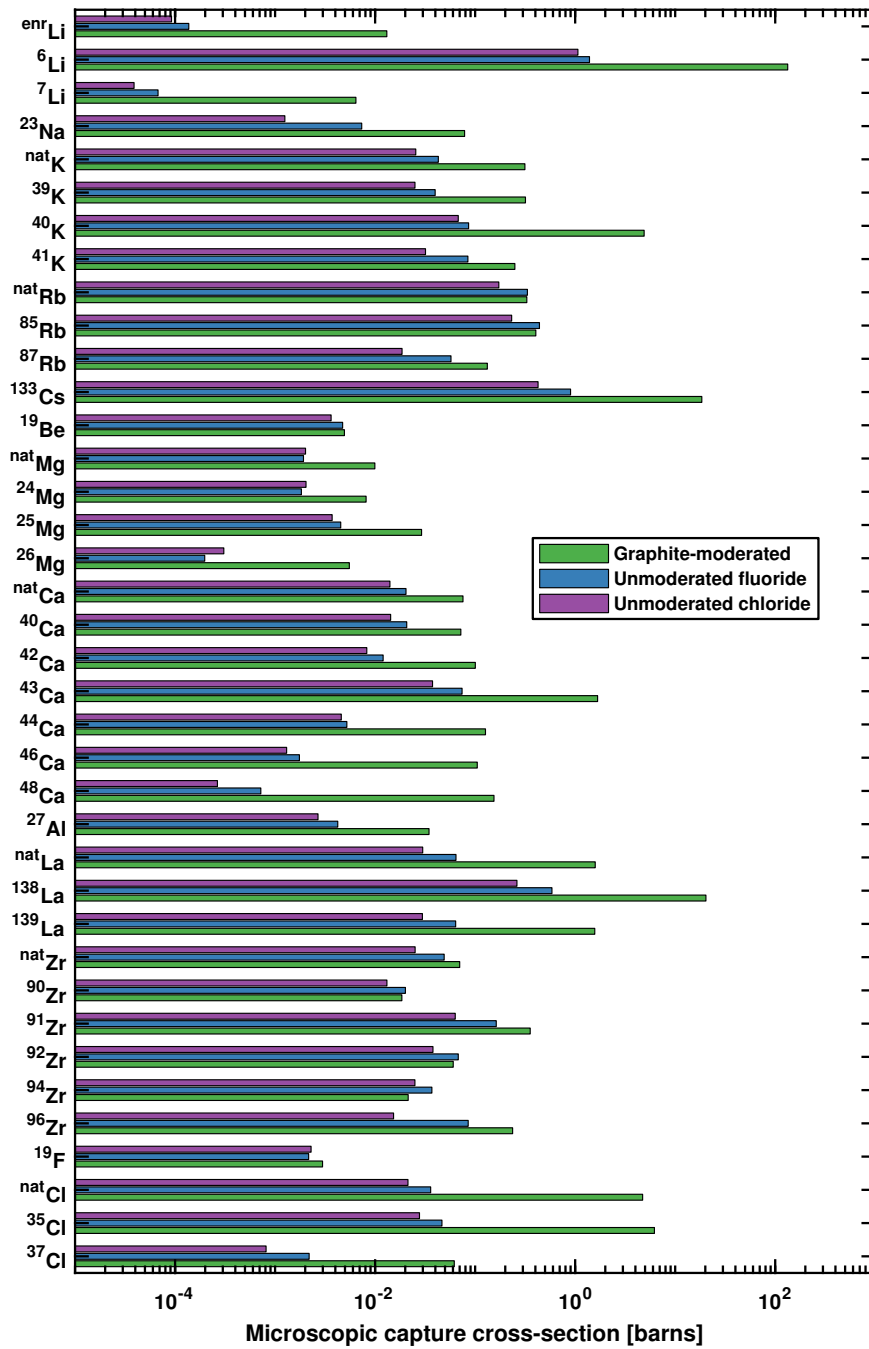


Figure 2.15 – Microscopic capture cross-section of candidate salt elements.

one can only choose to discard the whole inventory of that element (including the non-fission product part) or not to remove the element at all, leaving the FP in the salt mixture. It is obviously preferable to avoid that situation and exclude these elements from the base salt mixture. Elements for which this is the case, such as Rb, Cs, and Zr were therefore not investigated as potential components of fuel salt mixtures in this thesis.

Additional constraints on the allowable content of a given element fluoride exist. For example, BeF_2 is known to both increase the viscosity of the salt mixture with increasing content due to its tendency to form a near-glassy phase, as well as limiting plutonium solubility with increasing content (Beneš et al., 2013). It is therefore considered that the allowable content of BeF_2 is limited to approximately 30 mol %. ZrF_4 becomes increasingly volatile with increasing content, to the point of forming a mist above the salt melt and condensing in cold parts of the circuit if its content is too high. It is therefore considered important to limit its content to below 40 mol %.

Isotopic composition of elements

In most cases, elements selected for salt mixtures have a single isotope, such as Be, F and Na. However, the presence of several isotopes in some elements poses the question of the need for selective enrichment: it is warranted if the benefits outweigh the cost. This is arguably the case if the gain between the situation without and with enrichment is tremendous- or if the enrichment cost can be assumed to be low. Enrichment can thus be of interest in the following situations:

- the neutron capture cross-section of one or several isotopes is much greater than that of another isotope of the same element, or
- the neutron reactions on a given isotope produce troublesome elements, either because of their radioactivity, their capture cross-section, or of their chemical effects such as corrosion.

Of the elements selected in the previous section, two elements have been considered for enrichment:

Lithium is to be enriched in the isotope ^7Li due to the very large cross-section of ^6Li (its natural abundance varies between sample but is approximately 5 %) and its substantial tritium production through the large (n, α) cross-section of that isotope. Techniques for enriching Li exist and have been developed at ORNL. A reference ^6Li level of 50 appm was used in all the calculations involving Li.

Chlorine can be used without enrichment in a fast-spectrum reactor. However, the penalty due to the high capture cross-section of ^{35}Cl (its natural abundance being 75 %) makes the investigation of the performance of enriched chloride salts worthwhile. Moreover, both the increased production of ^{36}Cl , a β^- emitter with a half-life of 300 000 y, from ^{35}Cl as well as the increased production of sulfur isotopes provide an additional incentive to enriching chlorine. Chlorine should be suitable for enrichment using centrifuges as it has several compounds naturally in a gaseous state such as HCl whose isotopic mass ratios are favorable.

Melting point limits

One of the most important criterion for the feasibility of using a given salt mixture as fuel salt is its melting point. In MSRs, the main limiting factor on the core outlet temperature is due to materials: they need to retain enough of their strength for the safe operation of the reactor. Given a maximum outlet temperature due to material constraints, the maximum melting point is obtained by subtracting the core heat-up to get the inlet temperature, and then subtracting a safety margin from it yields a limit for the melting point of the mixture.

At the time of ORNL studies, the maximum outlet temperature was set to 704 °C (or 1300°F) because of the degradation of tensile properties of Hastelloy N beyond that limit. Assuming a core heat-up of 100 °C and a safety margin of 50 °C, results in a maximum melting temperature of 550 °C.

More recent studies such as those of the MSFR assume the availability of more modern alloys than Hastelloy N, such as HN80MTY (Russian alloy) or EM-721 (French alloy), with greater high-temperature strength. Consequently, a higher maximum outlet temperature of circa 750 °C to 800 °C is considered feasible, thus giving a maximum melting point of 600 °C to 650 °C. In this thesis compositions with melting points up to approximately 550 °C were considered, and compositions with lower melting points preferred if possible.

Selected fuel salts

Using all the criteria outlined in the previous section, several fluoride and chloride mixtures were selected for investigation. The selected fluoride mixtures are referred to as:

- LiF–AnF₄ salt mixture (FLi) for LiF–ThF₄ and LiF–UF₄ mixtures that are modern reference fluorides,
- LiF–NaF–AnF₄ salt mixture (FLiBe) for LiF–BeF₂–ThF₄ and LiF–BeF₂–UF₄, that are historical reference fluorides,
- LiF–BeF₂–AnF₄ salt mixture (FLiNa) for LiF–NaF–ThF₄ and LiF–NaF–UF₄, that have a reduced Li content,
- NaF–BeF₂–AnF₄ salt mixture (FNaBe) for NaF–BeF₂–ThF₄ and NaF–BeF₂–UF₄, that are devoid of Li but contain Be,
- NaF–KF–AnF₄ salt mixture (FNaK) for NaF–KF–ThF₄ and NaF–KF–UF₄, that are interesting alternatives to other salts because they are devoid of Li and Be.

Ternary mixtures such as FLiNaK and FLiNaBe were briefly considered but not found to differ significantly from the corresponding binary mixtures and thus not found to be of particular interest.

The chloride-based mixtures investigated are based on sodium chloride, since it is difficult to find ternary or more complex diagrams in the open literature. Other alkali metal fluorides can be envisaged, such as lithium or potassium chloride, but these are expected to thermalize and

2.4. Fuel Salts and Materials

absorb neutrons, respectively. Addition of magnesium chloride was shown to not influence the melting point substantially (Beneš and Konings, 2008c) so its use was not investigated.

Table 2.1 – Selected fluoride salt compositions and their melting point and calculated density at 900 K.

Salt	An	LiF	NaF	KF	BeF ₂	ThF ₄	UF ₄	PuF ₃	M. P. °C	Density g/cm ³	Ref.
% mol											
FLi	Th	72				28			555	4.59	¹
	U	73					27		490	4.67	¹
	MA	no mixture with low enough melting point (Eutectic at 744 °C)									²
FLiBe	Th	72			16	12			525	3.29	³
	U	72			16		12		500	3.36	³
	MA	71			28.5			0.5	500	1.9	²
FLiNa	Th	32	50			18			525	3.79	¹
	U	15	63				22		485	4.11	¹
	MA	no mixture with low enough melting point (Eutectic at 620 °C)									²
FNaBe	Th		72		18	10			469	3.05	³
	U		72		14		14		463	3.43	³
	MA		71.2		26.1			2.6		2.4	²
FNaK	Th		50	22		28			500?	4.15	⁶
	U		50	22			28		500	4.25	⁴
	MA	no mixture with low enough melting point (Eutectic at 567 °C)									²
FLiNaBe	MA	20.3	57.1		21.2			1.3	502	2.24	⁵
FLiNaK	MA	43.3	14	41.4				1.3	450	2.17	²

¹ Beneš et al. (2010) ² Beneš and Konings (2008b)

³ Capelli et al. (2014) ⁴ Thoma (1959) ⁵ Beneš and Konings (2009)

⁶ No data found, existence assumed based on U-containing composition

2.4.2 Structural Materials

Along with salt mixtures, several materials were used for calculations. They can be divided in two major categories with moderators on the one side and structural materials on the other. The moderators and structural materials and their compositions used in the equilibrium studies chapter are given in Table 2.3 below.

Chapter 2. Molten Salt Reactors

Table 2.2 – Selected chloride salt compositions and their melting point and calculated density at 900 K.

Salt	NaCl	ThCl ₄	UCl ₃	UCl ₄	PuCl ₃	M.P.	Density	Ref.
	% mol					°C	g/cm ³	
NaCl–ThCl ₄	50	50				≈500	3.32	¹
ThCl ₄		100				770	3.82	¹
NaCl–UCl ₃	68		32			520	3.32	²
NaCl–UCl ₃	60		40			590	3.64	²
NaCl–UCl ₃ –UCl ₄	15		15	70		≈500	3.64	³
UCl ₄				100		590	3.56	²
UCl ₃ –UCl ₄			20	80		545	3.79	³
NaCl–PuCl ₃	64				36	454	3.32	²

¹ Desyatnik et al. (1975) ² Beneš and Konings (2008a) ³ Desyatnik et al. (1971)

Moderators

Graphite is a common moderator that has been used in the nuclear industry for many decades and is the reference moderator in MSRs since the MSRP due to its low neutron absorption and chemical compatibility with the salt. It however has the major inconvenient of changing volume under neutron flux, first shrinking and then expanding, with both rates depending on neutron fluence and temperature of irradiation Robertson (1971). Its low lifetime at the neutron flux of the MSBR concept necessitated its replacement every 4 y, which results in substantial technical complications and additional radioactive waste.

Beryllium and Beryllium Oxide have similar neutronic properties and are both efficient moderators due to the extremely low neutron capture cross-section of ⁹Be. Moreover, ⁹Be has a high (n,2n) reaction cross-section which helps the neutron economy of the reactor. It has been used as neutron reflector in many research reactors and Beryllium Oxide was used as a moderator in the Aircraft Reactor Experiment (ARE). It was planned to use metallic Beryllium in the ART before the program was cancelled. Beryllium however has the disadvantage of producing a substantial amount of Tritium and Helium as well as being very toxic. Both are also incompatible with molten salts, as they would slowly dissolve both the metallic and oxide form.

Light and Heavy Water are common moderators that have the advantage of being liquid and thus not suffering from structural damage due to radiation. Moreover, they can be used as coolant as well. Hydrogen in light water is a powerful moderator and small amounts are capable of substantially thermalizing the neutron spectrum of a reactor, while Deuterium in heavy water is less effective at moderating neutrons due to its atomic

weight; a fact compensated for by its low neutron absorption. Both have the disadvantage of being miscible in molten salts and thus a separating material is needed.

Zirconium Hydride is a relatively uncommon moderator that has a high density of hydrogen atoms, making it a potent moderator. It has been used as a moderator in a few reactors such as in the fuel of the TRIGA series of research reactors. Zirconium Hydride has several allotropes due to deviations from stoichiometry of the Hydrogen, with its most stable phase at high temperature being the δ phase (Yamanaka et al., 1999). Zirconium hydride is also incompatible with molten salts and must be clad with another material. Additionally, at the expected temperatures of operation of an MSR an equilibrium partial pressure of Hydrogen close to atmospheric pressure is to be expected, further justifying the need for cladding.

Structural materials

Hastelloy N is the reference structural material for use in MSRs. Also called INOR-8 in the literature, it is a solid solution-strengthened nickel-base superalloy originally developed at ORNL to support MSR development (McCoy, 1969). Its major alloying elements are Molybdenum, Iron and Chromium, with the latter's content specifically tailored to obtain the optimum oxidation resistance in molten fluoride salts and in air. Indeed, Chromium is selectively oxidized and leached from the Nickel matrix by fluoride salts and thus its content must be kept low, while a minimum quantity of Chromium is necessary to impart oxidation resistance in air at high temperature. Its excellent corrosion resistance to clean molten fluoride salt has been demonstrated up to 871 °C and its mechanical strength remains sufficient at temperature at least as high as 704 °C (Olson et al., 2009). A deficiency in Hastelloy N was discovered thanks to its exposure to FPs-containing salts in the MSREs: the attack of and subsequent diffusion to grain boundaries of the alloy by Tellurium. Several solutions have been proposed, such as modifying the alloy composition Ignatiev et al. (2013) or changing the redox potential of the salts to oxidize Tellurium to its fluoride and dissolve it in the salt (Keiser, 1977a) and it is thus likely this problem can be overcome.

Other countries have developed variants of Hastelloy N such as MONICR in Czechia or GH3535 in China. Others have produced outright modifications of the alloy to increase its corrosion resistance such as the Russian alloy HN80MTY (with Titanium and Aluminium) and HN80M-VI (produced by vacuum induction melting). France has seen the development of an other, Nickel-Chromium-Tungsten-base series or alloys whose two main representative are called EM-721 and EM-722 Cury (2007).

Grade 316 Stainless Steel (SS316) is a common austenitic steel alloy alloyed with Molybdenum that has also been considered as a potential structural material for use with molten salts. Despite its large Chromium content it shows acceptable corrosion resistance in a clean salt environment, potentially due to slower diffusion of Chromium in an Iron matrix compared to a Nickel matrix (Zhu et al., 2015). Its tensile properties at high temperature are however less favorable than that of Hastelloy N.

Chapter 2. Molten Salt Reactors

Silicon Carbide (SiC) is a temperature resistant ceramic material with low neutron absorption, high radiation resistance (Snead et al., 2007), and good corrosion resistance properties with molten salts. High strength materials can be made by making compositions with SiC (SiC/SiC) or carbon fibers (C/SiC).

Table 2.3 – Selected moderator materials with their composition and density. Data taken from IAEA (2008) for all except Hastelloy, which instead was taken from (Robertson et al., 1970).

Material	Composition	Density [g/cm ³]
Graphite	C(bal.), B (2 appm)	1.8 (900 °C)
Be	Be (100 a %)	1.82 (900 °C)
BeO	Be (50 %), O (50 %)	2.83 (900 °C)
H ₂ O	H (66.6 %), O (33.3 %)	0.725 (300 °C)
D ₂ O	D (66.6 %), O (33.3 %)	0.725 (300 °C)
ZrH _{1.6}	Zr (bal.), H (2.16 wt%)	5.66 (900 °C)
SS316	Fe (bal.), Mn (2 wt%), Ni, (12 wt%), Mo (2.5 wt%), Cr (17 wt%)	7.8 (900 °C)
Hastelloy N	Ni (bal.), Mo (12 wt%), Cr (7 wt%), Fe (4 wt%)	8.65 (900 °C)
SiC	Si(50 %) C(50 %)	2.6 (900 °C)
Pb	Pb (100 %)	10.5 (300 °C)

Nuclear fuels

Finally, several fuel compositions were used in this thesis and are referred to as High-Enriched Uranium (HEU) (93% enrichment), LEU (20% enriched), Weapons-grade Plutonium (WGPu) (95% ²³⁹Pu), as well as Light Water Reactor Plutonium (LWRPu) and TRansUranic elements (TRU) from LWR SNF at a discharge burn-up of 60 GWd/t. Their isotopic compositions are reported on table 2.4.

Table 2.4 – Isotopic composition of start-up fuels

	²³³ U	HEU	LEU	WG Pu	LWR Pu	TRU
²³³ U	100 %					
²³⁵ U		93 %	20 %			
²³⁸ U		7 %	80 %			
²³⁷ Np						6.9 %
²³⁸ Pu					3.1 %	1.9 %
²³⁹ Pu				95 %	52.5 %	46.5 %
²⁴⁰ Pu				5 %	24.6 %	22.3 %
²⁴¹ Pu					12.2 %	1.2 %
²⁴² Pu					7.7 %	6.8 %
²⁴¹ Am						12.3 %
²⁴³ Am						1.9 %
²⁴⁴ Cm						0.1 %
²⁴⁵ Cm						0.1 %

3 Methods and Tools

In this chapter, the various methods and tools used in this thesis as well as a description of the fuel salts and materials used in the studies presented in the following chapters are described in more details.

3.1 Tools

This section describes the various computational tools that have been used to obtain most of the results presented in this thesis. First of all, the existing MATLAB environment and Serpent Monte-Carlo codes are introduced. Afterwards, the EQL0D fuel cycle procedure developed in the frame of this work is described in more details.

3.1.1 Serpent

Serpent Leppänen et al. (2015) is a continuous-energy Monte Carlo particle transport code developed since 2004 at the VTT Technical Research Centre in Finland. Originally developed as an alternative to the well-known Monte Carlo N-particle transport code (MCNP) focused on reactor physics applications using neutron transport such as spatial homogenization, group constants generation and criticality calculations, it now includes a wide range of capabilities such as photon transport, burn-up calculations, and coupled multi-physics simulations. Many of the output files produced by Serpent are in a MATLAB-compatible format, making the latter a natural solution for interfacing with Serpent.

In this thesis, Serpent was used for criticality calculations, as the source of microscopic cross-sections for burn-up with the EQL0D procedure, and for producing few-groups cross-sections to obtain full-core estimates based on lattice calculations. It was used in conjunction with the ENDF/B-VII.0 nuclear data library. For neutron transport calculations, 50 inactive (for fission source convergence) and 500 active cycles of 5000 neutrons each were used.

3.1.2 MATLAB

MATLAB (Matrix Laboratory) is a proprietary and commercial numerical computing environment using a weakly typed language of the same name developed by MathWorks since 1984. Originally developed to manipulate matrices and compute operations on them, it has grown to be capable of implementing large codes, make user interfaces, plotting data, as well as specialized computations for domains such as statistics, finance, control engineering and image processing.

During the work presented in this thesis, MATLAB was used to create the EQL0D procedure by interfacing the code to Serpent, taking advantage of the fact that Serpent outputs are mostly in a MATLAB-compatible format. Details on the EQL0D procedure for depletion calculations in Molten Salt Reactors is provided later in this chapter.

3.2 Applied Methods

Several computations have been performed in this thesis whose theoretical background must be first presented. This section also serves as a reference when results of such calculations are presented in the following chapters of this thesis.

3.2.1 Core Dimensions Estimation

The Serpent code used all along this thesis can be used to provided homogeneous macroscopic cross-sections in an arbitrary group structure, which can then be used to perform simple calculations using diffusion theory. The default group structure is a two-group structure with a group boundary of 0.65 eV, which is suitable to perform one- (for a fast reactor) or two-group (for a thermal reactor) calculations. This method is notably used to compute the critical core size in the lattice studies presented in the following chapter. Some details of the calculations performed are presented here, and are based on diffusion theory, itself derived from the time-independent one-group neutron diffusion equation in a homogeneous medium:

$$-D\nabla^2\phi + \Sigma_a\phi = \frac{\bar{\nu}\Sigma_f}{k_{\text{eff}}}\phi \quad (3.1)$$

In which ϕ is the neutron flux, D the diffusion coefficient, Σ_a and Σ_f the neutron absorption and fission cross-sections, $\bar{\nu}$ the average number of neutrons per fission, and k_{eff} the criticality eigenvalue. The left-hand side of the equation pertains to neutrons lost to leakage or absorption, and the right-hand side to neutrons generated by fission.

One-group critical bare core size

The equation can be simplified using the definition of the infinite multiplication factor k_∞ :

$$k_\infty = \frac{\bar{v}\Sigma_f}{\Sigma_a}$$

and of the neutron diffusion length \mathcal{L} :

$$\mathcal{L}^2 = \frac{D}{\Sigma_a}$$

into the following equation:

$$-\mathcal{L}^2 \nabla^2 \phi = \left(\frac{k_\infty}{k_{\text{eff}}} - 1 \right) \phi$$

One can subsequently define the geometrical B_g and material bucklings B_m :

$$B_g^2 = -\frac{\nabla^2 \phi}{\phi} \quad B_m^2 = \frac{1}{\mathcal{L}^2} \left(\frac{k_\infty}{k_{\text{eff}}} - 1 \right)$$

The geometrical buckling is dependent on the flux shape and thus the geometry, while the material buckling only depends on material properties. If they are made equal, the reactor will be critical, i.e. $k_{\text{eff}} = 1$.

In the case of a cylindrical core, there are two degrees of freedom: axial (height) and radial (radius). Assuming separation of variables, the geometrical buckling of a cylinder is:

$$B_g^2 = -\frac{\nabla^2 \phi}{\phi} = \left(\frac{\pi}{H} \right)^2 + \left(\frac{j_0}{R} \right)^2 \quad j_0 \approx 2.405 \dots$$

In which j_0 is the first zero of the Bessel function of the first kind of order zero, and H and R the extrapolated height and radius of the core, respectively.

There exists an optimum height-to-radius ratio that results in a minimum core volume for a given buckling. It can be derived by fixing the previous equation and replacing one of the two variables in the definition of the volume of the cylinder $V = \pi H R^2$ in which we can use the buckling definition to replace for H and then compute V :

$$H = \frac{\pi}{\sqrt{B_m^2 R^2 - j_0^2}} \Rightarrow V = \frac{\pi^2 R^3}{\sqrt{B_m^2 R^2 - j_0^2}}$$

The minimum of which can be found using:

$$\frac{\partial V}{\partial R} = \frac{3\pi^2 R^2 \sqrt{B_m^2 R^2 - j_0^2} - \frac{\pi^4 R^4}{\sqrt{B_m^2 R^2 - j_0^2}}}{B_m^2 R^2 - j_0^2} = 0 \Rightarrow B_m^2 = \frac{3j_0^2}{2R^2}$$

Chapter 3. Methods and Tools

Using this buckling into the equation for the height, one gets:

$$H = \frac{\sqrt{2}\pi}{j_0} R \approx 1.8475 \dots R = \alpha R$$

Which gives the optimum height-to-radius ratio α for a critical reactor of minimum volume per diffusion theory.

For a bare (unreflected) homogeneous fast reactor, a single group calculation is sufficient to get a good approximation of the critical core size. Assuming the previously derived result of a cylinder of optimal height-to-radius ratio, the critical dimensions can be obtained by equalizing the geometrical and material bucklings:

$$\frac{3}{2} \frac{j_0^2}{R^2} = \frac{k_\infty - 1}{L^2} \Rightarrow R = \sqrt{\frac{3}{2} \frac{j_0^2 L^2}{k_\infty - 1}}$$

This is obviously the extrapolated core radius, from which the real radius can be obtained using the transport correction:

$$R_{\text{true}} = R_{\text{ext}} - \frac{0.71}{\Sigma_{\text{tr}}}$$

Two-group critical bare core size

In the case of a bare thermal reactor the use of two groups is warranted. The neutron balance in diffusion theory takes the form of two equations instead of one:

$$-D_f \nabla^2 \phi_f + \Sigma_{a,f} \phi_f + \Sigma_{s,f \rightarrow \text{th}} \phi_f = \bar{v}_{\text{th}} \Sigma_{f,\text{th}} \phi_{\text{th}} + \bar{v}_f \Sigma_{f,f} \phi_f \quad (3.2)$$

$$-D_{\text{th}} \nabla^2 \phi_{\text{th}} + \Sigma_{a,\text{th}} \phi_{\text{th}} = \Sigma_{s,f \rightarrow \text{th}} \phi_f \quad (3.3)$$

In equation (3.2), D_f and D_{th} are the fast and thermal diffusion coefficients, ϕ_f and ϕ_{th} the fast and thermal fluxes, refer to the thermal and fast groups, respectively. Note that (n,xn) reactions were neglected in the above-mentioned equations. In a similar fashion as the one-group case, group-wise neutron diffusion lengths \mathcal{L}_{th} and \mathcal{L}_f can be defined:

$$\mathcal{L}_f^2 = \frac{D_f}{\Sigma_{a,f} + \Sigma_{s,f \rightarrow \text{th}}} = \frac{D_f}{\Sigma_{\text{rem},f}} \quad \mathcal{L}_{\text{th}}^2 = \frac{D_{\text{th}}}{\Sigma_{a,\text{th}}}$$

Using the definition of the buckling the first equation of (3.2) can be rewritten as follows:

$$(1 + \mathcal{L}_f^2 B^2) \phi_f = \frac{\bar{v}_{\text{th}} \Sigma_{f,\text{th}} \phi_{\text{th}}}{\Sigma_{\text{rem},f}} \left(1 + \frac{\bar{v}_f \Sigma_{f,f} \phi_f}{\bar{v}_{\text{th}} \Sigma_{f,\text{th}} \phi_{\text{th}}} \right) = \frac{\bar{v}_{\text{th}} \Sigma_{f,\text{th}} \phi_{\text{th}}}{\Sigma_{\text{rem},f}} e$$

with ϵ the fast fission factor of the four-factor formula. The second equation can be rewritten as:

$$(1 + \mathcal{L}_{th}^2 B^2) \phi_{th} = \frac{\Sigma_{s,f \rightarrow th}}{\Sigma_{a,th}} \phi_f = \frac{\Sigma_{s,f \rightarrow th}}{\Sigma_{rem,f}} \frac{\Sigma_{rem,f}}{\Sigma_{a,th}} \phi_f = p \frac{\Sigma_{rem,f}}{\Sigma_{a,th}} \phi_f$$

with p the resonance escape probability. Multiplying both equations finally yields:

$$(1 + \mathcal{L}_f^2 B^2) (1 + \mathcal{L}_{th}^2 B^2) = \frac{\bar{v}_{th} \Sigma_{f,th}}{\Sigma_{a,th}} \epsilon p = k_{\infty}$$

which is the criticality condition for a two-group calculation of a bare critical reactor.

3.2.2 Equilibrium reactivity break-down

Using the concept of equilibrium fuel cycle explained in the next section, one can compute the equilibrium reactivity of a given configuration. This reactivity can be broken down into components by a simple derivation, which is provided here. The reactivity is first derived using its definition:

$$\rho = \frac{k_{eff} - 1}{k_{eff}} \quad (3.4)$$

Knowing that the multiplication factor is the ratio of neutron production to neutron destruction:

$$k_{eff} = \frac{P}{D} = \frac{\bar{v}F + 2N_2 + 3N_3 + 4N_4}{L + C + F + N_2 + N_3 + N_4} \approx \frac{\bar{v}F + 2N_2}{L + C + F + N_2} \quad (3.5)$$

Where \bar{v} is the average number of neutrons per fissions, F the fission rate, C the capture rate (sum of all (n,0n) reactions), L the neutron leakage rate, and N_x the rate of the corresponding (n,xn) reaction. (n,3n) and (n,4n) reaction can be assumed to contribute very little to the neutron balance in most systems, and therefore ignored. Using the definition (3.5) in (3.4), one gets:

$$\rho = \frac{k_{eff} - 1}{k_{eff}} = \frac{(\bar{v} - 1)F + N_2 - C - L}{\bar{v}F + 2N_2} \quad (3.6)$$

In a closed fuel cycle, at equilibrium, all actinides are born from reactions on the main feed nuclide (fertile in the case of an isobreeding equilibrium):

$$F = F^{fert} + C^{fert} + N_2^{fert} \quad (3.7)$$

Additionally, the fertile nuclides should dominate the composition and thus largely be nearly the only source of (n,2n) reactions, thus:

$$N_2 \approx N_2^{fert}$$

Finally, the total capture rate can be split between the fertile contribution and the other nuclides:

$$C = C^{\text{fert}} + C^{\text{others}}$$

Combining (3.7) with (3.6), we finally obtain:

$$\rho = \underbrace{\frac{(\bar{v} - 2)F}{\bar{v}F + 2N_2^{\text{fert}}}}_{\text{Base reactivity}} + \underbrace{\frac{2N_2^{\text{fert}} + F^{\text{fert}}}{\bar{v}F + 2N_2^{\text{fert}}}}_{\text{Fertile bonus}} - \underbrace{\frac{C^{\text{others}}}{\bar{v}F + 2N_2^{\text{fert}}}}_{\text{Capture losses}} - \underbrace{\frac{L}{\bar{v}F + 2N_2^{\text{fert}}}}_{\text{Leakage losses}}$$

In the above-mentioned equation, the first term is only due to the fertile nuclide chosen and represents the maximum reactivity that would be achievable in a closed fuel cycle if other nuclides had zero absorption cross-sections. The two additional terms are for parasitic captures on other nuclides (fission products, structures, higher actinides) and leakage, respectively. They diminish the achievable reactivity, hence the minus signs. Using this equation, the reactivity at equilibrium can be broken down into single components and compared between configuration with for example changing spectra.

3.2.3 Density of salt mixtures estimation

While an extensive body of literature exists on some specific mixtures, many of the salt mixtures investigated in this thesis have not been thoroughly studied. Correlations based on measurements to obtain even the most basic properties are therefore non-existent and these must be obtained in another way for prospective calculations. The simplest way is to use the so-called law of additive molar volumes (Grimes, 1966), which assumes ideal solution behavior in the salt. This assumption is only true for some mixtures in given proportions and substantial deviations can appear in other cases. However, in most cases, it results in errors that are less than 5% (Williams et al., 2006). It is described by the simple equation below:

$$d(T) = \frac{\sum_i x_i m_i}{\sum_i x_i V_i(T)} \quad (3.8)$$

In which d is the density of the mixture, x_i the molar fraction of component i , m_i the molar mass of the component, and V_i its molar volume. Only the latter depends on temperature, and is therefore to be tabulated for single components; computing the density at different temperatures allows one to get a correlation for density as function of the temperature.

3.2.4 Nuclides removal

A distinct characteristic of MSRs is that of the volatility and insolubility of some of the FPs, which therefore leave the salt mixture. This process must therefore be taken into account in

the modelling. In this section, the behavior of FPs in MSRs is first detailed, based on data taken from the literature for fluoride salts. Without more complete information, the behavior of FPs in chloride salts was assumed to be the same, although there is evidence that some FPs such as zirconium could be more volatile in a chloride mixture. Subsequently, the modeling of FP removal is detailed.

Fission Product Behavior

<div>+1</div> <div>H</div>		Insoluble										<div>0</div> <div>He</div>					
<div>+1</div> <div>Li</div>	<div>+2</div> <div>Be</div>	Soluble										<div>0</div> <div>B</div>	<div>0</div> <div>C</div>	<div>0</div> <div>N</div>	<div>0</div> <div>O</div>	<div>-1</div> <div>F</div>	<div>0</div> <div>Ne</div>
<div>+1</div> <div>Na</div>	<div>+2</div> <div>Mg</div>	Sometimes soluble										<div>0</div> <div>Al</div>	<div>0</div> <div>Si</div>	<div>0</div> <div>P</div>	<div>0</div> <div>S</div>	<div>-1</div> <div>Cl</div>	<div>0</div> <div>Ar</div>
<div>+1</div> <div>K</div>	<div>+2</div> <div>Ca</div>	<div>0</div> <div>Sc</div>	<div>0</div> <div>Ti</div>	<div>0</div> <div>V</div>	<div>0</div> <div>Cr</div>	<div>0</div> <div>Mn</div>	<div>0</div> <div>Fe</div>	<div>0</div> <div>Co</div>	<div>0</div> <div>Ni</div>	<div>0</div> <div>Cu</div>	<div>0</div> <div>Zn</div>	<div>0</div> <div>Ga</div>	<div>0</div> <div>Ge</div>	<div>0</div> <div>As</div>	<div>0</div> <div>Se</div>	<div>-1</div> <div>Br</div>	<div>0</div> <div>Kr</div>
<div>+1</div> <div>Rb</div>	<div>+2</div> <div>Sr</div>	<div>+3</div> <div>Y</div>	<div>+4</div> <div>Zr</div>	<div>0</div> <div>Nb</div>	<div>0</div> <div>Mo</div>	<div>0</div> <div>Tc</div>	<div>0</div> <div>Ru</div>	<div>0</div> <div>Rh</div>	<div>0</div> <div>Pd</div>	<div>0</div> <div>Ag</div>	<div>0</div> <div>Cd</div>	<div>0</div> <div>In</div>	<div>0</div> <div>Sn</div>	<div>0</div> <div>Sb</div>	<div>0</div> <div>Te</div>	<div>-1</div> <div>I</div>	<div>0</div> <div>Xe</div>
<div>+1</div> <div>Cs</div>	<div>+2</div> <div>Ba</div>	<div>0</div> <div>Hf</div>	<div>0</div> <div>Ta</div>	<div>0</div> <div>W</div>	<div>0</div> <div>Re</div>	<div>0</div> <div>Os</div>	<div>0</div> <div>Ir</div>	<div>0</div> <div>Pt</div>	<div>0</div> <div>Au</div>	<div>0</div> <div>Hg</div>	<div>0</div> <div>Tl</div>	<div>0</div> <div>Pb</div>	<div>0</div> <div>Bi</div>	<div>0</div> <div>Po</div>	<div>0</div> <div>At</div>	<div>0</div> <div>Rn</div>	
<div>0</div> <div>Fr</div>	<div>0</div> <div>Ra</div>																
		<div>+3</div> <div>La</div>	<div>+3</div> <div>Ce</div>	<div>+3</div> <div>Pr</div>	<div>+3</div> <div>Nd</div>	<div>+3</div> <div>Pm</div>	<div>+3</div> <div>Sm</div>	<div>+3</div> <div>Eu</div>	<div>+3</div> <div>Gd</div>	<div>+3</div> <div>Tb</div>	<div>+3</div> <div>Dy</div>	<div>+3</div> <div>Ho</div>	<div>+3</div> <div>Er</div>	<div>+3</div> <div>Tm</div>	<div>+3</div> <div>Yb</div>	<div>+3</div> <div>Lu</div>	
		<div>0</div> <div>Ac</div>	<div>+4</div> <div>Th</div>	<div>+4</div> <div>Pa</div>	<div>+4</div> <div>U</div>	<div>+3</div> <div>Np</div>	<div>+3</div> <div>Pu</div>	<div>+3</div> <div>Am</div>	<div>+3</div> <div>Cm</div>	<div>0</div> <div>Bk</div>	<div>0</div> <div>Cf</div>	<div>0</div> <div>Es</div>	<div>0</div> <div>Fm</div>	<div>0</div> <div>Md</div>	<div>0</div> <div>No</div>	<div>0</div> <div>Lr</div>	

Figure 3.1 – Classification of relevant elements, including fission products in bold, with expected valence states and solubility.

The behavior of FPs in molten salt fuels is a complex issue due to the numerous variables it depends on: salt composition, temperature, redox potential, possible valence states, solubility limits, etc. Fortunately, these parameters are in a sufficiently narrow window in most designs so that strong differences are only encountered for a limited number of nuclides. Whether a given removal method can be used depends on the properties of the elements, but general rules can be drawn:

- Elements with low solubility will tend to diffuse toward a free surface and can be removed by methods such as He bubbling,
- Elements in a metallic state can be removed by plating on a surface such as graphite or structural metals,
- Elements with higher valence states forming stable fluorides and heavier halogens can be removed by fluorination,
- Elements with lower vapor pressure than salt components can be removed by distillation,

Chapter 3. Methods and Tools

- Most elements can be removed by reductive extraction,
- Leftover elements can always be removed by discarding the entire salt.

Other possible reprocessing methods include electrowinning and oxide precipitation, but these are not part of the reference processing schemes of the reactor concepts investigated in this paper. figure 3.1 features a classification of the main nuclides encountered in a liquid-fuel MSR and of their general behavior, as well as the methods that can be used to remove them from the salt.

Nuclides removal modeling

The removal of fission products is most often modeled with first-order removal and the concept of cycle times. It can be performed in two manners:

1. continuously, that is, simultaneously with fuel depletion, by introducing an additional proportional removal term in the Bateman equations, and
2. batch-wise, that is, at a single point in time.

Proportional removal of nuclides follows a law similar to radioactive decay. It can be used to model removal by the off-gas system using a removal constant λ_g generally shared by all concerned nuclides:

$$\frac{dn_i}{dt} = Q_i - \lambda_g n_i \quad (3.9)$$

in which Q_i is the net production rate for isotope i . A more practical quantity to characterize the removal rate is the cycle time $T_{cyc} = \frac{1}{\lambda}$. In the case of continuous processing the inventory cycle time is defined as the time needed to process the whole inventory V_{tot} at a rate \dot{v} :

$$\dot{v} T_{cyc} = V_{tot} \Rightarrow T_{cyc} = \frac{V_{tot}}{\dot{v}}$$

Continuous processing of soluble fission products follows a similar law, but nuclides are usually separated with a nuclide-specific efficiency ϵ_i :

$$\frac{dn_i}{dt} = -\lambda_{eff,i} n_i = -\epsilon_i \lambda_{proc} n_i$$

The λ removal rates can be inverted to obtain the cycle times, which in the case of processing are function of the volumetric processing rate \dot{v} and the total volume of salt V_{tot} :

$$\lambda_{eff,i} = \frac{1}{T_{eff,i}} = \epsilon_i \lambda_{proc} = \frac{\epsilon_i}{T_{proc}} = \epsilon_i \frac{\dot{v}}{V_{tot}}$$

Therefore a global balance has the following form:

$$\frac{dn_i}{dt} = -\overbrace{\frac{\dot{v}}{V_{\text{tot}}} n_i}^{\text{processed}} + \overbrace{(1 - \epsilon_i) \frac{\dot{v}}{V_{\text{tot}}} n_i}^{\text{returning}} = -\epsilon_i \frac{\dot{v}}{V_{\text{tot}}} n_i \quad (3.10)$$

Equation (3.9) thus indicated that the off-gas system removal is a particular case of the continuous processing with $\epsilon_i = 1$. In the case of batch-wise processing, the new number density $n_{i,1}$ is a fraction of the previous atomic density $n_{i,0}$, if the processing step is carried out after a time Δt :

$$n_{i,1} = \left(1 - \epsilon_i \frac{\dot{v}}{V_{\text{tot}}} \Delta t\right) n_{i,0} \quad (3.11)$$

The similar nature of continuous and batch-wise equations can be highlighted by computing the change in atomic densities in the batch-wise case:

$$\Delta n_i = n_{i,1} - n_{i,0} = -\epsilon_i \frac{\dot{v} \Delta t}{V_{\text{tot}}} n_{i,0} \quad (3.12)$$

Taking the limit $\Delta t \rightarrow 0$ of equation (3.12) yields equation (3.10).

3.2.5 Burn-up in Molten Salt Reactors

Burn-up is a common measure of fuel depletion used in fuel cycle studies and originates from solid-fueled reactor practice. It is often measured in terms of energy generated per unit mass of fuel (for example GWd/t) or in fissions per initial metal atom (%FIMA). This later definition is very close to that of FP mass created per initial actinide mass because the masses of actinides are similar and the mass of fission products created by fission is essentially the same as that of the actinide from which they were created.

Unlike in solid-fuel reactors however, fuel in MSRs is constantly mixed and therefore the burn-up history of different volumes of fuel is lost. Moreover, removal of fission products, be it naturally or artificially, not only biases the fission product distribution inside the fuel but also decreases the mass of FPs in the core, making the mass ratio of fission products in the core to the initial actinide mass invalid. Due to these two effects it is difficult to define a measurement of fuel depletion in an MSR in an unequivocal manner.

On the other hand, for most aspects related to neutronics aspects of the fuel cycle, the simplest metric is the mass of fission products inside the core per unit initial mass of actinides. While a precise but general definition is difficult to obtain, one can neglect the volatile fission products as a first approximation. In this case, the soluble FP fraction is proportional to the power density p , the removal cycle time T_{rem} and inversely proportional to the actinide density of

the fuel d_{HM} :

$$\text{Soluble FP fraction} \propto \frac{pT_{\text{rem}}}{d_{\text{HM}}} \quad (3.13)$$

3.2.6 Model of Breed-and-Burn in Molten Salt Reactors

As explained later in this thesis, MSRs can be operated in a Breed-and-Burn (B&B) cycle; that is, an open fuel cycle in which the reactor breeds its own fuel from a poorly fissile feed—without separation of actinides from the discharged fuel. To evaluate the ability of MSRs to operate in such a fuel cycle, a quick evaluation method was derived. A key difference between B&B in solid and liquid fuel reactors is that in liquid fuel reactors, fuels of different ages or burn-ups are constantly mixed together, whereas they remain separate in solid fuel reactors. This implies that cycle-average values are to be obtained in a different manner than a simple average. To this end, one must derive the burn-up distribution of both cases to understand the difference. Quantities of interest in the evaluation of the performance of candidate fuels or geometries for use in B&B reactors include the minimum and maximum burn-ups achievable, as well as the resulting multiplication factors.

The neutron excess method (Petroski et al., 2011; Heidet and Greenspan, 2012) uses a simple neutron balance for a unit element of fuel to compute the net number of neutrons produced as function of time or burn-up, based on the net number of neutrons produced after a given time in flux, which in the zero-dimensional case is given by:

$$P(t) = \int_0^t \bar{\nu}F(\theta) - A(\theta) d\theta = \int_0^t [\bar{\nu}\Sigma_f(\theta) - \Sigma_a(\theta)] \phi(\theta) d\theta \quad (3.14)$$

in which P is the net number of neutrons produced, $\bar{\nu}$ the average number of neutrons per fission, F and A the fission and absorption rates, and Σ_f and Σ_a the fission and absorption macroscopic cross-sections, and ϕ the neutron flux. The evolution of rates and cross-sections as function of time can be obtained by depleting a unit cell of the configuration of interest.

While this description is adequate to model a fuel element of a solid-fueled reactor, in an externally-cooled MSR the fuel is constantly mixed. At discharge, the fuel will be a mixture of elements that have spent different amounts of time in the core and therefore have been exposed to different fluences, unlike the fuel of a solid-fuel reactor which will have spent exactly the same amount of time in the core.

This difference can be modeled using the concept of Residence Time Distribution (RTD) of ideal reactors (Danckwerts, 1953). One can define an exit age distribution $E(t)$ describing the age (time spent in the reactor) of fuel taken from it and an internal age distribution $I(t)$ describing the age of the contents of the reactor. In the case of a so-called Plug Flow Reactor in

which the contents do not mix and spend the same amount of time in the reactor, these are:

$$E_{\text{SF}}(t) = \delta(t - \tau_{\text{dis}}) \quad I_{\text{SF}}(t) = \frac{1}{\tau_{\text{dis}}} [1 - H(t - \tau_{\text{dis}})] \quad (3.15)$$

in which δ is the Dirac delta function and H the Heaviside step function. This RTD models that of a single-batch solid-fuel (SF) reactor whose fuel is entirely discharged at a time τ_{dis} .

In the case of a MSR whose fuel is constantly discharged and replenished, the distribution is that of a so-called Continuously-Stirred Tank Reactor in which the liquid fuel (LF) is continuously mixed and discharged at a rate \dot{v} from a total fuel volume V :

$$E_{\text{LF}}(t) = \frac{\dot{v}}{V} \exp\left(-\frac{\dot{v}}{V} t\right) = \frac{1}{\tau} \exp\left(-\frac{1}{\tau} t\right) \quad I_{\text{LF}}(t) = E_{\text{LF}}(t) \quad (3.16)$$

in which the discharge cycle time $\tau = \frac{V}{\dot{v}}$ was defined, which is the time needed to discharge the whole fuel volume, and also the average residence time of a fuel element in the core, as will be shown later. It must be noted that the exit and internal distributions are equal since the contents of the reactor are supposed to be instantly and continuously mixed, therefore they have the same distribution. For comparison, the distributions are illustrated on fig. 3.2 below.

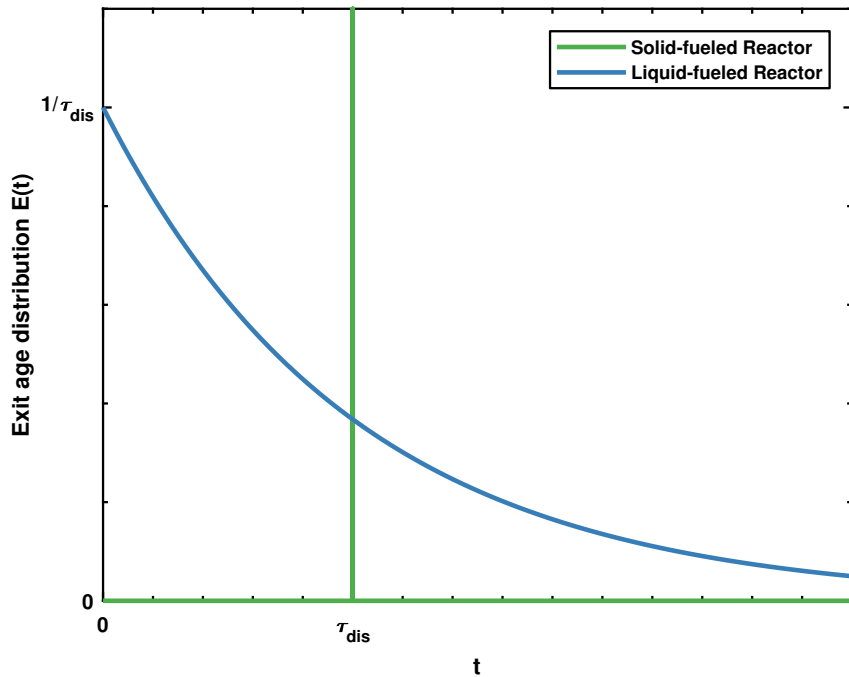


Figure 3.2 – Exit residence time distributions for solid- and liquid-fueled reactors of equal discharge and cycle times $\tau_{\text{dis}} = \tau_{\text{cycle}}$ as function of time.

The RTDs can be used to derive average values pertaining to the reactor. For example, the

Chapter 3. Methods and Tools

average age of fuel at discharge \bar{T}_{dis} and in the reactor \bar{T}_{in} is given by:

$$\bar{T}_{\text{dis}} = \int_0^\infty t E(t) dt \quad \bar{T}_{\text{in}} = \int_0^\infty t I(t) dt \quad (3.17)$$

Using equation (3.15) into (3.17) yields, for a solid-fueled reactor:

$$\begin{aligned} \bar{T}_{\text{dis,SF}} &= \int_0^\infty t \delta(t - \tau_{\text{dis}}) dt = \tau_{\text{dis}} \\ \bar{T}_{\text{in,SF}} &= \int_0^\infty t \frac{1 - H(t - \tau_{\text{dis}})}{\tau_{\text{dis}}} dt = \frac{\tau_{\text{dis}}}{2} \end{aligned}$$

While using (3.16) in (3.17) for a liquid-fuel reactor, one gets:

$$\bar{T}_{\text{dis,LF}} = \int_0^\infty t \frac{1}{\tau} \exp\left(-\frac{1}{\tau} t\right) dt = \tau \quad \bar{T}_{\text{in,LF}} = \bar{T}_{\text{dis,LF}} = \tau$$

In both cases the results are quite trivial: in a solid-fuel reactor the average age at discharge is the discharge time and the average age of fuel in the core is half of that, while in the case of solid fuel the average ages are equal to the average residence time.

Nevertheless RTDs can be used to obtain the net neutron excess at discharge of the fuel as function of the discharge time τ :

$$P(\tau) = \int_0^\infty dt E(t, \tau) \int_0^t d\theta P(\theta) \quad (3.18)$$

Computing (3.18) using (3.14) and (3.15) yield a trivial result:

$$P_{\text{SF}}(\tau) = \int_0^\infty dt \delta(t - \tau) \int_0^t d\theta P(\theta) = \int_0^\tau d\theta P(\theta) = P(\tau) \quad (3.19)$$

Equation (3.19) yields the trivial result that for a solid-fuel reactor the net number of neutrons produced at discharge of the fuel is given by $P(\tau)$. However, in the case of a liquid-fueled reactor, one gets:

$$P_{\text{LF}}(\tau) = \int_0^\infty dt \frac{1}{\tau} \exp\left(-\frac{1}{\tau} t\right) \int_0^t d\theta P(\theta)$$

The same process can be repeated for the number of neutrons absorbed A :

$$A(\tau) = \int_0^\infty dt E(t) \int_0^t d\theta A(\theta)$$

The equilibrium k_∞ can then be approximated by the ratio of neutrons produced to the neutrons absorbed:

$$k_\infty^{\text{eq}}(\tau) = \frac{P(\tau) + A(\tau)}{A(\tau)} = 1 + \frac{P(\tau)}{A(\tau)} \quad (3.20)$$

The differences between solid and liquid-fuel distributions can be further illustrated by comparing their neutron excess and k_{∞} distributions, as is done on figure 3.3 using a NaCl–UCl₃ salt. The minimum and maximum burn-ups are given by

$$P(B_{\min}) = P(B_{\max}) = 0$$

and are also visibly those point at which

$$k_{\infty}(B_{\min}) = k_{\infty}(B_{\max}) = 1$$

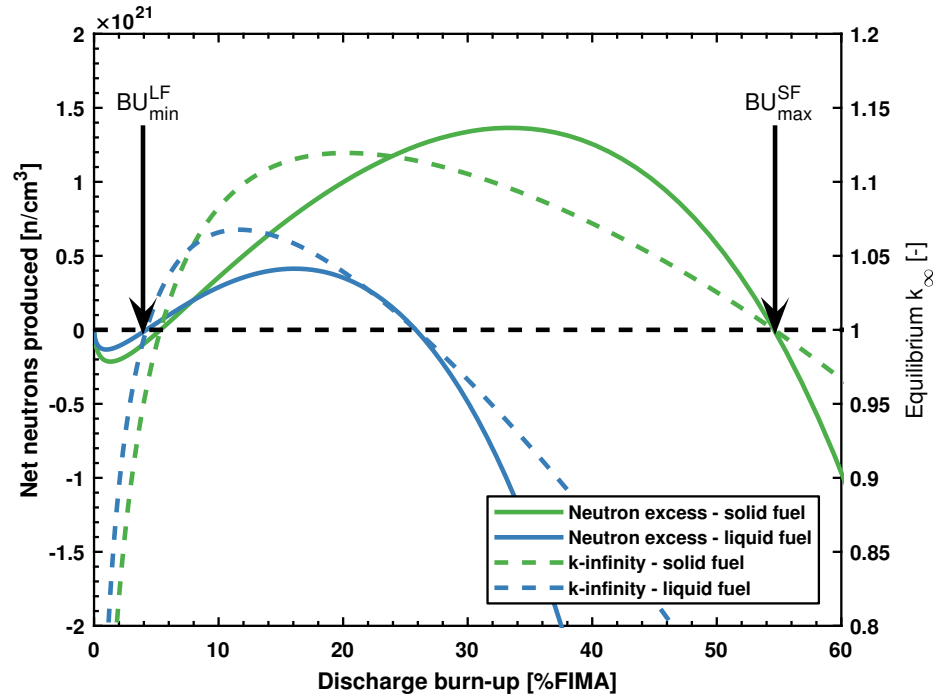


Figure 3.3 – Comparison of the neutron excess and equilibrium k_{∞} using solid-fuel-like and liquid-fuel-like distributions.

It can be noticed that in the case of the liquid-fuel distribution, the minimum discharge burn-up is slightly lower than that of the solid-fuel one, due to the fact that in a liquid-fuel core the oldest fuel (containing more fissile isotopes) is always present. On the other hand the maximum burn-up achieved in the solid-fuel case is substantially higher due to the fact that in a liquid-fuel core the oldest fuel is also partially removed before being burnt.

To validate the method, several test salts whose characteristics are detailed in Table 2.2 were computed using this model and discrete equilibrium points were calculated using the EQL0D procedure. The comparison of the results obtained by these two methods can be made using 3.4. The agreement is arguably satisfactory for scoping studies, although it should be noticed that the method seems to slightly underestimate the k_{∞} at equilibrium for Th-containing salts.

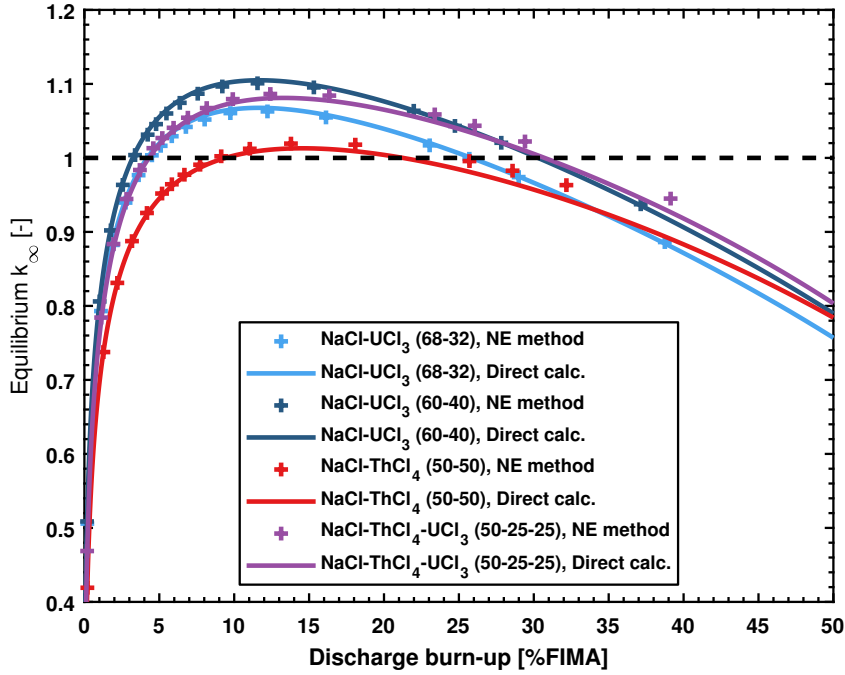


Figure 3.4 – Evaluation of the k_{∞} at equilibrium using direct calculation (crosses) and the neutron excess method (lines).

3.3 The EQL0D Procedure

The EQL0D procedure was inspired by the ERANOS-based equilibrium cycle procedure EQL3D that was developed at the Paul Scherrer Institute. Unlike EQL3D, which is a node-wise ERANOS-based depletion code meant for solid-fueled fast reactors, EQL0D is a point-depletion code to approximate mixing of circulating fuel. Three different versions of the code have been written, reflecting the evolution of simulation needs:

1. EQL0D-v1: ERANOS-based at a cell level, limited to some actinides and reaction channels,
2. EQL0D-v2: Serpent 2-based at a cell level, also limited to some actinides and reaction channels, and
3. EQL0D-v3: Serpent 2-based, with full nuclide modeling capabilities, and the subject of the present paper.

EQL0D-v3 is written using the MATLAB environment and the Serpent 2 Monte Carlo neutron transport code to generate microscopic reaction rates for depletion. The use of Serpent allows to model complex geometries which can appear in MSR designs. Additionally, Serpent can directly output burn-up matrices as well as other parameters of interest in a MATLAB format, simplifying the interaction of the procedure with Serpent. EQL0D was designed to handle two different types of depletion calculations:

1. fuel evolution over a finite number of steps like a standard depletion code, or
2. searching for equilibrium directly.

However, the procedure does not account for delayed neutrons precursors (DNP) drift that would slightly alter the neutron spectrum of the reactor, nor does it explicitly account for fuel circulation into areas of low or zero neutron flux which would alter fuel evolution to some extent.

In the following subsections, the main equations of the EQL0D procedure are first described. Afterwards, the computational scheme of EQL0D is outlined and further miscellaneous functions are introduced.

3.3.1 Bateman equations

The evolution of the concentration of nuclides in a nuclear fuel can be computed using the so-called Bateman equations (Bateman, 1910) that describe the change in concentration as a function of time for a given nuclide:

$$\frac{dn_i}{dt} = \underbrace{-\overline{\sigma_i \phi} n_i + \sum_{j \rightarrow i} \gamma_i \overline{\sigma_j \phi} n_j}_{\text{flux-induced reactions}} - \underbrace{\lambda_i n_i + \sum_{j \rightarrow i} \gamma_i \lambda_j n_j}_{\text{decay}},$$

in which n_i refers to the atomic density of nuclide i , $\overline{\sigma_i \phi}$ to the microscopic capture reaction rate on nuclide i , λ_i the decay constant for nuclide i , γ_i the fraction of all the reactions on nuclide j giving nuclide i (branching ratio or fission yield). In reality the microscopic capture reaction rate is time-dependent, but in practice it is assumed to be constant over the length of one or several time steps.

This equation can be written in a matrix form defining the burn-up matrix \mathbf{B} containing flux-dependent terms and the decay matrix \mathbf{D} :

$$\frac{d\vec{n}}{dt} = (\mathbf{B} + \mathbf{D}) \vec{n} \quad (3.21)$$

This equation is solved by taking the exponential for sum of the matrices:

$$\vec{n}(t + \Delta t) = \exp(\Delta t (\mathbf{B} + \mathbf{D})) \vec{n}$$

In liquid fuel reactors, fission, activation, corrosion and decay products are removed, either naturally or by Helium bubbling or by fuel processing. Moreover, removed products need to be replaced by adequate elements such as actinides or carrier salt elements. These removal or addition operations can be carried out in a continuous or batch-wise manner, and be classified into four basic processing operations:

Chapter 3. Methods and Tools

- Continuous removal of volatile and insoluble nuclides
- Continuous processing of soluble nuclides
- Batch-wise processing of soluble nuclides
- Continuous or batch-wise addition operations, which will be treated separately.

In the following paragraphs, each one will be explicated with the exception of nuclide addition operations which are discussed later on.

Continuous removal of volatile fission products can be simulated by adding the previously discussed proportional removal term of equation (3.10) to the Bateman equations. Thus, a matrix Λ for the removal of volatile and gaseous fission products by the off-gas system can be added to (3.21):

$$\frac{d\vec{n}}{dt} = (\mathbf{B} + \mathbf{D} - \Lambda) \vec{n}, \quad (3.22)$$

This matrix can be explicitly written element-by-element using the Kronecker delta δ_{ij} :

$$\Lambda_{ij} = \begin{cases} \delta_{ij} \lambda_g & \text{if } i \in \{\text{removed by off-gas}\} \\ 0 & \text{otherwise} \end{cases}$$

Continuous removal of soluble elements by the pyro-processing plant can be modeled in a similar manner to (3.22) by adding a continuous processing matrix \mathbf{P} :

$$\frac{d\vec{n}}{dt} = (\mathbf{B} + \mathbf{D} - \Lambda - \mathbf{P}) \vec{n}$$

which is explicitly written:

$$P_{ij} = \begin{cases} \delta_{ij} \epsilon_i \lambda_p & \text{if } i \in \{\text{processed}\} \\ 0 & \text{otherwise} \end{cases}$$

Batch-wise removal of soluble elements can be performed using a matrix form of equation (3.12). The new composition vector \vec{n}_1 is given by:

$$\vec{n}_1 = (\mathbf{I} - \Delta t \mathbf{P}) \vec{n}_0$$

provided that the time step Δt is smaller than the cycle time of the removal process.

3.3.2 Coupled Bateman equations

If the system consists only of a single material, removed nuclides cannot be accounted for afterwards. In some cases, removed nuclides must be tracked, such as when estimating the total radioactive inventory of the reactor and processing plant complex, estimating noble

metal deposition on surfaces, isolating Pa to let it decay outside of the flux, etc. This can be achieved by using a secondary material and coupling their respective Bateman equations.

This can be illustrated by applying it to a complex system as that of Two-fluid Molten Salt Breeder Reactor (MSBR(2f)), containing the fuel (f), the blanket (b), the Pa decay and feed storage (s), the off-gas system (g) and the pyroprocessing plant (p), which in matrix form gives:

$$\frac{d}{dt} \begin{bmatrix} \vec{n}^f \\ \vec{n}^b \\ \vec{n}^s \\ \vec{n}^g \\ \vec{n}^p \end{bmatrix} = \begin{bmatrix} \mathbf{T}^f & 0 & 0 & 0 & 0 \\ 0 & \mathbf{T}^b & 0 & 0 & 0 \\ -\frac{V^f}{V^s} \mathbf{A}^f & -\frac{V^b}{V^s} \mathbf{A}^b + \frac{V^b}{V^s} \mathbf{R}_{Pa} & \mathbf{D} & 0 & 0 \\ \frac{V^f}{V^g} \Lambda & \frac{V^b}{V^g} \Lambda & 0 & \mathbf{D} & 0 \\ \frac{V^f}{V^p} \mathbf{P} & \frac{V^b}{V^p} \mathbf{P} & 0 & 0 & \mathbf{D} \end{bmatrix} \begin{bmatrix} \vec{n}^f \\ \vec{n}^b \\ \vec{n}^s \\ \vec{n}^g \\ \vec{n}^p \end{bmatrix}$$

in which:

$$\begin{aligned} \mathbf{T}^f &= \mathbf{B}^f + \mathbf{D} - \Lambda - \mathbf{P} + \mathbf{A}^f \\ \mathbf{T}^b &= \mathbf{B}^b + \mathbf{D} - \Lambda - \mathbf{P} - \mathbf{R}_{Pa} + \mathbf{A}^b \end{aligned}$$

In the previous equations, the ratios of volumes guarantee a conservation of the number of atoms moved from one material to the other assuming constant volumes during the time-step.

3.3.3 Nuclide addition operations

Beside removal of nuclides, the fuel composition can also be modified by addition of nuclides, which is used for three main reasons:

1. maintaining the mass or number of atoms constant,
2. keeping the reactor critical,
3. controlling the redox potential.

These three types of operations are explained in this section.

Refueling operations

First, keeping the mass or number of atoms constant is mainly used to refuel the reactor with actinides. It can however also be used to maintain the composition of the carrier salt. Similarly to nuclides removal, this can be performed in a continuous or batch-wise manner. Generally, the constraint on the amount fed has two characteristics:

1. one can keep the amount of all nuclides, only actinides or actinides and fission products constant,

2. the amount kept constant can be the number of atoms or the mass.

In a continuous manner, one can define an addition matrix \mathbf{A} so as to keep the total mass constant regardless of \vec{n} , using the vector of atomic masses $\vec{m} = (m_1, m_2, \dots, m_N)$:

$$\begin{aligned} \frac{dM_{\text{tot}}}{dt} &= \vec{m} (\mathbf{B} + \mathbf{D} - \mathbf{\Lambda} - \mathbf{P} + \mathbf{A}) \vec{n} = 0 \\ \Rightarrow \vec{m} \mathbf{A} &= -\vec{m} (\mathbf{B} + \mathbf{D} - \mathbf{\Lambda} - \mathbf{P}) \end{aligned}$$

One can thus build \mathbf{A} to fulfill this condition. If the material is to be refueled with feed nuclides $f \in F$ with a mass fraction μ_f , one gets the following terms:

$$A_{ij} = -\delta_{if} \frac{\mu_f}{m_f} \sum_k m_k (B_{kj} + D_{kj} - \Lambda_{kj} - P_{kj})$$

This definition, in effect, creates virtual reactions on nuclides nuclides being destroyed that produce nuclides in the feed.

Criticality control operations

An advantage of liquid-fuel MSRs is the ability to control long-term reactivity changes due to fuel burn-up by addition or removal of certain elements or isotopes. For example, a Th breeder MSR may have a positive reactivity swing that could be compensated by Th additions. Alternatively, a burner MSR will need a regular make-up of fissile material, the quantity of which could be criticality-driven.

The criticality search algorithm in EQL0D uses user-input nuclide vectors detailing which nuclides can be added to or removed from the fuel to increase or decrease reactivity to within an acceptable margin of a given target k_{eff} . This mode can be used in two modes:

1. A simple addition mode, in which nuclides are removed or added from the fuel regardless of keeping the mass constant, or
2. A mode keeping the total mass constant in which nuclides that are removed or added are compensated for by the addition or the removal of another nuclide group.

For example, in the case of MSBR(2f), the reactivity is controlled by simple additions or removal from the fuel of uranium fed from the blanket. In the case of MSBR and MSFR however, criticality is controlled by addition or removal of uranium which are compensated for by removal or addition of thorium from the fuel so as to keep the total mass of actinides in the fuel constant.

Redox potential control operations

In MSRs, the salt potential must be controlled to prevent excessive corrosion of the container materials. In the case of a fluoride salt carrier with U as fissile material, the fission process releases free fluorine atoms since the average valence of FPs is lower than that of U in UF_4 . In the Molten Salt Reactor Experiment (MSRE), the excess fluorine was captured by contacting metallic Be with the salt to scavenge free fluorine atoms. Other reactor concepts such as the MSFR foresee the use of a U buffer by varying the ratio of UF_4 to UF_3 atoms.

In EQL0D, elements have been assigned valence states based on their expected behavior in a fluoride salt as described on figure 3.1. Unknown elements have been assigned a valence state of 0 but are not expected to influence results substantially due to their very low concentrations during fuel evolution. If so desired, single values can be manually overridden to account for an average valence between several possible valence states, for example when using a U redox buffer.

The excess or default of fluorine in a mixture can be computed by multiplying atomic densities n_i with their expected valence v_i .

$$\bar{v} = \sum_i n_i v_i$$

Once corrected by the addition or removal Δn of replacement nuclides r of atomic fraction α_r compensating exactly the change in fluorine Δn_F :

$$\left. \begin{aligned} \bar{v}_1 &= \bar{v}_0 + \Delta n \sum_r \alpha_r v_r - \Delta n_F = 0 \\ \Delta n + \Delta n_F &= 0 \end{aligned} \right\} \Rightarrow \left\{ \begin{aligned} \Delta n &= -\frac{\bar{v}_0}{1 + \sum_r \alpha_r v_r} \\ \Delta n_F &= -\Delta n \end{aligned} \right.$$

Computational scheme

As was previously mentioned, EQL0D is designed for the simulation of both:

1. fuel evolution over a finite number of steps like a standard depletion code, or
2. searching for equilibrium directly.

For this purpose, EQL0D uses two loops, as depicted on figure 3.5:

1. an outer loop in which Serpent is called and the burn-up matrices for the system are created, and
2. an inner loop in which the system is solved and batch-wise processes (refueling operations, redox and criticality control) are performed.

The role of the outer loop is to update cross-section and flux data; the inner loop depletes materials, refuels them and performs other operations such as criticality and redox potential control. In equilibrium mode, the inner and outer loops are run until user-input convergence

Chapter 3. Methods and Tools

criteria are fulfilled and equilibrium is reached. In the general mode, each loop is run several times according to user input.

The default convergence criterion for equilibrium calculations is that of the maximum relative change of the concentration of nuclides below a given threshold whose default value is 0.001 (0.1 %):

$$\max_i \left(\left| \frac{N_i^{\text{previous}} - N_i^{\text{current}}}{N_i^{\text{previous}}} \right| \right) < \text{Threshold}$$

Burn and decay matrices for burnable materials and analog reaction rates for criticality search are obtained from Serpent while the fuel processing matrices introduced previously are created by the routine. To solve the Bateman equations, EQL0D uses the Chebyshev Rational Approximation Method (CRAM) (Pusa and Leppänen, 2013) implemented in MATLAB at order 16.

The concept of equilibrium fuel cycle is useful in the analysis of reactors that have a partly- or fully-closed fuel cycle, that is, in which part of or all the actinide vector is recycled in the core. In this case, provided the properties of the reactor and fuel cycle (total actinides mass, fission rate) are kept constant between cycles, that is, the reactor is refueled with feed to conserve its actinide mass, its fuel composition will eventually converge to an equilibrium. At that point, its actinide vector will not substantially change between comparable points in the cycle. The equilibrium is unique and independent of the initial fuel composition, hence the iterative scheme chosen for equilibrium calculations in EQL0D. This equilibrium state can be used to study intrinsic properties of the reactor and its associated fuel cycle. Moreover, if the feed only contains fertile isotopes such as ^{238}U or ^{232}Th , the composition will converge towards its natural iso-breeding state, in which case excess reactivity at equilibrium indicates that the reactor can operate as an iso-breeder.

Predictor-corrector step

Beside the iterative equilibrium calculation mode, EQL0D offers the possibility of computing the fuel evolution over burn-up steps of finite size, as in the case of standard burn-up codes. While in the iterative mode the evolution of the fuel composition is of little interest compared to the equilibrium itself, in the steps mode it is important. Therefore, a Constant Extrapolation/Linear Interpolation (CE/LI) predictor-corrector scheme, as named by Isotalo and Aarnio (2011), was implemented. In this scheme, an approximation of the end-of-step composition is first extrapolated using a linear interpolation between previous step and beginning-of-step reaction rates, and then corrected by linearly interpolating between first calculated beginning-of-step and first predicted end-of-step reaction rates. The predictor step

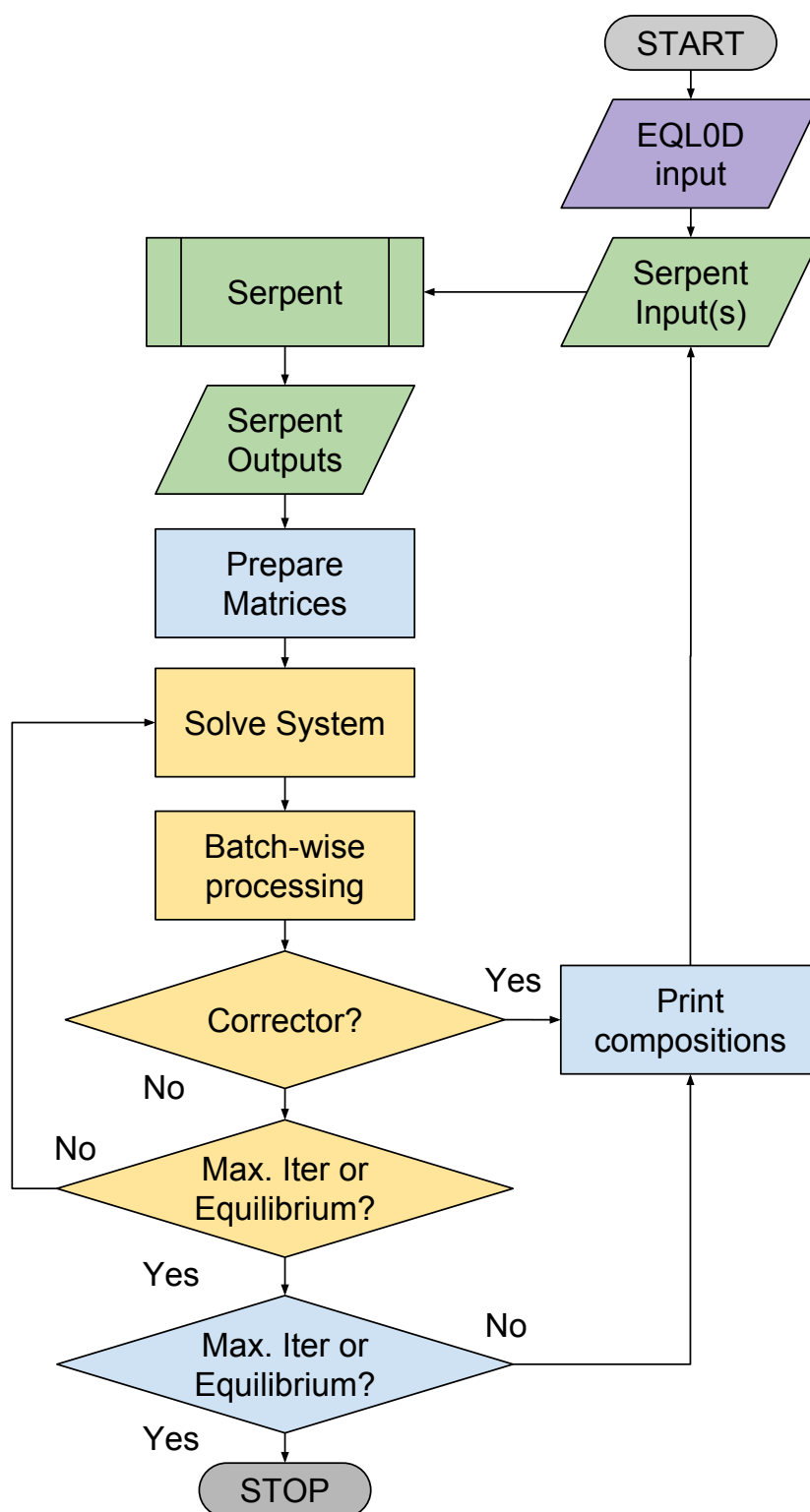


Figure 3.5 – Flowchart of the EQL0D procedure. The outer loop is colored in blue and the inner loop in orange.

first uses the Beginning of Step (BOS) reaction rates and yields:

$$\tilde{n}(t + \Delta t) = \exp(\Delta t \mathbf{T}_{\text{BOS}}) \tilde{n}(t)$$

The predicted composition $\tilde{n}^*(t + \Delta t)$ is then used to obtain updated reaction rates \mathbf{T}_{EOS} at the approximated end of the step. The corrected End of Step (EOS) compositions can then be computed over N_{steps} sub-steps by linear interpolation between the BOS and EOS rates:

$$\mathbf{T}_{\text{COR},j} = \left(1 - \frac{(j-1)}{N_{\text{steps}}}\right) \mathbf{T}_{\text{BOS}} + \frac{(j-1)}{N_{\text{steps}}} \mathbf{T}_{\text{EOS}}$$

and thus:

$$\tilde{n}\left(t + j \frac{\Delta t}{N_{\text{steps}}}\right) = \exp\left(\frac{\Delta t}{N_{\text{steps}}} \mathbf{T}_{\text{COR},j}\right) \tilde{n}\left(t + (j-1) \frac{\Delta t}{N_{\text{steps}}}\right)$$

3.3.4 Verification

Unfortunately, verification and validation of codes dedicated to MSRs is made difficult due to the scarcity of experimental data and the age of computational models that were used at the time of the MSRP. Nonetheless some level of verification can be achieved by using simple sanity checks, benchmark against similar codes and comparison with legacy ORNL, which is the subject of this section.

MSFR benchmark results

Aufiero et al. (2013) modified the Serpent 2 code directly to include continuous removal of FPs and refueling, as well as criticality-dependent feed of Uranium from the fuel to the blanket. This modification was originally applied to the EVOL neutronic benchmark of the MSFR. In the depletion part of this benchmark, the fuel evolution of an ^{233}U -started MSFR is computed over 200 EFPY. This depletion was computed using both codes and the ENDF/B-VII.0 library to minimize the differences coming from neutron transport calculations and nuclear data libraries.

The results given by both procedures are depicted on figure 3.6. Most quantities are in excellent agreement, except for the quantity of ^{233}U in the salt. It is due to the different criticality algorithms used by both codes and possibly small modelling differences between the two cases, as hinted by the slightly higher plutonium content in the case of EQL0D simulation. While improvement of the computational scheme is certainly possible, the agreement is judged sufficient for most purposes.

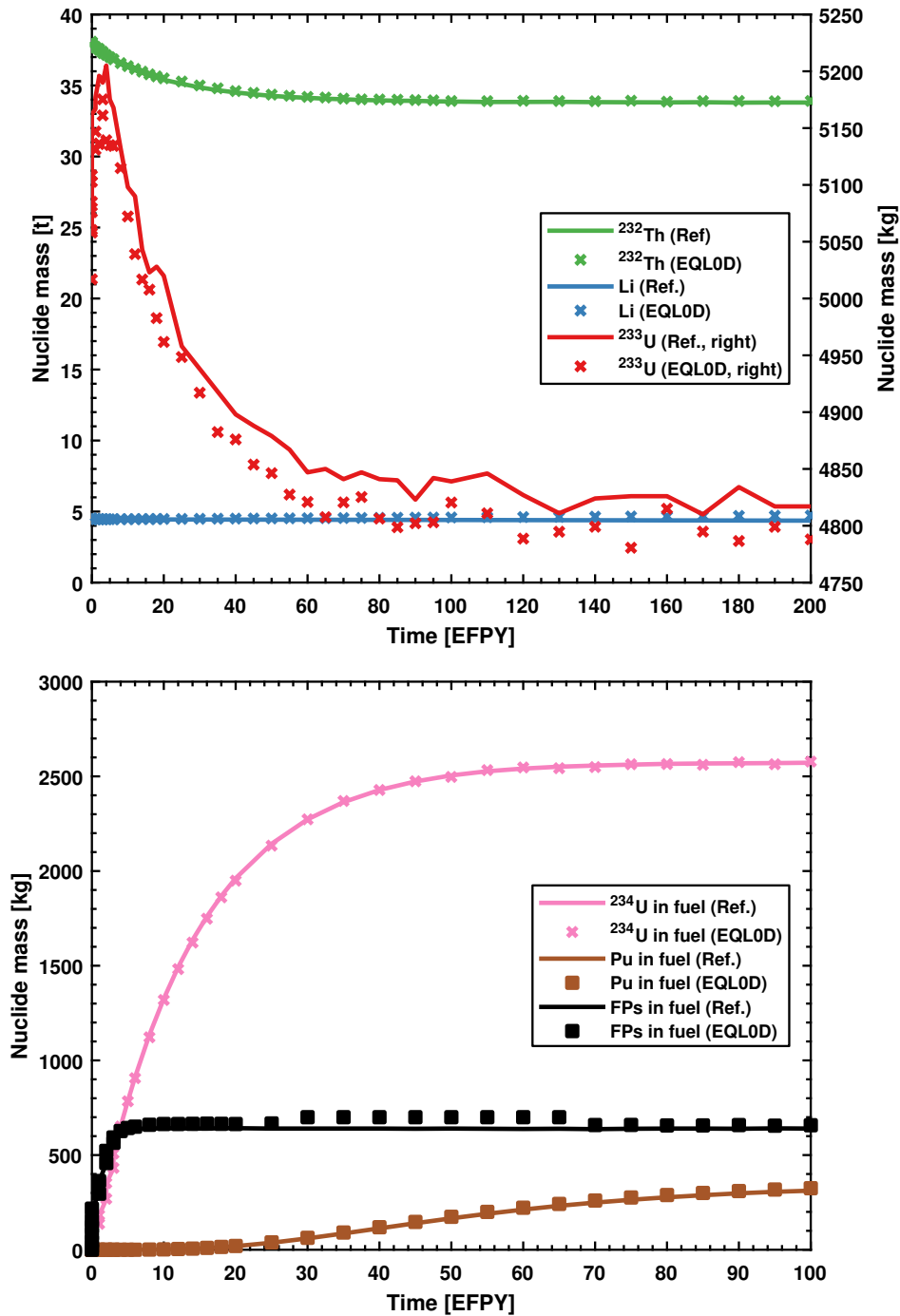


Figure 3.6 – Comparison of results obtained for the MSFR benchmark using Aufiero's modified Serpent and EQL0D.

Comparison with legacy ORNL data

An additional comparison can be carried out using results dating back to the times of the MSRP. In particular, Robertson (1971) gives equilibrium concentrations of selected fission

Chapter 3. Methods and Tools

products for the reference MSBR configuration, which can be obtained with EQL0D and compared to ORNL numbers. Table 3.1 compares these with those predicted by EQL0D, as well as the absorption fraction (ratio of absorptions to those in fissile materials: ^{233}U , ^{235}U and ^{239}Pu). The Volatile Yield Fraction is the fraction of the cumulative yield of the chain carried by the volatile nuclide, calculated using data from England and Rider (1994).

Table 3.1 – Comparison of equilibrium concentrations and absorption fractions of selected fission products as reported by ORNL and predicted EQL0D for MSBR.

		Densities [10^{24} at/cm ³]			Absorption Fraction			Volatile
		ORNL	EQL0D	Diff.	ORNL	EQL0D	Diff.	
Sr	90	8.5×10^{-6}	1.3×10^{-5}	53%	2.1×10^{-4}	1.1×10^{-5}	-95%	58%
Zr	91	4.6×10^{-7}	5.2×10^{-7}	13%	2.8×10^{-5}	2.4×10^{-5}	-13%	29%
	93	1.7×10^{-6}	1.7×10^{-6}	0%	2.2×10^{-4}	2.1×10^{-4}	-5%	2%
Ba	137	5.1×10^{-7}	7.6×10^{-7}	48%	4.9×10^{-5}	5.7×10^{-5}	17%	66%
	140	1.0×10^{-7}	1.3×10^{-7}	26%	2.4×10^{-5}	1.4×10^{-5}	-42%	24%
La	139	1.7×10^{-7}	2.4×10^{-7}	43%	3.3×10^{-5}	6.0×10^{-5}	81%	46%
Ce	144	2.6×10^{-7}	2.7×10^{-7}	4%	2.9×10^{-5}	9.4×10^{-6}	-68%	5%
Pr	141	2.0×10^{-7}	2.0×10^{-7}	2%	5.8×10^{-5}	6.8×10^{-5}	17%	0%
	143	1.0×10^{-7}	1.0×10^{-7}	1%	2.3×10^{-4}	2.1×10^{-4}	-9%	0%
Nd	143	2.4×10^{-7}	2.5×10^{-7}	4%	1.5×10^{-3}	1.5×10^{-3}	-3%	0%
	145	2.1×10^{-7}	2.2×10^{-7}	3%	4.2×10^{-4}	4.3×10^{-4}	2%	0%
Pm	147	8.2×10^{-8}	7.7×10^{-8}	-6%	1.3×10^{-3}	8.9×10^{-4}	-32%	0%
	148	1.3×10^{-9}	3.6×10^{-10}	-72%	5.4×10^{-4}	1.5×10^{-5}	-97%	0%
	148m		3.7×10^{-10}	-43%		2.6×10^{-4}	-49%	
Sm	149	4.5×10^{-9}	5.3×10^{-9}	18%	6.5×10^{-3}	7.3×10^{-3}	13%	0%
	150	4.6×10^{-8}	4.5×10^{-8}	-3%	1.2×10^{-4}	1.3×10^{-4}	11%	0%
	151	1.3×10^{-8}	1.2×10^{-8}	-11%	1.4×10^{-3}	1.6×10^{-3}	13%	0%
	152	2.2×10^{-8}	2.2×10^{-8}	0%	2.9×10^{-5}	4.1×10^{-4}	1297%	0%
Eu	153	5.7×10^{-8}	5.5×10^{-8}	-4%	7.5×10^{-4}	6.1×10^{-4}	-18%	0%
	154	1.7×10^{-8}	7.2×10^{-9}	-58%	4.9×10^{-4}	4.5×10^{-4}	-8%	0%
	155	2.7×10^{-9}	3.4×10^{-9}	24%	7.0×10^{-4}	7.0×10^{-4}	0%	0%
Oth.					5.1×10^{-4}	1.3×10^{-3}	159%	
Tot.					1.5×10^{-2}	1.4×10^{-2}	-7%	

While several nuclides show good agreement with ORNL data, several nuclides also show substantial discrepancies. However, the total fission product absorption fraction is in good agreement.

Discrepancies for nuclides of low atomic numbers seem to be linked to the fact that they have volatile (Xe, Kr) nuclides in their decay chain and that most of the yield of the chain is carried by these nuclides. These could be attributed by differences in modeling between ORNL results and the models used in this paper, as plating out and deposition to graphite was not modeled in this work. However, the numerical stability of the solutions of the Bateman equations depend on the eigenvalues of the matrix, which can have very different orders of magnitude and thus cause instabilities, especially for nuclides with very short half-lives (Pusa and Leppänen, 2013). Therefore it is possible that the model used by ORNL may be too simplistic.

As ^{148}Pm is mostly born from captures on ^{147}Pm , they cannot be attributed to the fission yield. Accounting for $^{148\text{m}}\text{Pm}$ seems to reduce the discrepancy to the order of magnitude caused by lower absorption on the precursor nuclide, ^{147}Pm . The difference in ^{151}Sm could be due to the higher capture rate which would lower its equilibrium concentration, while that of ^{149}Sm seem to be due to differences in fission yields. The discrepancy in ^{154}Eu seems to be due to the fission yield, as it is born directly from fission without having precursor fission products.

4 Equilibrium Closed Fuel Cycle Performance in an Infinite Lattice

4.1 Introduction

The first part of this thesis was dedicated to the investigation of the characteristics of potential MSR designs at equilibrium in a closed fuel cycle. Indeed, any reactor operated on a closed fuel cycle with a fertile-only feed (^{232}Th or ^{238}U) will eventually reach an isobreeding equilibrium that is intrinsic to the reactor and its fuel cycle.

Positive reactivity at equilibrium is a measure of the breeding potential of the reactor as the fertile-to-fissile ratio can be increased to keep the reactor critical and generating excess amounts of fissile material. On the other hand, negative reactivity at equilibrium must be compensated for by adding fissile material at the reactor, meaning the reactor is a net burner of fissile material.

However, positive reactivity at equilibrium also mirrors the neutron budget of the reactor and thus implies that neutrons can be spent to transmute and eventually burn nuclides with low fissibility such as minor actinides.

The results presented in this chapter were obtained at the infinite lattice level, which means that neutron leakage must additionally be taken into account. In effect, this means that some of the excess reactivity must be spent to compensate for neutron losses through leakage. This factor was considered through the calculation of the bare (unreflected) critical sizes of the corresponding configurations using one- or two-group neutron diffusion (as previously explained in section 3.2.1) and the few-group cross-sections produced for the equilibrium.

Specifically, in the case of thermal-spectrum MSRs, the performance and characteristics of several combinations of fuel salt and moderating materials were studied. The properties of the salts and materials that are mentioned in this chapter were previously outlined in section 2.4.

4.2 Assumptions

The assumptions made to carry out the infinite lattice study presented in this chapter are first outlined in this section.

4.2.1 Lattice geometry

The selected geometry is that of an infinite hexagonal lattice of cylindrical fuel salt channels embedded in a moderator matrix. On a two-dimensional level, the lattice can be described with a set of two parameters, and in this work, that of:

- the salt volume fraction s describing the moderation level and
- salt channel radius r describing the heterogeneity level

were used. Other parameters used in the literature include the salt channel diameter, lattice pitch, ratio of moderator atoms to actinide atoms, etc.

It must be noted that due to the circular and hexagonal shapes used respectively for the fuel channel and moderator element, some values of the fuel share cannot be achieved as the largest circle that fits in an hexagon is that hexagon's inscribed circle. Indeed, the salt volume fraction is given by:

$$s_{\max} = \frac{\pi r_{\text{in}}^2}{2\sqrt{3}r_{\text{in}}^2} = \frac{\pi}{2\sqrt{3}} \approx 0.907 \quad (4.1)$$

Salt fractions higher than this value cannot be represented using cylindrical channels in an hexagonal lattice, therefore only the 100 % share was computed using homogeneous square cells containing only salt.

The influence of the salt channel radius r and salt volume fraction s on the heterogeneity of the geometry is illustrated in figure 4.1 below.

It must also be mentioned that some moderators are either chemically incompatible with salts (Be, BeO, ZrH) or miscible (Heavy and Light Water) and thus necessitate a barrier to separate them from the salt. As a first approximation, this barrier was neglected, but its impact is investigated in the section dedicated to partial effects.

4.2.2 Closed fuel cycle

A wide range of parameters can be changed in such a study, therefore reference values were selected for the base cases and the investigation of the influence of individual parameters was done separately in a sensitivity study of selected cases.

The reference parameters were selected to be:

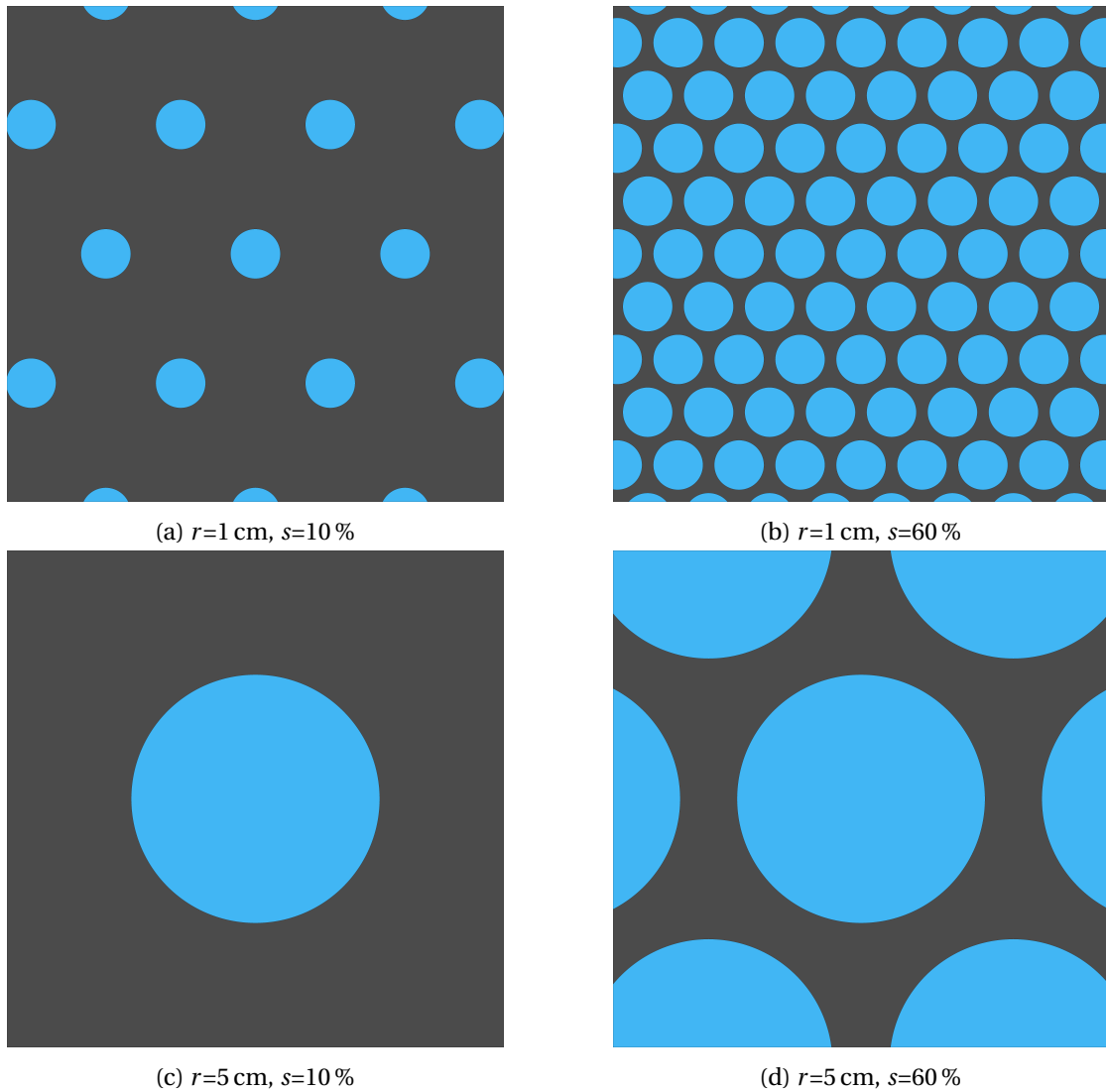


Figure 4.1 – Illustration of the variation of channel radius and salt volume fraction on the lattice geometry. The fuel salt is depicted in blue and the moderator in dark grey. The side of the squares is 20 cm long.

- 10 W/cm^3 for the power density, which is relatively low in the aim of not penalizing thermal-spectrum configurations,
- 30 s for the removal cycle time of volatile fission products, which is a commonly assumed value in the literature, and
- 30 EFPD for the reprocessing cycle time of the soluble fission products, a low value (rapid fuel reprocessing) selected to first minimize the influence of fission products on the results.
- No losses of actinides during reprocessing.
- The total mass of actinides and fission products was kept constant and equal to the initial mass of actinides.

4.3 Results

The results presented here are divided in two sections for the U-Pu cycle on the one hand and the Th-U cycle on the other.

The goal of a moderation level study such as this one is to search for moderated configurations that provide some advantage over a non-moderated configuration, generally in the form of lower fuel volumes and inventories.

4.3.1 Uranium-Plutonium cycle

In the U-Pu cycle, the fertile feed only consists of ^{238}U , which has the advantage of being more fissile by fast neutrons than ^{232}Th and that its main and secondary fissile nuclides, such ^{239}Pu and ^{241}Pu produce a larger number of neutrons per fission (approximately 2.9). Both of these advantages substantially increase the neutron budget of the reactor.

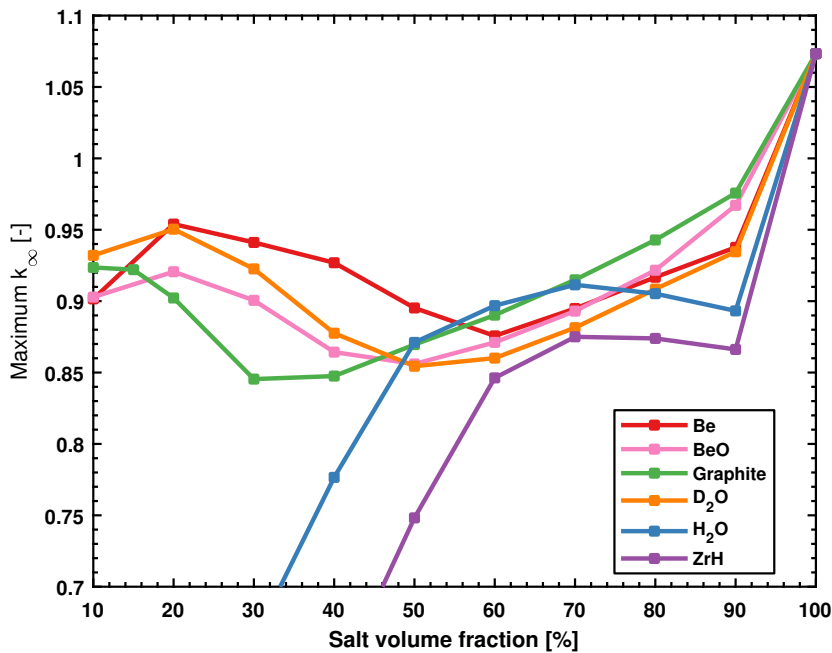


Figure 4.2 – Maximum reactivity in fluoride salts in U-Pu cycle as function of moderator.

The maximum reactivity achievable as function of the moderator used for a given salt volume fraction is depicted on figure 4.2 below for a $\text{LiF}-\text{UF}_4$ salt, which is expected to perform the best.

However, an isobreeding equilibrium in a closed U-Pu cycle and in a thermal spectrum is impossible due to the build-up of higher actinides with low fission propability. An illustration of that phenomenon can be obtained using the reactivity decomposition of equation (3.6).

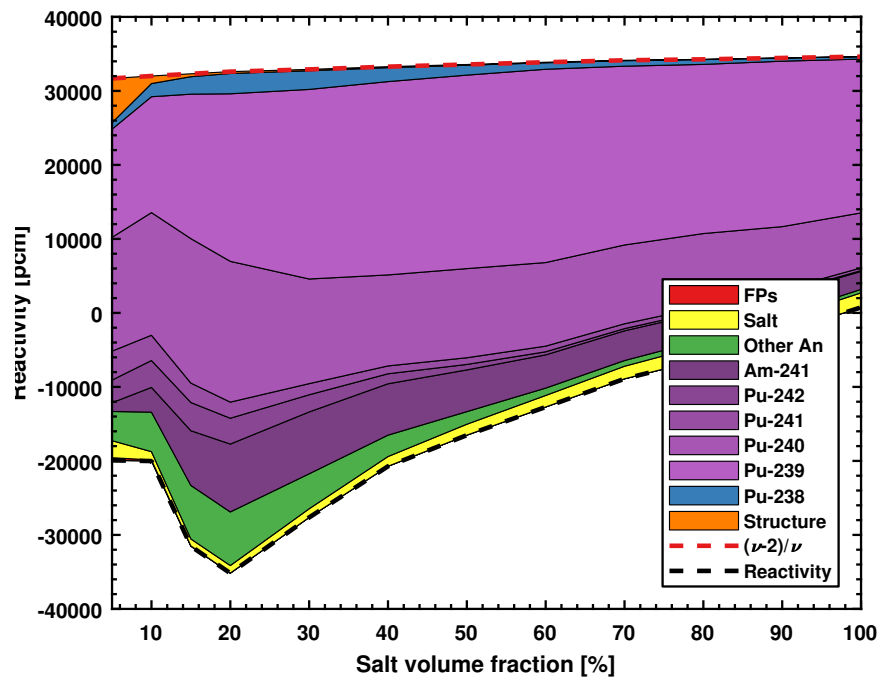


Figure 4.3 – Equilibrium reactivity decomposition of $\text{LiF}-\text{UF}_4$ in a graphite lattice and closed U-Pu cycle

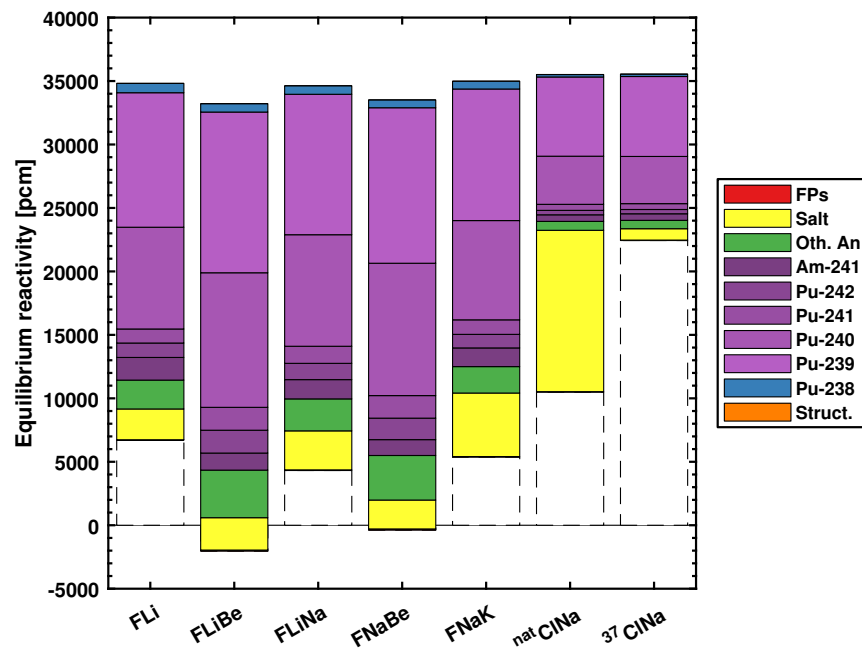


Figure 4.4 – Equilibrium reactivity decomposition of salts in fast spectrum and U-Pu cycle

It is depicted for the case of a $\text{LiF}-\text{UF}_4$ salt at equilibrium in a graphite moderated lattice with channel radius $r = 1$ cm on figure 4.3 below. The sum of the base and bonus reactivities is given by the top value of the bar, and each subsequent part is the reactivity consumed by a given nuclide or set of nuclide at equilibrium. The dashed area under the bar, is present at all, is the leftover reactivity.

The initial excess reactivity of approximately 30 000 pcm provided by the U-Pu cycle is depicted with a red dashed line. Subsequent neutron captures of other nuclides consume that reactivity down to the point of the black dashed line which is the available reactivity. Obviously, it is strongly negative in all but the unmoderated case (100% salt volume fraction), meaning that none of these configurations is suitable for an isobreeder in the U-Pu cycle.

In fast spectrum on the other hand, the performance of FLi, FLiNa, and FNaK is acceptable (see figure 4.4) and the performance of chlorides, especially enriched chlorides, is exceptional with more than 22 000 pcm reactivity in the enriched case.

4.3.2 Thorium-Uranium cycle

Unlike the U-Pu cycle, the Th-U cycle has a smaller neutron budget due to the lower number of neutrons per fission produced by ^{233}U (approximately 2.5). However, the high fission probability of ^{233}U compared to that of higher fissile nuclides means that a smaller proportion of the equilibrium actinide vector is made of higher nuclides, and therefore this budget is spent more efficiently. The equilibrium k_∞ of all computed configurations is summarized on figure 4.5 below.

Configurations of interest at equilibrium are given by a high excess reactivity (high k_∞), to a level comparable than that of the fast (unmoderated) case. One can quite simply notice the excellent performance of configuration in the top left corner of the figure, composed of mixes of salts and moderators with low parasitic captures (Be, BeO, Graphite and D_2O). The best performing salt is $\text{LiF}-\text{ThF}_4$, followed by $\text{LiF}-\text{BeF}_2-\text{ThF}_4$ in some configurations. On the other hand, $\text{NaF}-\text{KF}-\text{ThF}_4$ and $\text{NaF}-\text{BeF}_2-\text{ThF}_4$ show poor performance in a moderated spectrum. Moreover, the performance of H_2O and ZrH is very poor for all fuel salts due to the steady decrease of the reactivity with increased moderation.

A better comparison of the performance of the various moderators can be obtained by comparing the infinite reactivity at equilibrium for a single salt, which is done on figure 4.6 below for the FLi salt as function of the salt volume fraction. The results show the highest k_∞ achievable for a given salt volume fraction for any salt channel radius within the 1 cm to 10 cm.

Apart from Be-moderated cases with exceptional reactivity due to the (n,2n) reaction of ^9Be the largest reactivity budget is obtained for fast-spectrum cases. A decomposition of the reactivity lost by neutron capture in various nuclides in the Thorium-Uranium cycle in fast-spectrum is given on figure 4.7 below for the candidate salts.

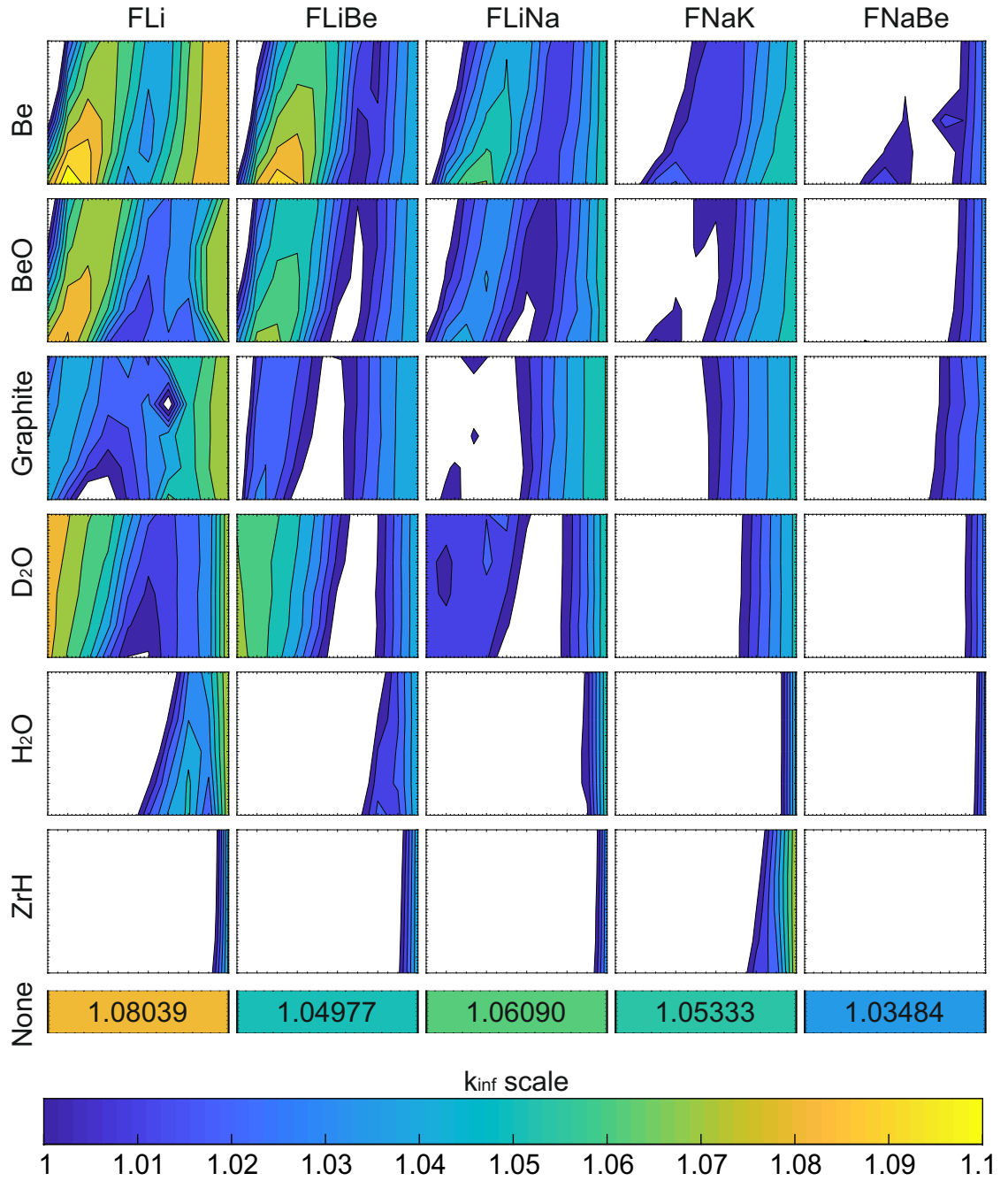


Figure 4.5 – Equilibrium reactivity as function of salt and moderator in closed Th-U cycle. The horizontal axis of each figure represents the salt volumetric share and the vertical axis the salt channel radius. The domain colored in white is subcritical ($k_{\infty} < 1$) at equilibrium.

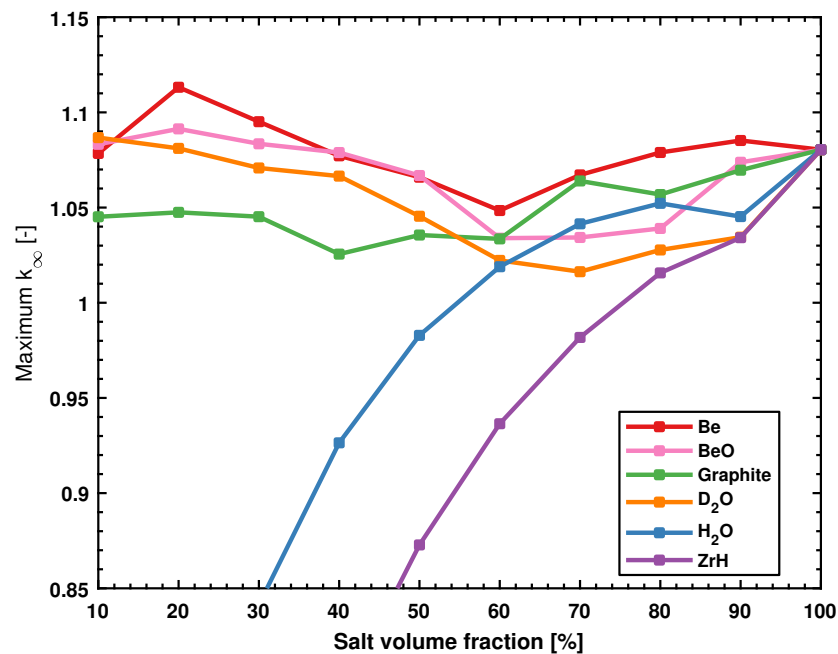


Figure 4.6 – Maximum reactivity in fluoride salts in Th-U cycle as function of moderator.

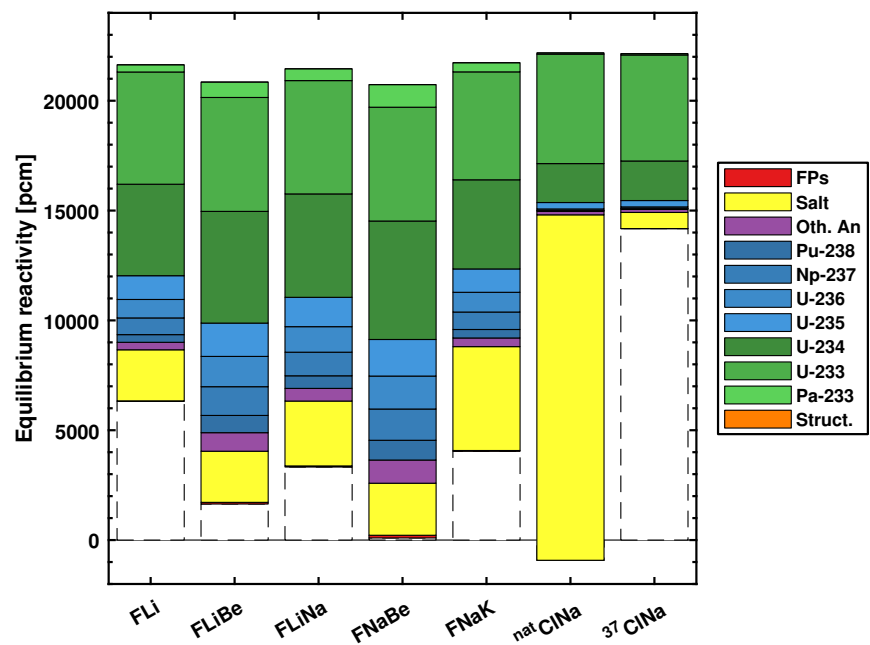


Figure 4.7 – Equilibrium reactivity decomposition of salts in fast spectrum and Th-U cycle

The best-performing fluoride-based salt is arguably $\text{LiF}-\text{ThF}_4$, followed closely by $\text{LiF}-\text{NaF}-\text{ThF}_4$ and $\text{NaF}-\text{KF}-\text{ThF}_4$, both of which could be used to replace FLi fuel salts to lower tritium production due to the presence of Li, at the cost of lower breeding performance and larger inventories however. It must be recalled that the $\text{NaF}-\text{KF}-\text{ThF}_4$ mixture used here is hypothetical. $\text{LiF}-\text{BeF}_2-\text{ThF}_4$ and $\text{NaF}-\text{BeF}_2-\text{ThF}_4$ show lower and much lower performance, likely due to a slightly softer spectrum due to the presence of Be, as well as their lower actinide fraction in the salt.

The neutron spectra of unmoderated fluoride salts is given on figure 4.8 below. One notices the relatively softer spectra of FLiBe and FNaBe which are linked to the presence of Be as well as their lower actinide content. FLiNa, FNaBe and FNaK are also noticeably softer on the thermal side of the spectrum because of the large scattering resonance of ^{23}Na around 2.8 keV. FNaK is otherwise somewhat harder than FLi in some regions. Chloride-based salts have however noticeably harder spectra as visible on figure 4.8.

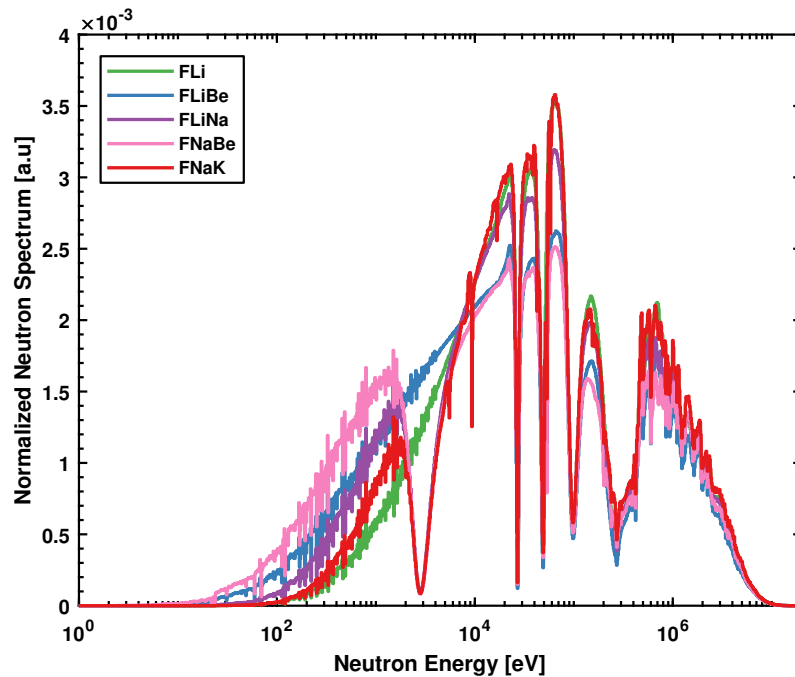


Figure 4.8 – Normalized neutron spectrum of unmoderated fluoride salts in an infinite lattice.

Concerning chloride salts however, the difference between natural and enriched chlorine cases is tremendous, as the natural chlorine $\text{NaCl}-\text{ThCl}_4$ case is subcritical at equilibrium and thus cannot be operated as an isobreeder, while the enriched case shows a large reactivity margin. The difference with the previously presented U-Pu case using natural chlorine, which shows positive reactivity at equilibrium, is mostly due to the lower neutron budget of the Th-U cycle and to the increased concentration of chlorine atoms in the Thorium-containing chloride salts due to Th being in a tetrachloride form while Uranium is a trichloride.

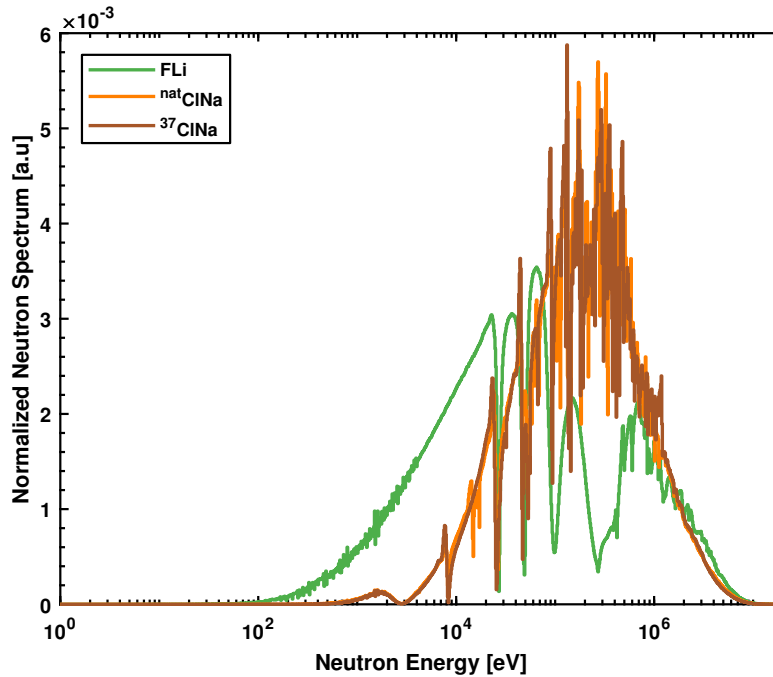


Figure 4.9 – Normalized neutron spectrum of unmoderated chloride salts in an infinite lattice.

4.4 Separate Effects

A large number of other parameters can affect the previously presented results. Therefore, the influence of the most important of these parameters on the equilibrium characteristics of MSR was investigated using smaller-scale parametric studies. Notably, the influence of the introduction of a cladding material in the case of the best-performing moderators was studied. Additionally, the influence of the power density on the equilibrium critical inventory was investigated for selected salts. Finally, the impact of the soluble FP reprocessing rate on the isobreeding core fuel salt volume necessary was evaluated.

4.4.1 Effect of cladding material

Several of the moderators that perform well in a closed Th-U cycle with several salts are either chemically incompatible with salts (e.g. Be) and would be dissolved, or are miscible (e.g. Heavy Water) with salts and thus a material must be used to keep them separate. However, the list of potentially compatible materials is quite short and include essentially metallic alloys or silicon carbide.

The effect of the introduction of a 1 mm thick cladding tube in the hexagonal matrix on the equilibrium reactivity reserve as function of the salt volume fraction was computed for Be- and D₂O-moderated lattices and is depicted on figure 4.10 below.

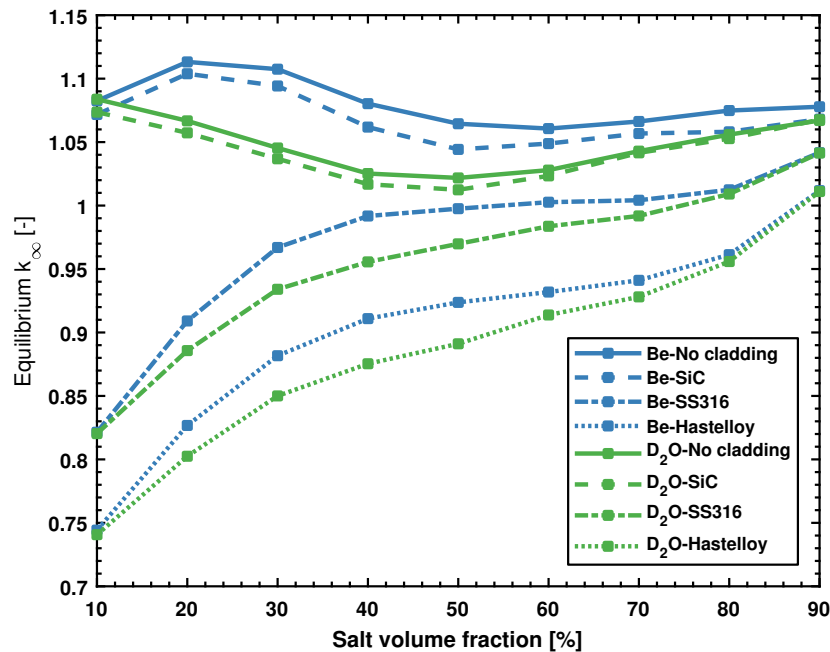


Figure 4.10 – Effect of 1 mm cladding of various materials on the infinite reactivity at equilibrium in the Th-U cycle with a LiF–ThF₄ salt.

The effect is noticeably strong for metallic materials (SS316, Hastelloy N), making the lattice subcritical at equilibrium in the case of both moderators, making this configuration particularly unattractive. The effect is less punishing in the case of SiC due to its low absorption, however manufacturing SiC structure is still technically challenging to this day. It is possible that Chemical Vapor Deposition (CVD) would provide a way of coating solid moderating materials such as Be, however it is unlikely to provide a stable structure as would be necessary in the case of a liquid moderator such as heavy water.

4.4.2 Effect of Protactinium capture

Power density, defined as the power per unit volume of fuel salt, has a particular impact in the case of a Th-U cycle due to the long half-life (27 days) of the intermediate ²³³Pa produced by neutron capture on ²³²Th. If ²³³Pa undergoes a neutron reaction such as neutron capture or (n,2n) before decaying to ²³³U, the breeding performance of the reactor will be decreased. The former reaction is substantially more likely in a thermalized neutron spectrum and therefore moderated configurations sometimes foresee the separate extraction of Pa on a short cycle (typically 3 days) to ensure its proper decay to ²³³U. It is especially effective in the case of high power densities because of the reduced time between neutron captures they imply.

The impact of power density on the isobreeding equilibrium was computed for a FLi-fueled

graphite-moderated case (10% salt volume fraction) with and without Pa isolation, for a FLi-fueled and a NaCl-fueled unmoderated cases. The impact can be quantified by computing the isobreeding core size and its corresponding core salt volume, which is depicted on figure 4.11 below.

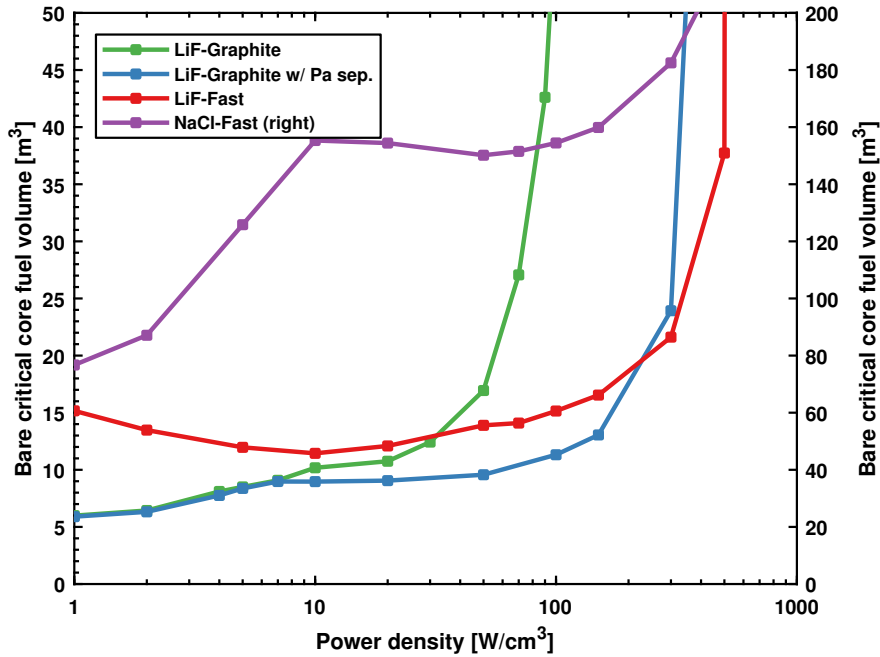


Figure 4.11 – Effect of power density on the isobreeding fuel salt volume for fluorides in a thermal and fast spectrum.

Visibly, the Protactinium capture effect is much stronger in a thermal spectrum, as the critical fuel salt volume quickly increases beyond a power density of 40 W/cm^3 . This effect can be alleviated by Pa separation and isolation on a short cycle for power densities up to 150 W/cm^3 . Fast-spectrum configurations show less sensitivity to the power density than their moderated counterparts despite their inherently higher critical fuel volumes.

4.4.3 Effect of reprocessing cycle time

A more general effect than that of ^{233}Pa capture is that of the reprocessing cycle time, that is, the speed of removal of FP, which influences reactivity through increased parasitic captures. Recalling the behavior of the mass fraction of FP from equation (3.13), the influence of the reprocessing cycle time can be studied by selecting a low power density to minimize the effect of ^{233}Pa capture and vary the cycle time accordingly.

It can be deduced from results given on figure 4.12 that moderated designs are much less tolerant to high fractions of fission products and thus necessitate fast fuel processing, compared

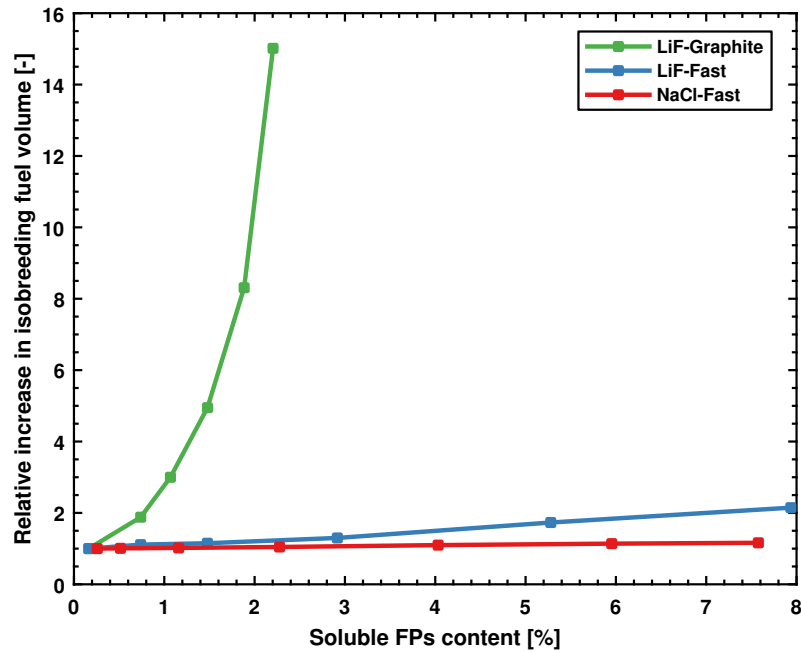


Figure 4.12 – Effect of reprocessing cycle time and FPs content on the isobreeding fuel salt volume for fluorides and chlorides in a thermal and fast spectrum.

to fast-spectrum designs. Indeed, their critical fuel volume quickly increases beyond a FP content of 0.5 % while comparatively the fast-spectrum designs are nearly unaffected.

Interestingly, an optimum FP fraction can be found from the point of view of salt volumes processed. Indeed, for a given cycle time and thus FP concentration, the volume of fuel salt that must be reprocessed is given by the isobreeding volume divided by the cycle time, as depicted on figure 4.13.

This effect is explained by the competing trends of shorter cycle times simultaneously decreasing the isobreeding fuel volume while increasing the speed at which it must be reprocessed. Interestingly, the optimum for fast-spectrum reactors seems to be situated at quite high FP concentrations.

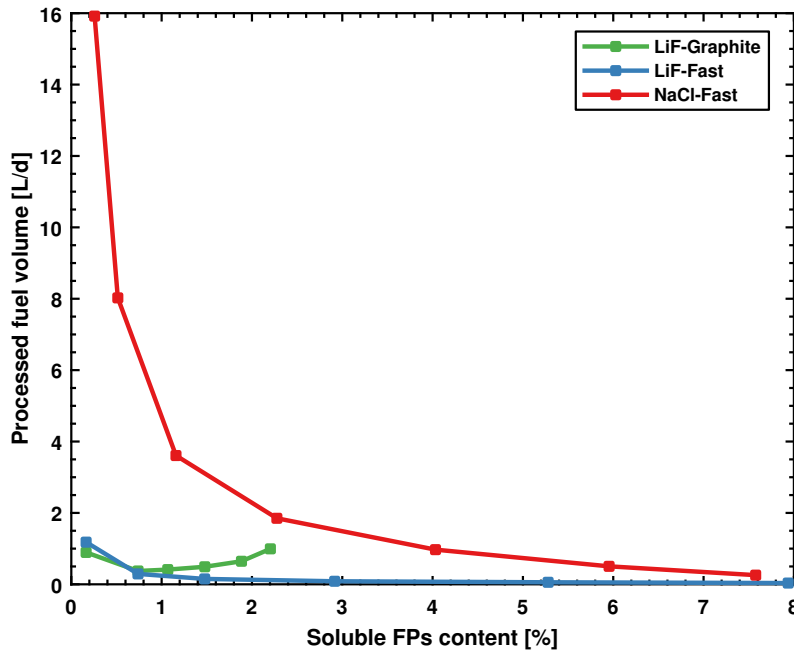


Figure 4.13 – Effect of reprocessing cycle time and FPs content on the isobreeding fuel salt volume to be processed per day for fluorides and chlorides in a thermal and fast spectrum.

4.5 Conclusions

The results presented in this chapter highlight the impossibility of running a moderated MSR on a closed U-Pu cycle, while it remains possible in the case of a fast spectrum in both fluorides and chlorides. However, the use of a U-Pu cycle in fluoride salts and in a fast spectrum does not provide any substantial advantage over that of a closed Th-U and was thus not further considered.

Moreover, the investigation of several moderators (Be, BeO, Heavy Water, Water and ZrH) yielded no promising alternatives to graphite as for what concerns an isobreeding reactor in a closed fuel cycle. While Be and Heavy Water showed interesting results, the neutronic penalty caused by the necessity of cladding said moderators with a corrosion-resistant material that could separate them from the fuel salts is prohibitive. Additionally, the same investigations conducted with several alternative salts to the reference FLi and FLiBe salts showed no compelling candidate for use in an iso-breeding closed fuel cycle.

The impact of high power densities on the equilibrium-critical isobreeding inventory in the case of a thermal spectrum MSR becomes noticeable in the cases without Pa isolation. Without said separation the necessary inventory exceeds that of a fast spectrum reactor above a power density of 7 W/cm^3 . From a proliferation point of view, it is however preferable to avoid isolation of Pa which produces separated ^{233}U with a high level of purity.

5 Transition to Equilibrium in a Closed Fuel Cycle

5.1 Introduction

In the previous chapter, it was established that the only practical configurations to operate an isobreeding MSR in closed fuel cycle were:

1. Graphite-moderated, fluoride-fueled MSRs,
2. Unmoderated, fluoride-fueled MSRs and
3. Unmoderated, chloride-fueled MSRs.

Representative designs of the first two types were selected based on existing reactors: the single-fluid MSBR and two-fluid MSBR(2f) graphite-moderated reactors designed by ORNL and the two-fluid fast-spectrum MSFR designed by CNRS. For the chloride reactors, three simplified designs based on the results of the previous chapter were established, two using the U-Pu cycle and natural and enriched chloride salts, and one using the Th-U cycle using enriched chloride salt.

In this chapter, the characteristics of these six cores are studied during their transition to equilibrium, including their initial critical load. For this purpose, a logarithmically increasing number of step between cross-section recalculations with Serpent was used while keeping the time step constant at 30 days. The numbers of step for each of the 23 cycles was thus 2, 2, 2, 5, 7, 9, 11, 14, 18, 23, 29, 37, 47, 60, 76, 97, 123, 157, 200, 255, 325, 414 and 528, which gives 73770 days total or 202.11 years.

5.2 Fluoride-fueled Reactors

Of the three selected fluoride-fueled reactor, two are graphite moderated and one is a fast-spectrum reactor. Their main characteristics are given on Table 5.1 and their core layout on Figure 5.1. Their detailed fuel cycle parameters are given in table 5.2.

MSBR(2f), MSBR and MSBR are well-established designs with precise fuel cycle parameters

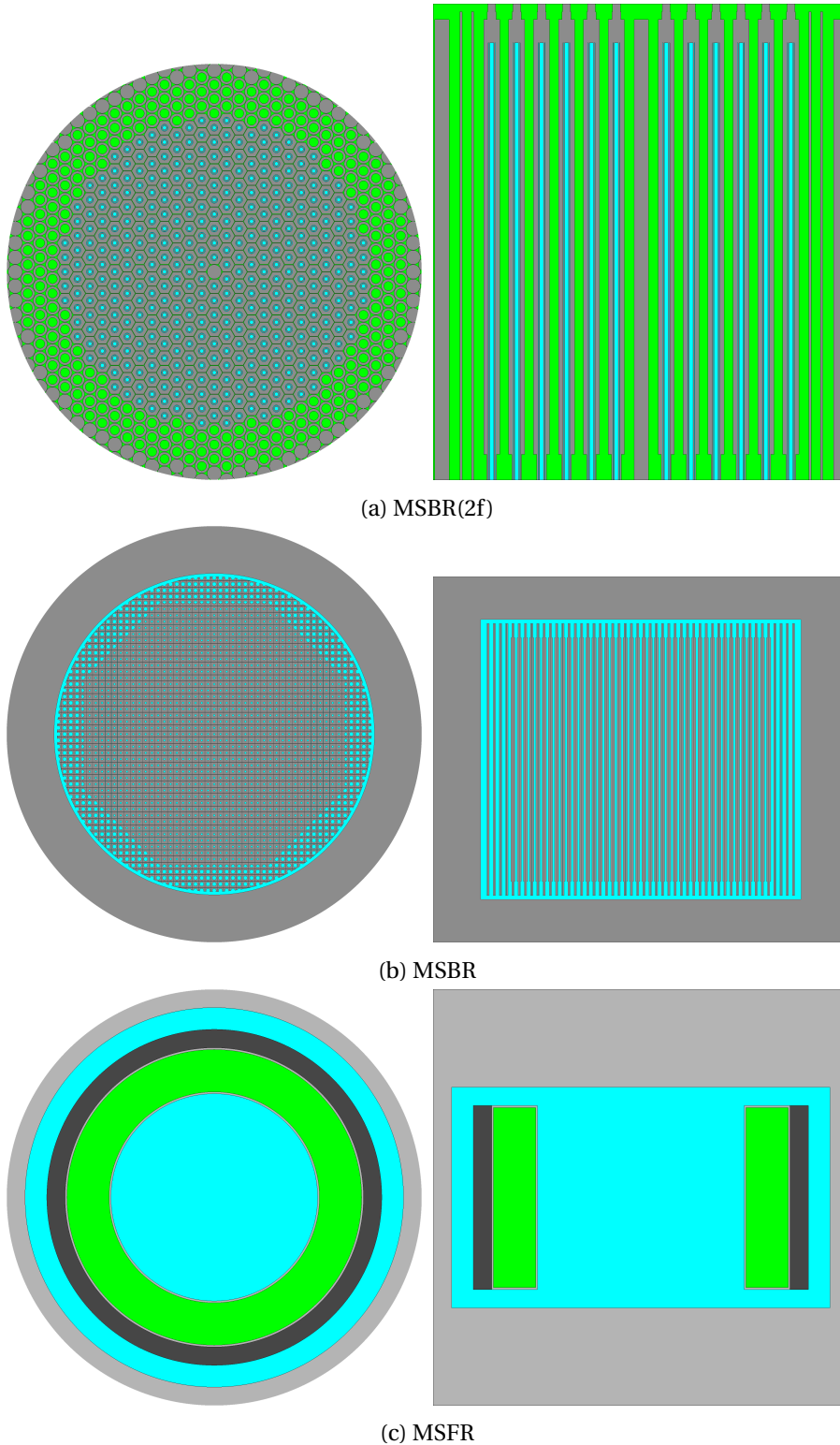


Figure 5.1 – Comparison of the core models of simulated reactors (not to scale). The fuel salt is depicted in light blue, the blanket salt in light green, the graphite in dark gray, structural materials in light gray, and boron carbide in black.

5.2. Fluoride-fueled Reactors

Table 5.1 – Reference characteristics of the fluoride-fueled MSRs used in this chapter.

Reactor	Type	MSBR(2f) ¹	MSBR ²	MSFR ³	MW _{th}
		Two-fluid	Single-fluid, Two-zone	Two-fluid	
	Power	556	2250	3000	
	Moderator	Graphite	Graphite	None	
Dimensions	Core ⁴	4.04 × 3.05	3.96 × 5.25	2.25 × 2.25	m
	Blanket ⁵	0.38	None	0.46	m
	Reflector ⁵	0.15	0.76 (radially)	1.0 (axially)	m
Fuel	Salt	LiF–BeF ₂ –UF ₄	LiF–BeF ₂ –AnF ₄	LiF–AnF ₄	
	Mixture	68.5-31.3-0.2	71.7-16-12.3	77.5-22.5	mol %
	Density	2.03	3.33	4.1	g/cm ³
	Volume	10.5	48.7	18	m ³
Blanket	Salt	LiF–BeF ₂ –ThF ₄		LiF–ThF ₄	
	Mixture	71-2-27	None	77.5-22.5	mol %
	Density	4.4		4.1	g/cm ³
	Volume	19.9		7.7	m ³

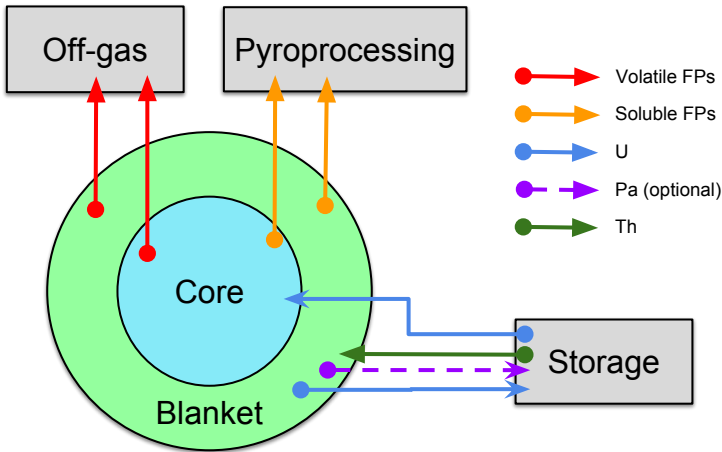
¹ Robertson et al. (1970) ² Robertson (1971) ³ Heuer et al. (2014)

⁴ Height x Diameter ⁵ Thickness

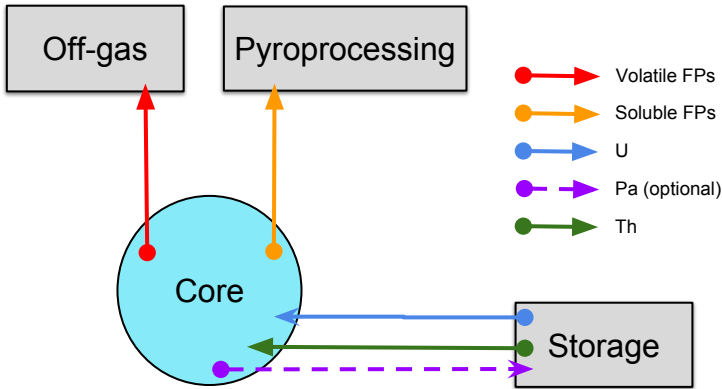
using reference values. Their fuel cycle schemes are depicted on figure 5.2 below and the cycle times used for reprocessing in the models are given in table 5.2.

MSBR(2f) is a pure two-fluid breeder: the fuel salt does not contain Thorium and thus relies exclusively on its blanket for breeding. Optionally, Protactinium can be extracted on a short cycle from the blanket to increase the breeding gain by minimizing parasitic captures on ²³³Pa. Since the fuel salt does not contain Thorium, it can be reprocessed using vacuum distillation which will remove the most important absorbers such as lanthanides. Before distilling the salt the Uranium in it must be removed by fluorination. FPs behavior was assumed to match the more recent MSBR data, notably in terms of solubility of noble metals. Cycle times were taken from Robertson et al. (1970): insoluble FPs are removed with a cycle time of 20 s, while most soluble FPs are removed with a cycle time of 110 d (thus corresponding to a fuel salt processing rate of 95 L/d) and other soluble FPs not removed by distillation (Rubidium, Cesium, Zirconium) with a cycle time of 1825 d to model salt discard. These cycle times apply to both the fuel and blanket. Additionally, Uranium and Protactinium isotopes, if the latter is isolated, are removed from the blanket on a 1.1 d cycle.

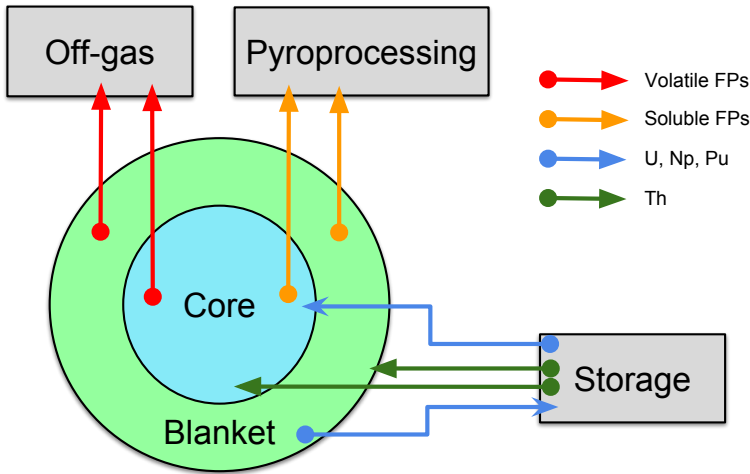
MSBR is a single-fluid breeder and thus breeding takes place in the fuel salt, which therefore



(a) MSBR(2f)



(b) MSBR



(c) MSFR

Figure 5.2 – Comparison of the fuel cycle of MSBR(2f), MSBR and MSFR.

5.2. Fluoride-fueled Reactors

Table 5.2 – Individual cycle times assumed for FPs and equivalent efficiencies in the case of known inventory cycle time.

Group	Nuclides	MSBR(2f)	MSBR	MSFR
Off-gas		20 s	20 s	43 s
Fuel process.		N/A	10 d	450 d
¹⁹ F activ.	N, O	N/A	N/A	43 s
Noble gases	He, Ne, Ar, Rn, Kr, Xe	20 s	20 s	
Noble metals	Ru, Rh, Pd, Ag, Nb, Mo, Tc, Sb, Te Se			450 d (100%)
	Zn, Ga, Ge, As	N/A	N/A	
	Cd, In, Sn	110 d	200 d (5%)	
Zirconium	Zr	1825 d		
Alkali metals	Rb, Cs		3435 d (0.3%)	
Alkali-earths	Sr, Ba	110 d		
Halogens	Br, I		60 d (17%)	
Lanthanides	Y, La, Ce, Pr, Nd, Pm, Sm, Gd Eu Tb		50 d (20%) 500 d (2%) N/A	
	Dy, Ho, Er, Tm, Yb	N/A	N/A	

contains Thorium. MSBR fuel is reprocessed by liquid Bismuth Reductive Extraction (RE) which allows to separate FPs from actinides in a salt containing Thorium. In this model, cycle times for various FP groups based on Robertson (1971) have been applied: 20 s for insoluble FPs, and 50 d for most soluble FPs, while some are removed with a lower efficiency (higher cycle time) and others such as alkali metals and alkali-earth (Rubidium, Strontium, Cesium, Barium) with a 3435 d to simulate salt discard for these nuclides not removed by reductive extraction or fluorination. The actual cycle time of the whole inventory is 10 d, corresponding to a processing rate of 4870 L/d. Finally, Protactinium can be isolated on a 3 d cycle.

MSFR is a two-fluid breeder but the fuel salt contains Thorium along with the blanket salt. The fuel processing scheme used is that of the EVOL benchmark, in which insoluble FPs are removed from the salts by the off-gas system with a 43 s cycle time while soluble FPs are removed on a 450 d cycle (equivalent to a 40 L/d rate) by liquid Bismuth reductive extraction. One major difference compared to MSBR is the removal of alkali metals and alkali-earths by

reductive extraction, which may be possible because of the lack of Beryllium in the fuel salt. Moreover, soluble FPs are removed from the blanket salt with a 19250 d cycle time (0.4 L/d rate). Uranium, Neptunium, and Plutonium are removed from the blanket and fed to the fuel salt on a 192.5 d cycle (40 L/d rate), with an efficiency of 99 % for Uranium and Neptunium and 90 % for Plutonium, respectively.

5.2.1 Initial inventory

First, the question of the beginning-of-life critical load for each reactor must be answered. The natural choice for the first load of a Th cycle reactor is ^{233}U , however, it is currently not readily available in sufficient amounts. Nevertheless, this scenario is applicable to reactors started once a fleet of Th-cycle reactors has been established and thus remains of interest.

For MSBR(2f) and MSBR, the impact of using a different blanket (MSBR(2f)) and fuel (MSBR) salt was investigated. In the case of MSBR(2f) the alternative blanket salt was selected to have a lower Th concentration ($\text{LiF}-\text{BeF}_2-\text{ThF}_4$, 72-14-14 mol % instead of $\text{LiF}-\text{ThF}_4$, with 27 mol % Th). In the case of MSBR, the selected alternative fuel salt was $\text{LiF}-\text{ThF}_4$ (73-27 mol %) for its higher PuF_3 solubility at the cost of a higher melting point.

The initial loads necessary are given in Table 5.3 for the reference salts and Table 5.4 for the alternative salts. Values in italic exceed the maximum PuF_3 solubility in the salt considered. These were computed by increasing the amounts of fissile material in the fuel salt without compensation in the case of MSBR(2f) and compensated for by adjusting the amount of ^{232}Th in the fuel salts in the case of MSBR and MSFR so as to keep the total concentration of actinides constant. Additionally, the loads in the reference salts per unit thermal power are compared on figure 5.3.

Table 5.3 – Initial loads necessary to start each reactor for each start-up fuel using reference salts.

	MSBR(2f)		MSBR		MSFR	
	mol%	kg	mol%	kg	mol%	kg
^{233}U	0.176	253	0.204	1203	2.6	5012
LEU	2.54	3096	1.82	10924	18.4	35688
HEU	0.283	408	0.308	1837	4.525	8778
WG <u>Pu</u>	0.112	161	0.11	666	<i>4.18</i>	<i>8233</i>
LWR <u>Pu</u>	3.2	<i>3761</i>	2.7	16348	<i>5.1</i>	<i>10063</i>
EQL ^a	0.399	566	0.48	2844	4.77	9208

^a Actinide vector at equilibrium, without ^{232}Th

In the case of high-enrichment fuels (^{233}U , HEU, WGPu) the loads are acceptably small and should have a minor impact on the melting point of the fuel salt, while for a LEU start-up, the

Table 5.4 – Comparison of initial loads necessary to start MSBR(2f) and MSBR using alternative salts.

	MSBR(2f) ^a		MSBR ^b	
	mol%	kg	mol%	kg
²³³ U	0.124	178	0.469	226
LEU	1.16	1738	6.1	29872
HEU	0.21	335	0.85	4136
WGPu	0.063	91	0.11	666
LWRPu	1.53	2027	4.99	24682

^a Using a LiF–BeF₂–ThF₄ blanket salt.

^b Using a LiF–ThF₄ fuel salt.

concentration is large enough to influence the melting point and density to some degree, but these were not considered here.

In the case of a LWRPu start-up however, the degraded isotopics impose a high amount of Pu in the fuel salt. The necessary concentrations are all above the solubility limits of the fuel salts of the respective reactors. The solubility limit of PuF₃ in LiF–BeF₂, at the inlet temperature of the MSBR(2f) (Ferris et al., 1971), is approximately 0.3 mol %. In MSBR, it is approximately 0.9 mol % in LiF–BeF₂–ThF₄ at 550 °C (Sood et al., 1975) and in MSFR approximately 3.84 mol % at 600 °C in LiF–ThF₄ (Sood et al., 1975).

A higher PuF₃ solubility can be achieved by changing the salts or increasing the inlet temperatures. In MSBR(2f) the most likely candidate is LiF–ThF₄, and therefore Th would need to be included in the fuel salt, substantially changing the whole reactor concept, because it would not be recovered in the processing scheme of the reactor. In the case of a WGPu start-up however, the critical concentrations of PuF₃ in MSBR(2f) and MSBR are below the solubility limits and thus are feasible, while it is not the case in MSFR.

5.2.2 Equilibrium properties

Having determined the possible start-up fuels and the necessary initial inventories, the characteristics of the closed cycle equilibrium can be studied. The transition to a closed Th cycle equilibrium was computed using ²³³U in the initial load for each reactors.

In this section, the equilibrium properties of the MSBR(2f), MSBR and MSFR designs are presented and compared. Of interest are the equilibrium actinide vector, as well as the influence of the absence or presence of Pa isolation on the breeding performance and production of ²³²U as proliferation barrier.

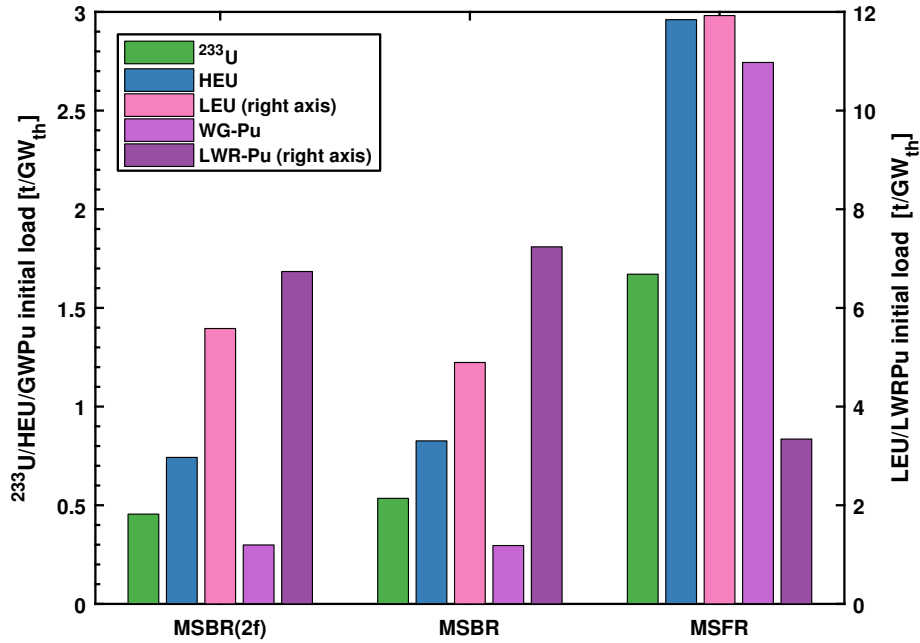


Figure 5.3 – Comparison of initial critical load per thermal power.

Actinide vector

The actinide composition at equilibrium is an intrinsic characteristic of the reactor and fuel cycle couple. On figure 5.4, the masses of major nuclides, with the exception of ^{232}Th in the Th-U cycle is represented per unit of thermal power for all three reactors.

As is evident on the plot, the MSBR(2f) and MSBR are very comparable at equilibrium despite their very different power levels. The equilibrium mass of non- ^{232}Th actinides being proportional to the ratio of the ^{232}Th cross-section to that of the other actinides, it is higher in a fast-spectrum and thus the equilibrium masses are higher for the MSFR. However, the ratios are essentially similar despite spectral differences: ^{233}U makes up approximately half of the non-Th isotopes, ^{234}U makes up a quarter of that and higher actinides the other quarter.

Breeding performance

Breeding performance at equilibrium can be quantified using several indicators, amongst which are:

- the breeding gain, representing the net excess mass of ^{233}U produced per unit of time,
- the fuel yield, the fraction of the initial critical mass produced per unit of time, and
- the doubling time, which is the time needed to accumulate a critical mass at the breeding rate at equilibrium.

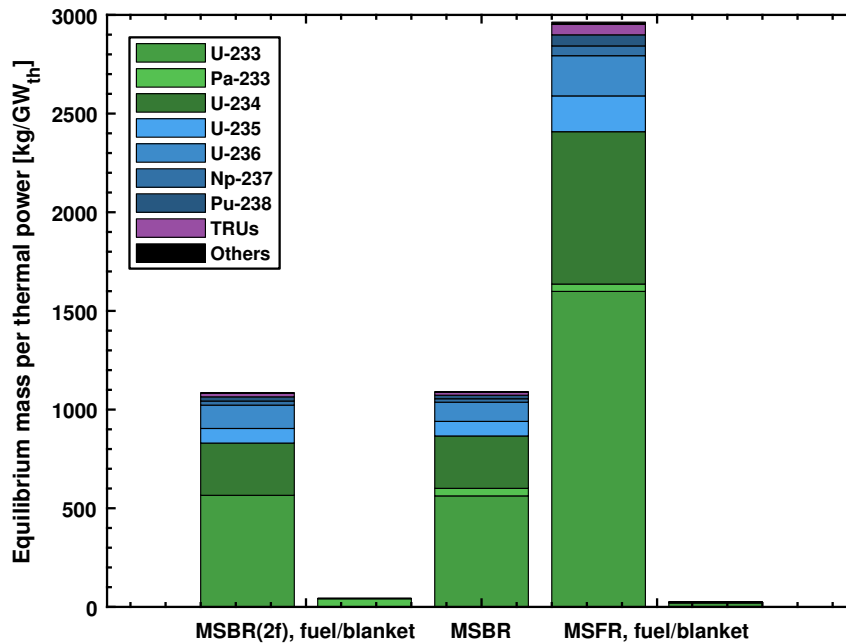


Figure 5.4 – Comparison of nuclide masses in the equilibrium vector.

These parameters are compared between designs and in the presence or absence of Pa separation in table 5.5.

Table 5.5 – Comparison of breeding parameters at equilibrium of the three reactors.

		Without Pa separation			With Pa separation		
		MSFR(2f)	MSBR	MSFR	MSBR(2f)	MSBR	MSFR
Breeding Gain	[kg/EFY]	6.2	17.2	36.2	9.5	69.1	37.5
Fuel Yield	[%/EFY]	2.5	1.4	0.7	3.8	5.7	0.8
Doubling Time	[EFY]	40.7	70.1	138.3	26.5	17.4	133.5

For MSBR(2f) the impact of Pa separation on breeding is substantial, as it nearly doubles the doubling time. However, the 40.7 EFY doubling remains practical in its absence.

In the case of MSBR however, the impact of Pa separation is tremendous, as the doubling time more than triples without it, reaching 70.1 EFY, which is impractical given the very fast processing speed of the reactor.

Pa separation from the blanket has a very limited impact on MSFR, as can be expected due to the fast spectrum and dilution level of the protactinium in the blanket. Pa isolation from the fuel would further decrease the doubling time but the incentives to do so are limited.

^{232}U content in U vector

^{232}U produced in the Thorium cycle is one of the potential barriers to diversion of the fissile U vector because of the strong gamma emitters present in its decay chain. It is produced by four main pathways:

1. $^{233}\text{U} \xrightarrow{n,2n} ^{232}\text{U}$
2. $^{233}\text{Pa} \xrightarrow{n,2n} ^{232}\text{Pa} \xrightarrow{\beta^-} ^{232}\text{U}$
3. $^{232}\text{Th} \xrightarrow{n,2n} ^{231}\text{Th} \xrightarrow{\beta^-} ^{231}\text{Pa} \xrightarrow{n,\gamma} ^{232}\text{Pa}$
4. $^{230}\text{Th} \xrightarrow{n,\gamma} ^{231}\text{Th} \xrightarrow{\beta^-} ^{231}\text{Pa} \xrightarrow{n,\gamma} ^{232}\text{Pa}$

The first three depend on a threshold (n,2n) reaction and the ^{232}U content can therefore be expected to be higher in a fast neutron spectrum. The three last pathways depend on reactions of Pa isotopes and therefore Pa isolation will decrease the ^{232}U content in the U vector. The fourth reaction depends on the presence of ^{230}Th which makes a small fraction of natural Thorium due to the decay of natural ^{238}U . In the present work, cases with up to 200 ppm ^{230}Th in the Th vector were computed to investigate its influence on the ^{232}U production.

The ^{232}U content in the U vector of both fuel and storage for all three reactors in the absence or presence of Pa isolation and ^{230}Th in the Thorium vector are depicted on figure 5.5.

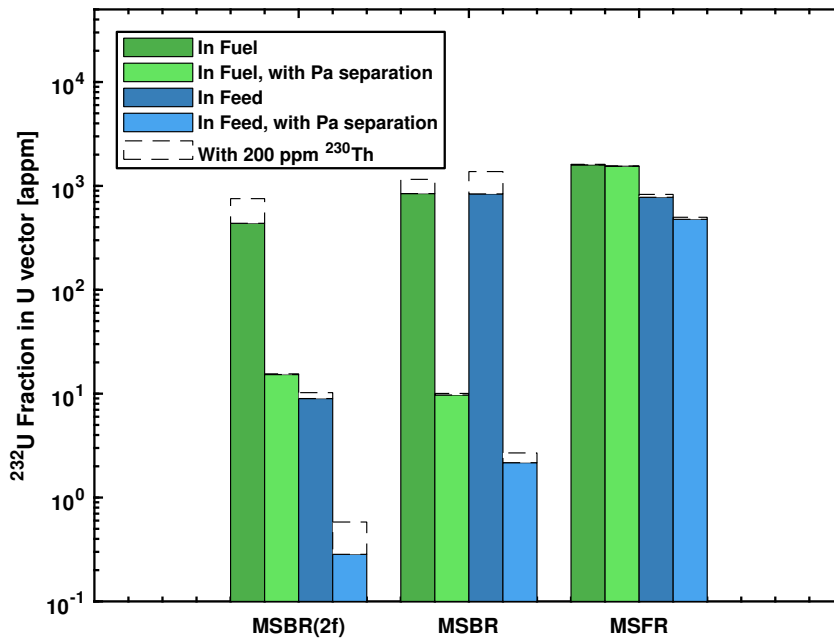


Figure 5.5 – Comparison of ^{232}U content in fuel and feed materials at equilibrium.

The ^{232}U fraction is highest (1600 ppm in the fuel for the base case) for the MSFR due to its fast spectrum, and this fraction is practically unaffected by Pa removal or the presence of ^{230}Th in the Thorium vector because the $^{233}\text{U}(n,2n)$ reaction dominates in this spectrum.

In the cases of MSBR(2f) and MSBR the ^{232}U contents are 440 and 840 ppm in the fuel for their respective base cases. This amount is substantially reduced by Pa isolation and decreases by two orders of magnitude to values as low as 0.2 and 2 ppm in the feed, respectively. The amount is practically doubled by the presence of ^{230}Th in the Th vector: it becomes 732 ppm and 1170 ppm in the fuel and 0.4 ppm and 3.5 ppm in the case of Pa isolation, respectively.

According to Kang and Hippel (2001), the ^{232}U content necessary to fulfill the International Atomic Energy Agency (IAEA)'s self-protection standards for fissile material (dose rate of 1 Svkg/h at 1 m), is 2.4% (24000 ppm). Given the values depicted on figure 5.5, one can conclude that the U in the system is far from those requirements and as such the separation of Pa should be avoided in the fuel cycle.

5.2.3 Transition to equilibrium state

Having ascertained the possibility of starting each of the reactors using each potential fuels, the transition to a closed Th-cycle equilibrium can be computed.

In the following calculations, each reactor is loaded with a critical amount of a given fuel and fed with the bred ^{233}U and a complement of the selected fuel to keep the reactor critical. Once the reactor can breed sufficient amounts of ^{233}U to sustain itself, the complementary feed is removed and the excess ^{233}U bred is removed and stockpiled.

Cumulative fuel mass inserted

The transition scenarios have two phases:

1. all bred ^{233}U is also fed to the fuel and the feed material is used to bridge the gap and keep the reactor critical,
2. once the bred ^{233}U is sufficient to keep the reactor critical on its own, the excess amount produced, if any, is stored.

The first quantity of interest is the cumulative amount of feed material that needs to be fed along its self-bred ^{233}U to the reactor to keep it critical until excess production of ^{233}U can be achieved. It is depicted on figure 5.6.

Contrarily to the initial load necessary, the subsequent amounts of fuel needed are comparatively small in the case of the fast-spectrum MSFR, compared to MSBR(2f) and MSBR. From the point of view of the fed quantities, no reasonable transition could be achieved using LEU in MSBR(2f) and MSBR, while a questionable transition can be achieved using LWRPu in MSBR(2f) but not in MSBR. In MSFR however, a transition can be practically reached in all cases, including LEU, because it can efficiently breed from ^{238}U . In the thermal-spectrum reactors, HEU performs better than WGPu, while the opposite is true in MSFR, due to the larger neutron budget of plutonium in a fast spectrum. Moreover, the amounts fed per unit

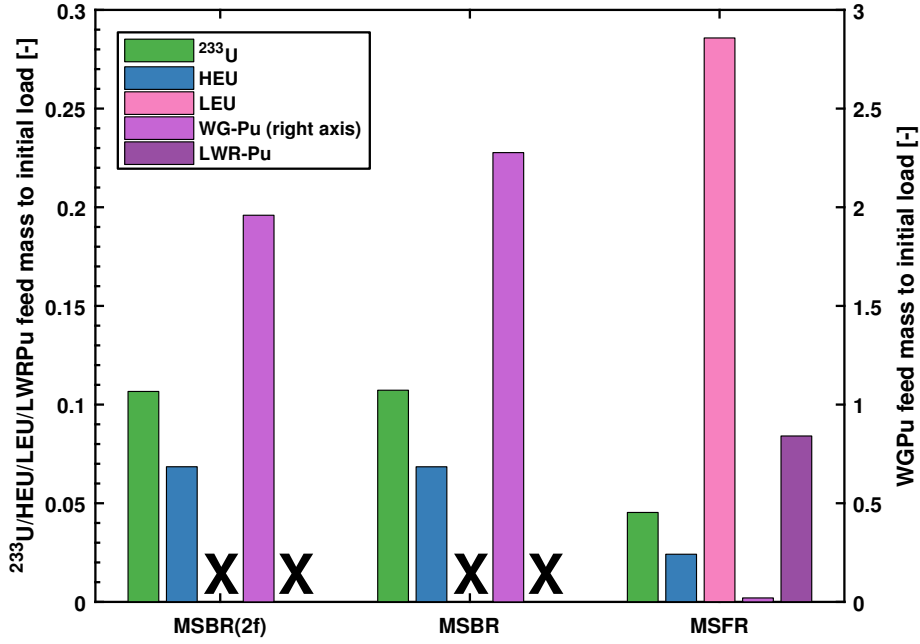


Figure 5.6 – Cumulative mass of each feed necessary to reach excess ²³³U production relative to initial load.

thermal power are comparable for MSBR(2f) and MSBR.

Neutron balance evolution

Detailing the contribution of each nuclide to the neutron balance further informs on the performance of each feed material. Assuming $k_{\text{eff}} = 1$, one has:

$$\bar{\nu} - 1 = \sum_i \frac{C_i}{F} + \frac{L}{F} \quad (5.1)$$

in which $\bar{\nu}$ is the average number of neutrons per fission, C_i the capture rate of nuclide i , L the leakage rate and F the total fission rate. Using this equation the number of neutron lost to leakage and to capture on individual nuclides can be explicated. This decomposition is given on figure 5.7 for all three reactors for the ²³³U-started scenario, figure 5.8 for the enriched uranium scenarios, and 5.9 for the Plutonium-started scenarios. It must be noted that in the case of MSFR, the thick axial Nickel-based alloy reflectors decrease leakage to a minimum and its contribution is thus barely visible.

An important target for a Th cycle breeder is that at least a neutron be captured on ²³²Th, which is visibly the case at equilibrium in all scenarios. However at the beginning of some scenarios too many neutrons are consumed by individual nuclides, such as in the case of

WGPu-started scenarios in thermal spectrum. In this particular case several years are needed to consume the Pu isotopes that absorb too many neutrons, explaining the larger mass of feed needed in that particular scenario and this despite the increase in $\bar{\nu}$ due to the presence of plutonium. In the HEU-started scenarios however, the ^{232}Th capture remains above unity.

As for the MSFR the opposite effect is true: in the MSFR spectrum the ^{235}U absorption is visibly higher while not contributing to a substantial increase of the overall $\bar{\nu}$ as is visible in the HEU-started scenario. In the LEU-started scenario, the ^{232}Th capture is substantially below unity, but is compensated by the ^{238}U capture, producing Pu isotopes that temporarily increase the neutron budget, however making the transition extremely long. The balance of the Pu-started scenarios is quite similar, even though the decrease in ^{232}Th capture is quicker in the LWRPu case. Additionally, more neutrons are lost to transplutonium nuclides.

Conversion ratio

To explain the difference in performance of the different possible feeds, one may turn to the conversion ratio, defined as the ratio of fissile nuclides created by decay of intermediate nuclides such as ^{233}Pa and ^{239}Np or direct capture on nuclides such as ^{234}U and ^{240}Pu to fissile nuclides destroyed by fission and capture:

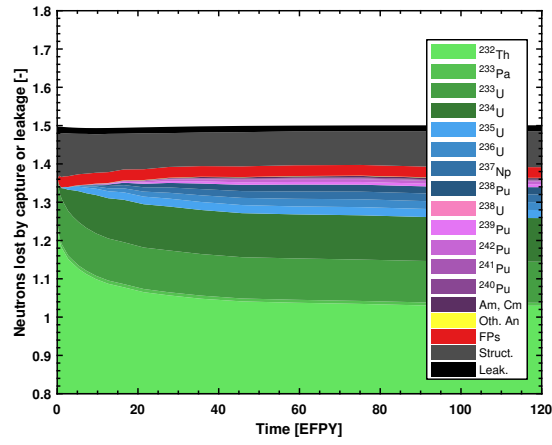
$$\text{CR} = \frac{\lambda_{\text{Pa}} N_{\text{Pa}} + \lambda_{\text{Np}} N_{\text{Np}} + \sum_{\text{oth. fertile}} C_i}{\sum_{\text{fissile}} (F_i + C_i)} \quad (5.2)$$

The results of this computation are depicted on figure 5.10 below. Regardless of the reactor considered, the ^{233}U -started scenarios reach a positive breeding gain the fastest due to the excellent fission probability of ^{233}U compared to other fissile nuclides. In the thermal-spectrum reactors the HEU-started cases reach a conversion ratio above unity quicker than the WGPu scenarios, thus explaining the larger amounts of feed needed in the latter cases. LEU-started cases in thermal spectrum however never reach a positive breeding gain, explaining the ever increasing amounts of feed necessary in those cases. In MSFR the situation is reversed and Pu-started scenarios reach a positive breeding gain faster than HEU and LEU-started scenarios.

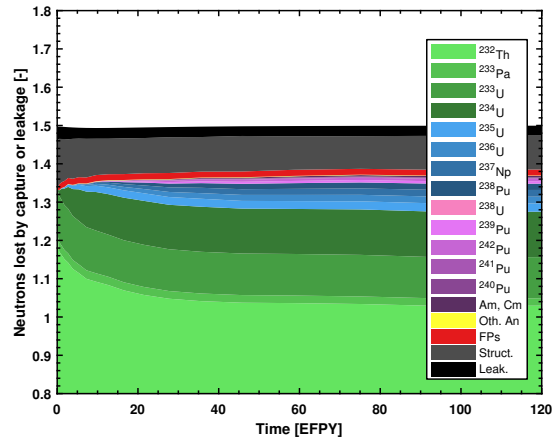
Doubling time

Once the addition of the respective feed of each scenario has stopped, the excess uranium, mostly ^{233}U produced is removed from the fuel or the blanket of the reactor and stockpiled. The evolution of the ^{233}U stockpile can be compared to the initial amount of ^{233}U needed for reactor start-up (see figure 5.11) and the time needed to reach this quantity, called the first doubling time.

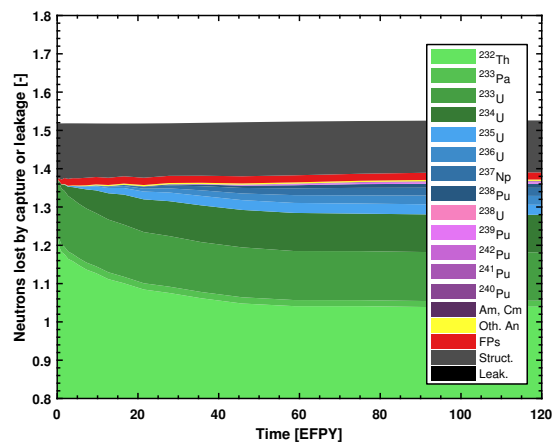
The shortest first doubling times are achieved in the case of the MSBR(2f) which combines a



(a) MSBR(2f)

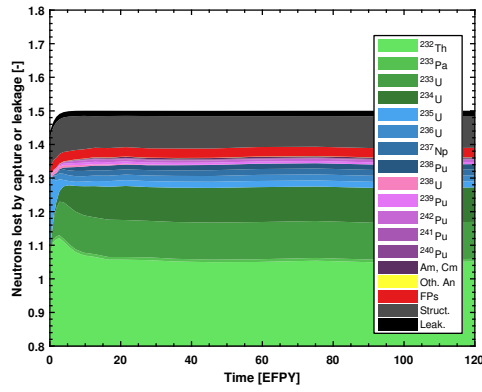


(b) MSBR

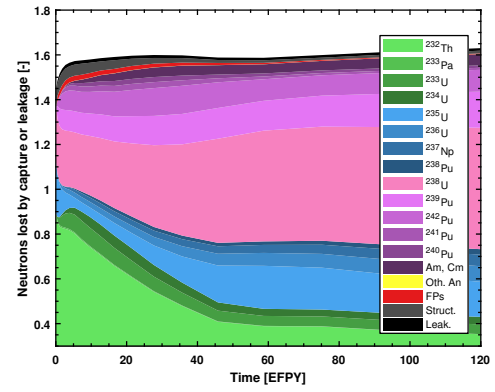


(c) MSFR

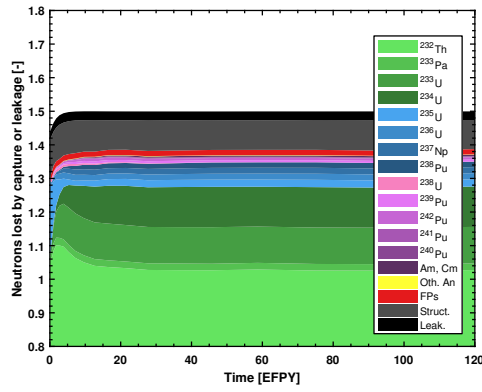
Figure 5.7 – Neutrons per fissions consumed by capture or leakage in each reactor in the ^{233}U -based transition scenarios.



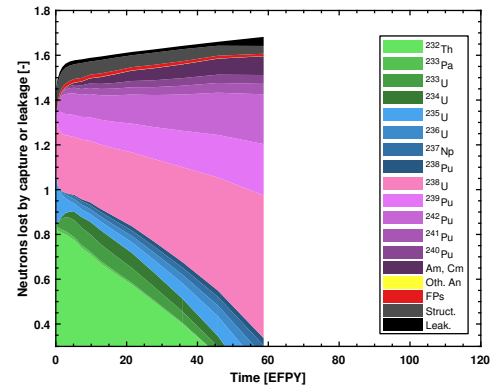
(a) MSBR(2f), HEU



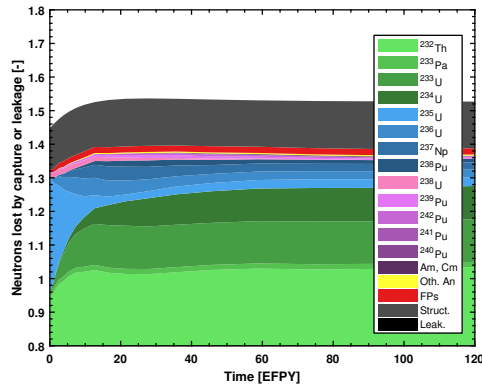
(b) MSBR(2f), LEU



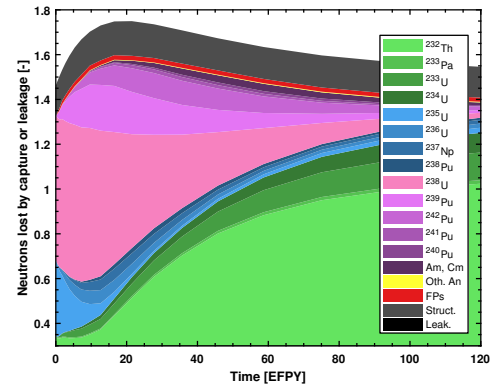
(c) MSBR, HEU



(d) MSBR, LEU



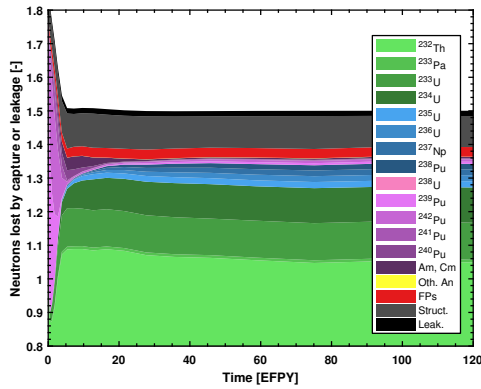
(e) MSFR, HEU



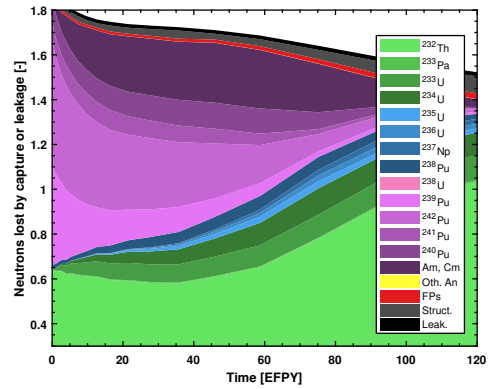
(f) MSFR, LEU

Figure 5.8 – Neutrons per fissions consumed by capture or leakage in each reactor in the enriched Uranium-based transition scenarios.

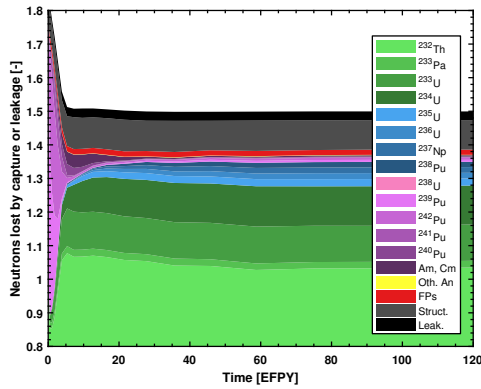
Chapter 5. Transition to Equilibrium in a Closed Fuel Cycle



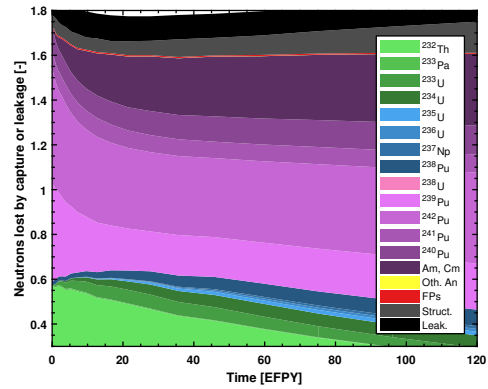
(a) MSBR(2f), WGPu



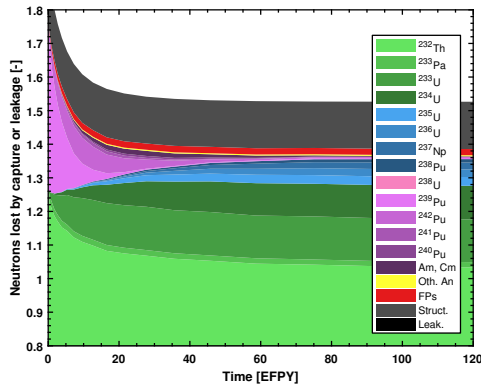
(b) MSBR(2f), LWRPu



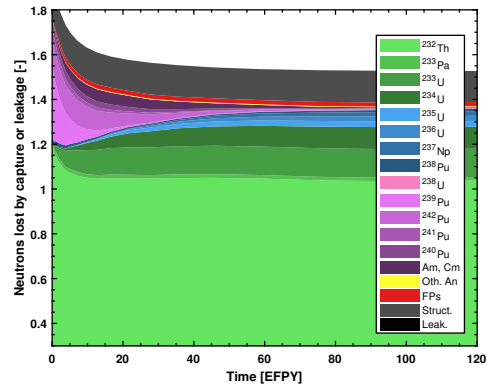
(c) MSBR, WGPu



(d) MSBR, LWRPu

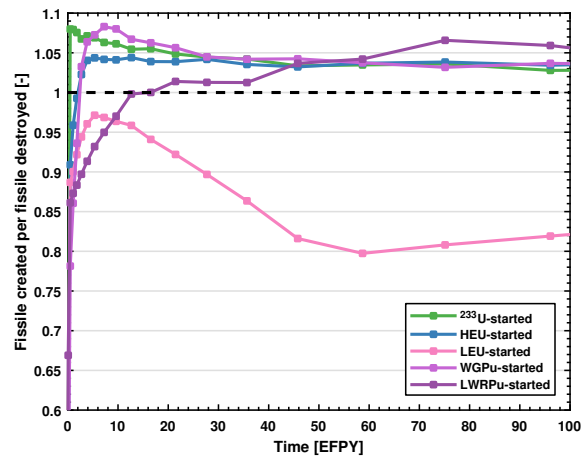


(e) MSFR, WGPu

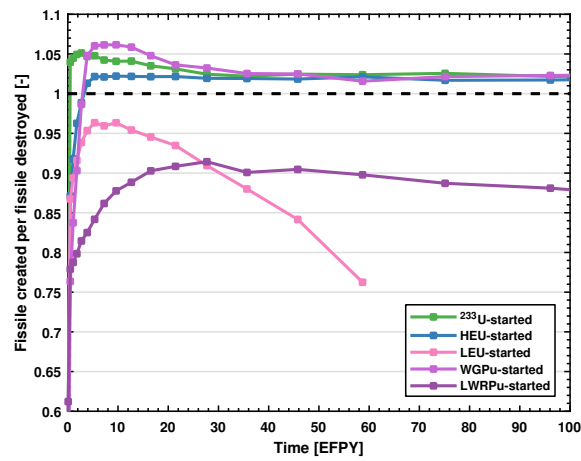


(f) MSFR, LWRPu

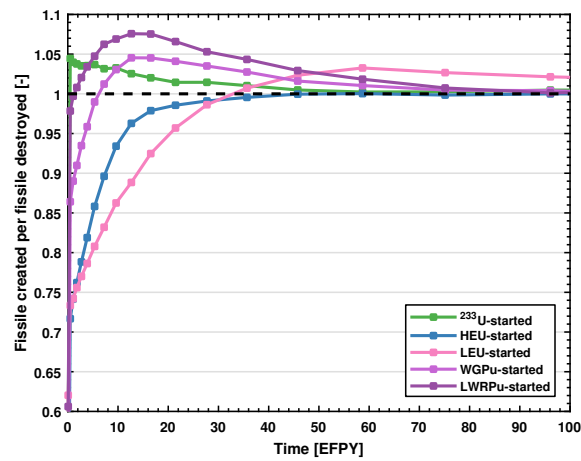
Figure 5.9 – Neutrons per fissions consumed by capture or leakage in each reactor in the Plutonium-based transition scenarios.



(a) MSBR(2f)

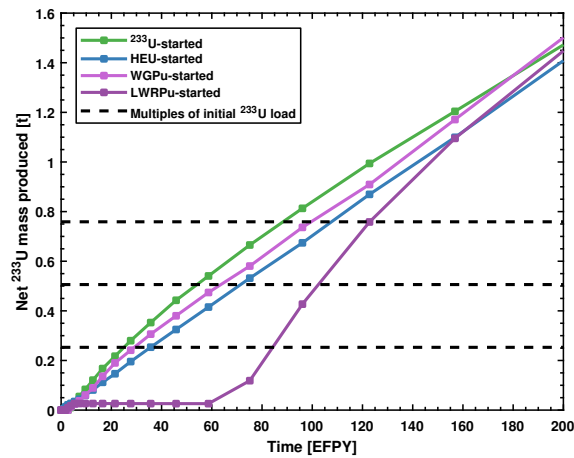


(b) MSBR

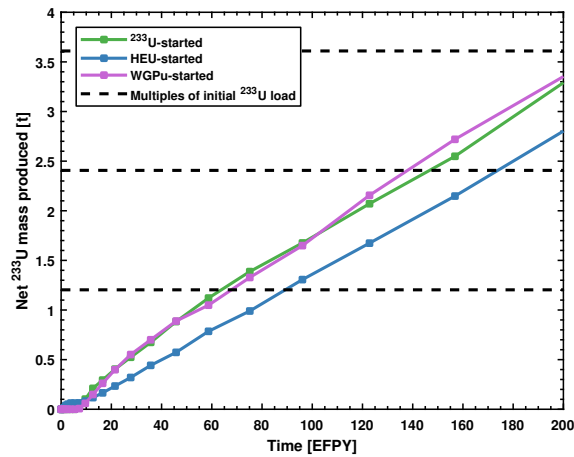


(c) MSFR

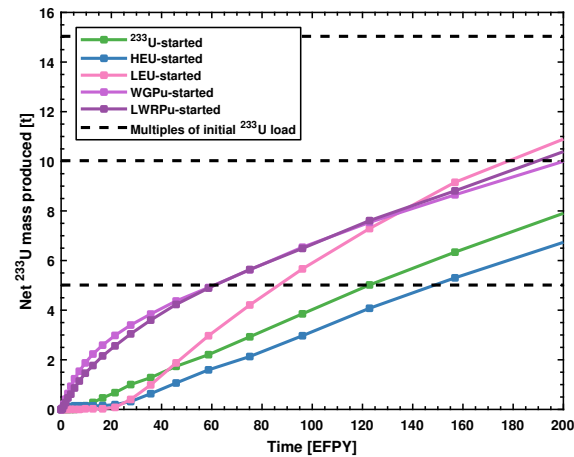
Figure 5.10 – Conversion ratio of all three reactors in different feed scenarios as function of time.



(a) MSBR(2f)



(b) MSBR



(c) MSFR

Figure 5.11 – Net ^{233}U mass produced during the transition and corresponding doubling times.

low initial inventory with substantial breeding capability due to its breeding blanket, while the longest doubling times are achieved with the MSFR due to the large initial inventory and comparatively low reprocessing rate and thus low breeding rate of this particular case. Regarding differences between feed materials, LEU and HEU-based scenarios generally have longer doubling time than WGPu- and LWRPu-based scenarios in the case of MSFR, which is explained by the large neutron budget of Pu isotopes. In the case of the LWRPu transition in MSBR(2f) however, the poorer fissile quality of the Pu vector substantially increases the doubling time.

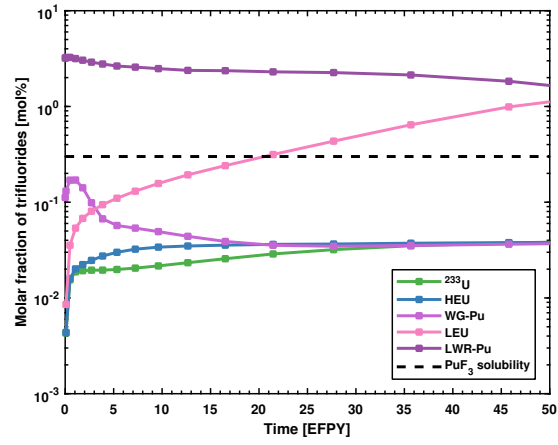
Concentration of trifluorides

The solubility limit for PuF_3 was discussed previously in the context of the initial inventory of each reactor in Pu-started scenarios. However, it is often considered that all trifluoride-forming elements (mostly transuranics and lanthanides) share the same solubility limit. It is thus possible for scenarios started with other nuclear fuels to produce sufficient amounts of trifluorides to exceed the solubility limit.

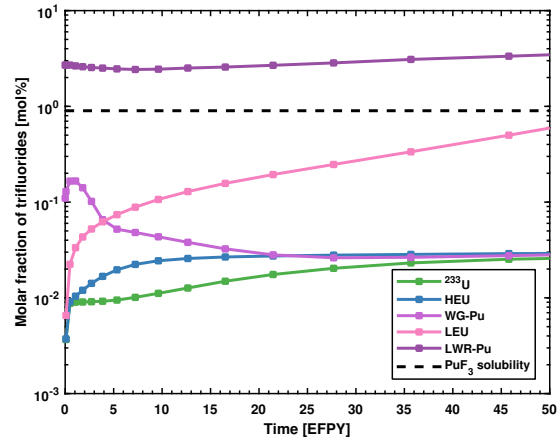
The evolution of the concentration of trifluorides during each transition scenario and the solubility limit of PuF_3 corresponding to the fuel salt of interest are depicted on figure 5.12.

In MSBR(2f) the solubility limit is exceeded at Beginning of Life (BOL) in the LWRPu-started scenario and after approximately 20 EFPY in the LEU-started scenario. In MSBR, the LWRPu scenario suffers from a similar limitation and the LEU-started scenario reaches the solubility limit shortly after 50 EFPY, further invalidating this scenario.

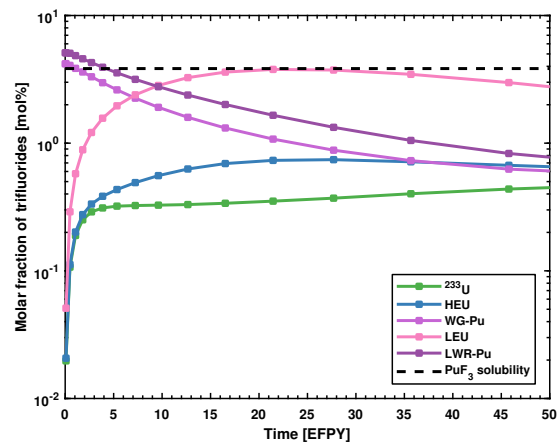
In MSFR both the WGPu and LWRPu scenarios have PuF_3 content above the solubility limit at BOL, but the solubility limit is also reached in the case of a LEU start-up after approximately 20 EFPY.



(a) MSBR(2f)



(b) MSBR



(c) MSFR

Figure 5.12 – Molar concentration of trifluorides during transition to equilibrium compared to the PuF_3 solubility limit in simulated reactors.

5.3 Chloride-fueled Reactors

For comparison with fluoride-fueled reactors, simplified single-fluid chloride-fueled reactors were investigated. As they are fueled with chloride salts, solubility of Plutonium is sufficient and that of Transplutonium elements is not expected to be problematic. Three cases were selected for further investigation: two in a closed U-Pu cycle using natural and enriched chlorine, and one in a Th-U cycle using enriched chlorine. Their characteristics are given on table 5.6 and their simple core layout on figure 5.13 below. As for fuel cycle parameters, the same values as that of MSFR were used.

Table 5.6 – Characteristics of the chloride-fueled configurations used in this section.

		U-Pu natural Cl	U-Pu enriched Cl	Th-U enriched Cl
Reactor	Type	Single-fluid	Single-fluid	Single-fluid
	Power	3000 MW _{th}	3000 MW _{th}	3000 MW _{th}
	Moderator	None		
Fuel	Salt	NaCl–UCl ₃	Na ³⁷ Cl–U ³⁷ Cl ₃	Na ³⁷ Cl–Th ³⁷ Cl ₄
	Composition	68-32 mol %	68-32 mol %	50-50 mol %
	Density	3.32 g/cm ³	3.32 g/cm ³	3.32 g/cm ³
	Volume	134 m ³	19.1 m ³	65.8 m ³
Blanket		None		

The thermal power of 3000 MW_{th} was chosen by analogy with the fluoride-fueled MSFR. The cores are composed of a cylindrical cavity filled with the fuel salt and surrounded on all side by a 100 cm thick Hastelloy N reflector, in a layout similar to that of the MSFR by replacing blankets with a radial reflector. The cooling loops and their fuel volume were neglected for simplicity. The cores were dimensioned to be isobreeding in a closed fuel cycle on a 450 d cycle time for soluble fission products, similarly to MSBR.

5.3.1 Initial inventory

Due to the absence of major limitations on the TRU chloride content in the fuel, the chloride-fueled concepts were only considered for start-up with LWR TRU. The initial loads in mass and molar units are given on table 5.7 below.

The initial fissile inventories are noticeably larger than that of the MSFR due to the large

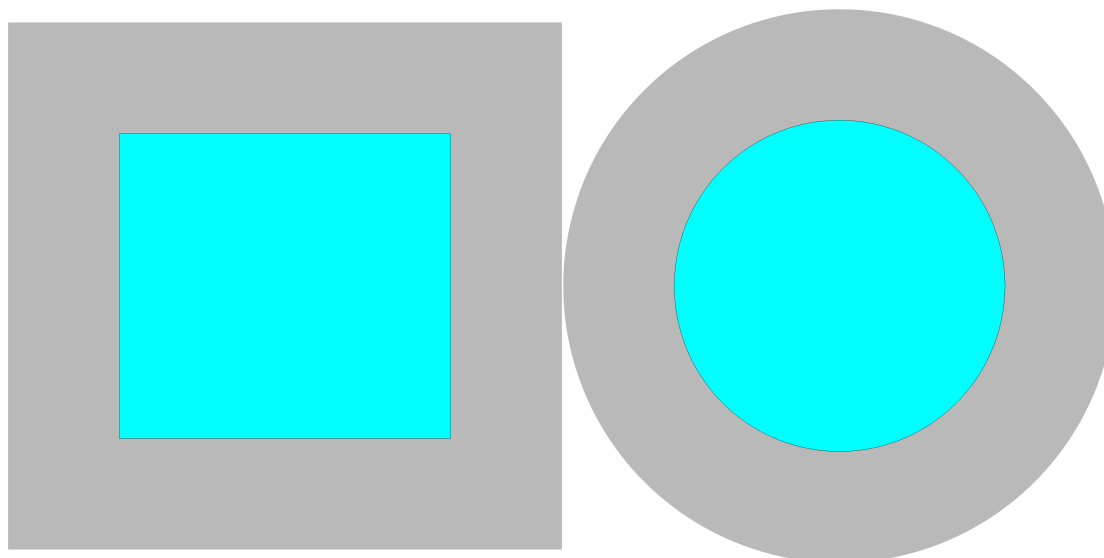


Figure 5.13 – General core model used for chloride-fueled reactors. The fuel salt is depicted in light blue and structural materials in light gray.

Table 5.7 – Initial TRU loads necessary to start each chloride concept.

	U-Pu-nat		U-Pu-enr		Th-U-enr	
	mol%	kg	mol%	kg	mol%	kg
TRU	7.92	22455	7.15	7128.5	9.98	24084
Np	0.55	1532	0.49	486	0.69	1644
Pu	6.23	17666	5.63	5609	7.85	18948
Am	1.12	3210	1.02	1019	1.42	3443
Cm	0.02	45.8	0.01	14.5	0.02	49
²³⁸ U	24.08	67807	24.85	24600		
²³² Th					40.03	93556

5.3.2 Equilibrium

Actinide vector

The actinide composition at equilibrium is an intrinsic characteristic of the reactor and fuel cycle couple. On figure 5.4, the masses of major nuclides, with the exception of ²³²Th in the Th-U cycle is represented per unit of thermal power for all three reactors.

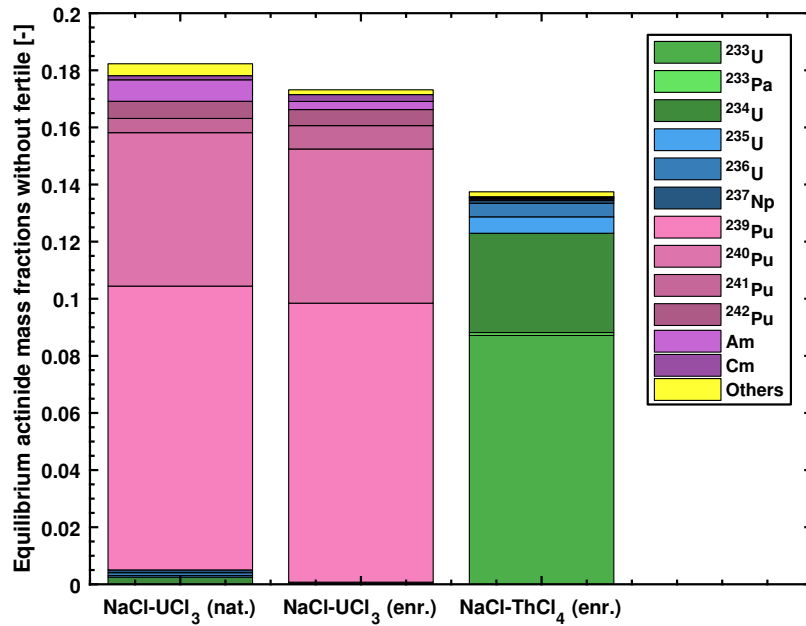


Figure 5.14 – Comparison of nuclide masses in the equilibrium vector of chloride-fueled designs.

5.3.3 Transition to equilibrium state

Similarly to the fluoride-fueled reactors case, the three chloride-fueled cores were depleted to equilibrium. Criticality was adjusted by adding more TRU fuel if the core became subcritical, while it was adjusted by removing excess Plutonium for the Uranium-Plutonium cycle cases or Uranium for the Thorium-Uranium cycle case.

Conversion ratio

The conversion ratio can be computed in a similar manner to what was done for the fluoride-fueled reactors using equation (5.2). The results are depicted on figure 5.15.

It is manifest that the conversion ratio exceeds unity from the very beginning of the transition, which is explained by the very high breeding capability of these cores and their very high tolerance to TRUs due to the very hard neutron spectrum. Interestingly, breeding is able to compensate for the initial reactivity loss due to the appearance of fission products and initial depletion of the fuel so that no fuel insertion must be carried out to keep the reactor critical in any of the three cases presented here.

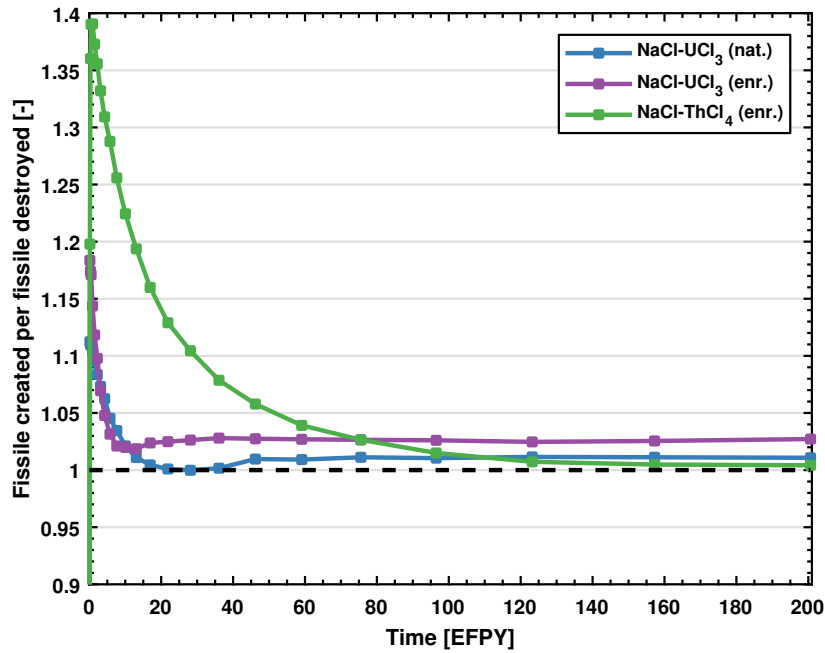


Figure 5.15 – Conversion ratio of chloride reactors during transition.

Neutron balance evolution

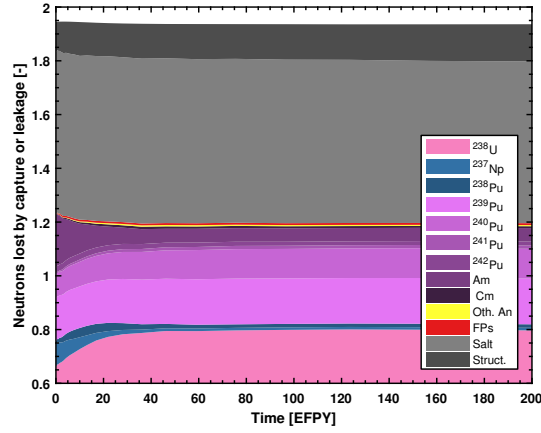
The evolution of the neutron balance can also be computed for the chloride cases using equation (5.1). The results are depicted on figure 5.16.

The neutron balance essential stabilizes after 40 EFPY for the two Uranium-Plutonium cycle reactors, while it takes more than 140 EFPY for the Thorium-Uranium cycle. Unsurprisingly, nearly 0.6 neutrons per fission are captured by the fuel salt using natural chlorine, a much more substantial fraction than in the case of the fluoride reactors investigated before. In all cases however, another substantial capture of neutrons happens in the structural materials (vessel and reflector).

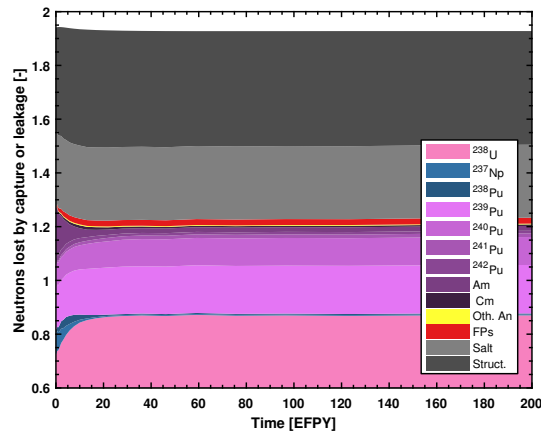
Excess fissile mass generated

The investigated cores were dimensioned according to the equilibrium results obtained in an infinite lattice in the study presented in the previous chapter and are thus expected to be close to isobreeding. However, the reactors are kept critical during the transition by insertion (if subcritical) or removal (if supercritical) of fissile material from the fuel. The net amount of fissile removed in all three cases as a fraction of the initial Pu load is depicted on figure 5.17.

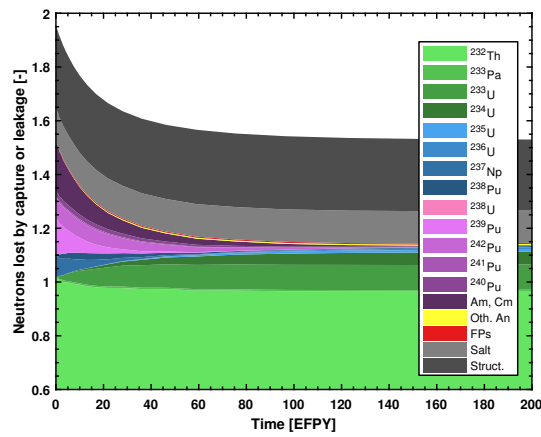
The amount of excess fissile material produced is thus less than 0.05 % of the initial Plutonium load, confirming the essentially isobreeding behavior of the reactors.



(a) NaCl–UCl₃ (nat.)



(b) NaCl–UCl₃ (enr.)



(c) NaCl–ThCl₄ (enr.)

Figure 5.16 – Neutrons per fissions consumed by capture or leakage in each reactor in the transition scenario.

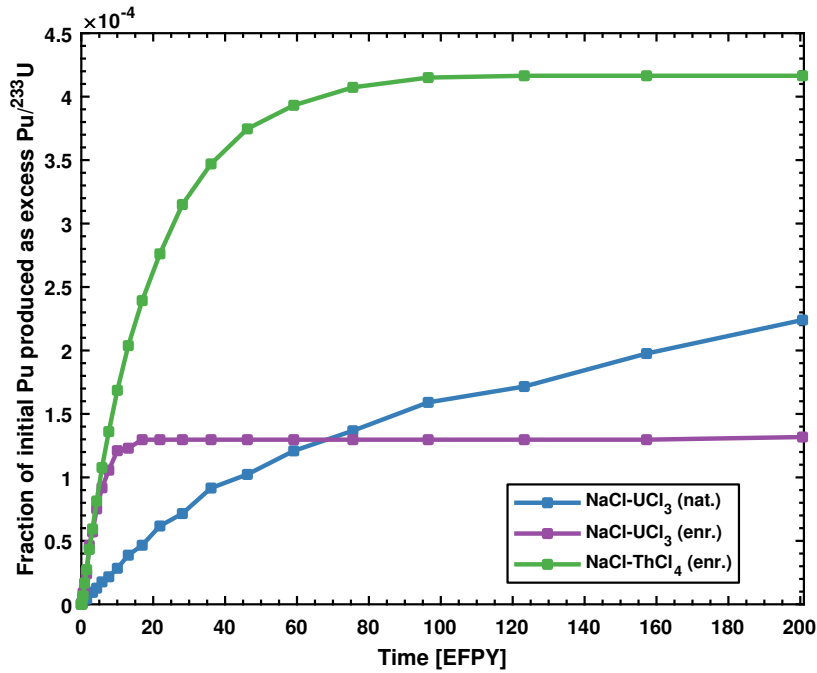


Figure 5.17 – Excess fissile material generated in chloride-fueled reactors transition.

Sulfur production

Sulfur isotopes are produced by irradiation of chlorine isotopes through several reactions, amongst which are:

1. $^{35}\text{Cl} \xrightarrow{n,p} ^{35}\text{S} \xrightarrow{\beta^-} ^{35}\text{Cl}$
2. $^{37}\text{Cl} \xrightarrow{n,p} ^{37}\text{S} \xrightarrow{\beta^-} ^{37}\text{Cl}$
3. $^{35}\text{Cl} \xrightarrow{n,\gamma} ^{36}\text{Cl} \xrightarrow{\beta^-} ^{36}\text{S}$
4. $^{37}\text{Cl} \xrightarrow{n,2n} ^{36}\text{Cl} \xrightarrow{\beta^-} ^{36}\text{S}$
5. $^{35}\text{Cl} \xrightarrow{n,2n} ^{34}\text{Cl} \xrightarrow{\beta^+} ^{34}\text{S}$
6. $^{35}\text{Cl} \xrightarrow{n,\alpha} ^{32}\text{P} \xrightarrow{\beta^-} ^{32}\text{S}$
7. $^{36}\text{Cl} \xrightarrow{n,\alpha} ^{33}\text{P} \xrightarrow{\beta^-} ^{33}\text{S}$
8. $^{37}\text{Cl} \xrightarrow{n,\alpha} ^{34}\text{P} \xrightarrow{\beta^-} ^{34}\text{S}$

In the case of a natural chlorine, the (n,γ) reaction on ^{35}Cl , having a large and non-threshold reaction could be expected to dominate the production of sulfur isotopes, however the long half-life of ^{36}Cl precludes this. Instead, the (n,α) reactions on ^{35}Cl and ^{37}Cl dominate the production because of their relatively large cross-sections. The concentration of all sulfur isotopes in the fuel salts is depicted on figure 5.18 below.

Obviously, the natural chlorine case show the highest concentration which becomes close to 1 mol% after 200 EFPY, a very substantial amount susceptible of being a problem for the

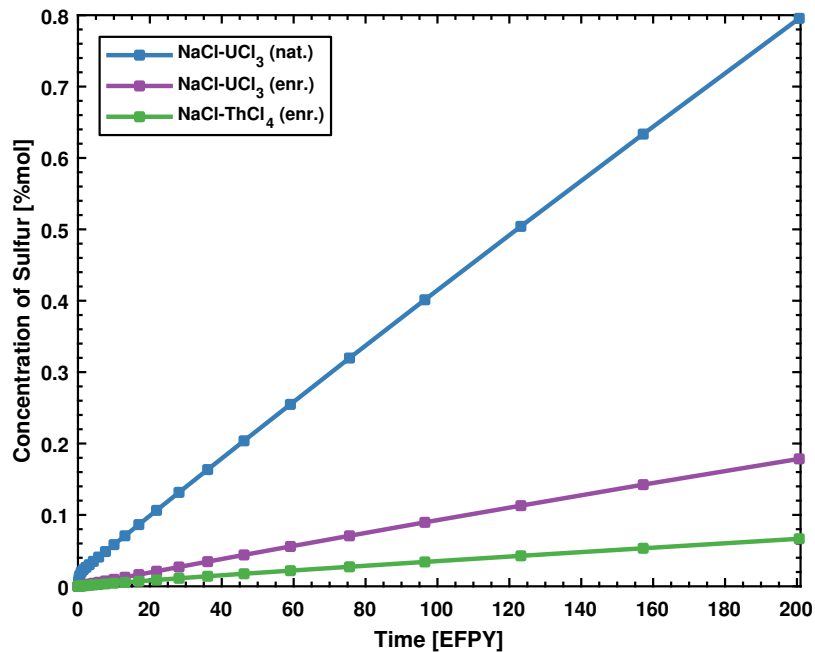


Figure 5.18 – Sulfur production in chloride reactors.

reactor. In this simulation however, it was supposed that no process would remove sulfur from the fuel, which is a conservative assumption since it could be removed by fuel processing.

5.4 Conclusions

Based on the conclusions of the previous chapter, existing thermal- and fast-spectrum fluoride-fueled concepts in a closed Thorium-Uranium were selected and their initial inventories, equilibrium properties and transition to equilibrium using several potential fuels were investigated without substantial changes to their designs.

The results show that the limitations on the solubility of transuranics forming trifluorides is a severely limiting factor in fueling these reactors using SNF Plutonium or TRUs. In all three reactors, the inventories necessary for start-up exceeded the limit. In the thermal-spectrum reactors, WGPu could be used as an alternative, but the applicability of this scenario is limited to disposal of Plutonium from dismantled nuclear weapons.

Additionally, further problems were encountered when using alternative start-up fuels such as LEU. In MSBR(2f), the transition necessitated excessive amounts of LEU to be able to proceed. In MSBR, the transition proved impossible because LEU had to be inserted to the point of removing all ^{232}Th from the fuel salt, defeating the purpose of the reactor. In MSFR, the solubility limit of the bred PuF_3 was reached after several years. Alternatively, HEU could

Chapter 5. Transition to Equilibrium in a Closed Fuel Cycle

be used to fuel these reactors, but proliferation concerns make this solution rather unlikely.

Nevertheless, the fast-spectrum concept showed the best potential in transitioning to a closed fuel cycle from SNF actinides and thus could be considered for optimization by changing the fuel salt composition to increase the solubility of trifluorides. Possible routes include the decrease of the Thorium fraction in the salt or the introduction of other elements in the salt mixture.

Alternatively, simplified chloride-fueled concepts were drawn from the calculations of the previous chapter. Three separate configurations using natural chlorine in a Uranium-Plutonium cycle, enriched chlorine in the same cycle, and enriched chlorine in a Thorium-Uranium cycle were laid out using parameters similar to that of the MSFR.

All three configurations proved capable to transitioning to a closed fuel cycle using TRU as initial fuel and without necessitating further fuel make up. However, the configuration with the smallest inventory was obtained using enriched chlorine in a Uranium-Plutonium cycle, with an in-core volume twice as large as that of MSFR, a substantial penalty.

Nevertheless, in view of the incineration of existing waste, initial inventories may not be of importance, unless one desires to maximize the amount of power generated from a fixed stockpile.

Finally, the amount of radiotoxicity created by reactors operating on a closed cycle at equilibrium can be compared by assuming a given amount of actinide losses and compared to the production of radiotoxicity from discharged actinides from LWR SNF. Actinide losses of 1 % and 0.1 % were assumed. The results of this computation are given on figure 5.19 below.

Most configurations are thus producing less waste through losses per unit power generated than that of actinides from LWR SNF except that of the $\text{NaCl}-\text{UCl}_3$ fueled by natural chlorine with 1 % losses. The same configuration with 0.1 % losses shows a reduction of the radiotoxicity generated by one order of magnitude, along with the enriched chlorine and MSFR cases with 1 % losses. The latter configurations with 0.1 % losses show a reduction of the radiotoxicity by two orders of magnitude compared to LWR SNF. The enrichment of chlorine may thus prove advantageous if the efficiency of the separation processes cannot be brought as high as 99.9 %.

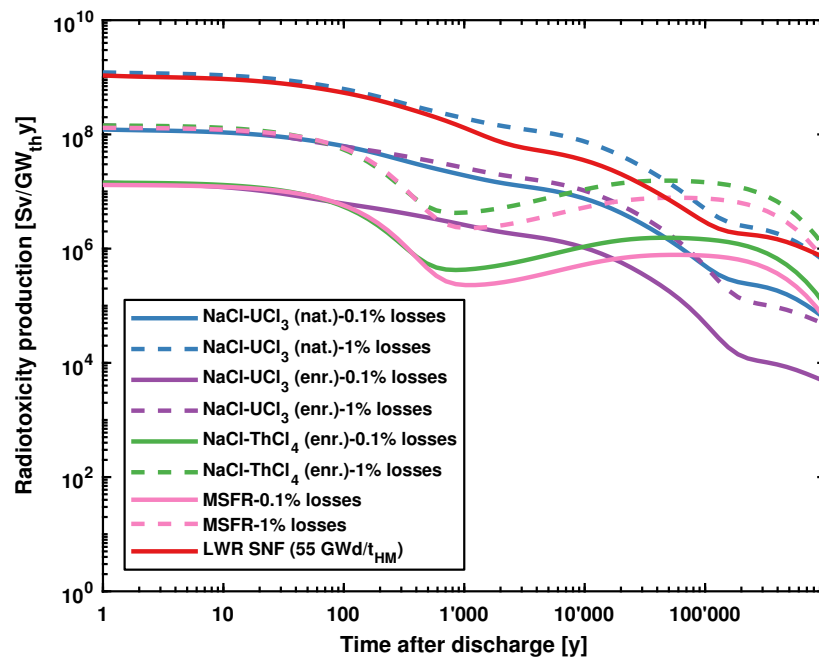


Figure 5.19 – Radiotoxicity production per unit energy produced due to reprocessing losses in closed fuel cycle.

6 Open Fuel Cycles

6.1 Introduction

In the previous chapter, the performance of fluoride- and chloride-fueled designs in a closed fuel cycle was investigated, including their transition to equilibrium using several fuels of interest. It was shown to be feasible to operate such reactors in a closed fuel cycle, however, this possibility relies on the feasibility of fuel processing to remove FPs from the fuel salt. While such processes have been demonstrated at a laboratory scale, their applicability remains uncertain. Therefore, the feasibility of running MSRs in two types of open fuel cycles without fuel reprocessing, B&B and once-through, was investigated from a neutronics point of view.

6.2 Breed-and-Burn Fuel Cycle

B&B reactors are an old idea dating back to at least the time of the Second International Conference on the Peaceful Uses of Atomic Energy (Feinberg and Kunegin, 1958) during which Feinberg highlighted the practicality of not having to reprocess the fuel of a fast reactor during the cycle. It has been investigated by researchers such as Klaus Fuchs (Fuchs and Hessel, 1961), which investigated the possibility of an homogeneous B&B reactor and Edward Teller (Teller et al., 1995) which brought the idea of a gas-cooled and thorium-fueled B&B reactor. Japanese researchers (Sekimoto et al., 2001) have brought the idea of a fission wave propagating uniaxially to avoid the radial redistribution of heat sources in the core which complicates core design. Most recently the company Terrapower has been developing a sodium-cooled Travelling Wave Reactor (TWR) since 2006 (Hejzlar et al., 2013). Interested readers are referred to a recent article (Lopez-Solis and François, 2017) which reviews the concept in many more details.

Fundamentally, a B&B reactor is a reactor capable of operating on fertile-only feed in an open cycle without actinide separation from its discharged fuel, by opposition to a classical type of breeder reactor, called a *seed-and-blanket* reactor, in which the fissile is mostly bred in a blanket which is reprocessed at relatively low discharge burn-up to produce new fuel. It must

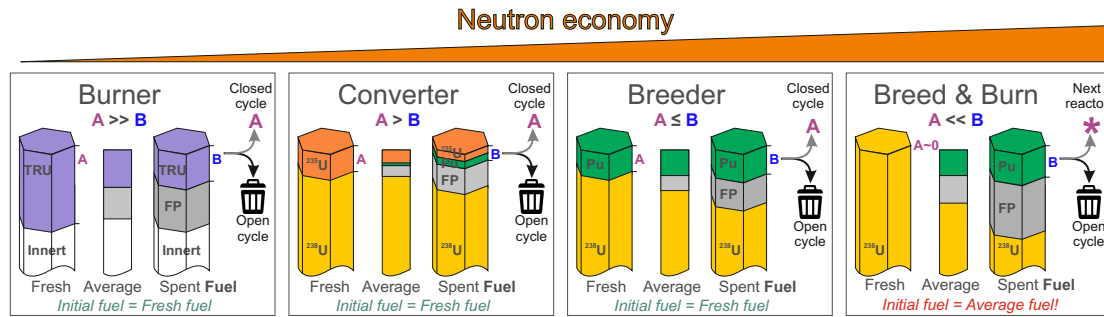


Figure 6.1 – Principle of B&B compared to classical converters and breeders.

be mentioned that there are two main variants of B&B reactors:

- TWRs, in which a fission rate propagates as a wave in a static fuel, and
- Standing Wave Reactors (SWRs), in which the fuel is moved and thus the fission rate does not propagate.

While TWRs are simpler because it is not necessary to shuffle fuel in the core, the technological challenges posed by the fluences necessary to achieve B&B are substantial. In SWRs, the fuel can be moved to regions where it is the most effective depending on its burn-up: for example, highly burnt fuel need not be in a high flux region as it will be a net neutron absorber. Therefore, cladding fluence can be decreased compared to the TWR. Moreover, in the case of strictly static fuel, inhomogeneity of the neutron flux due to the finite size of the core leads of a loss of efficiency in the fuel because of lower burn-up at the extremities of fuel assemblies. It has been proposed to make the fuel move radially as well as axially (3D shuffling) to alleviate this limitation (Qvist et al., 2015).

The necessity of conserving a positive breeding gain without FP removal applies stringent requirements on the neutron economy of the reactor. Therefore, the design space is generally limited to reactors possessing:

- a hard neutron spectrum to limit parasitic neutron captures on structural materials and fission products,
- a large core to lower neutron leakage, usually coming at the cost of worsened safety parameters (such as void reactivity worth) in liquid metal fast reactors,
- an actinide-dense fuel form to further improve both previous factors.

Technologically, one of the most limiting factor is the maximum allowable fluence on the cladding because its integrity must be guaranteed with sufficient safety margins.

However, a third type of B&B can be conceived when implemented in an externally-cooled MSR in which the primary coolant is the fuel salt, which would bring an alternative. It has the advantages that:

- the fuel being homogeneously mixed, there is no loss of fuel efficiency due to flux

inhomogeneities,

- the absence of cladding tubes implies that fluence would not be a limiting factor,
- the void reactivity will remain negative.
- the properties of molten salts should allow higher outlet temperatures than are possible in a liquid metal-cooled reactor.

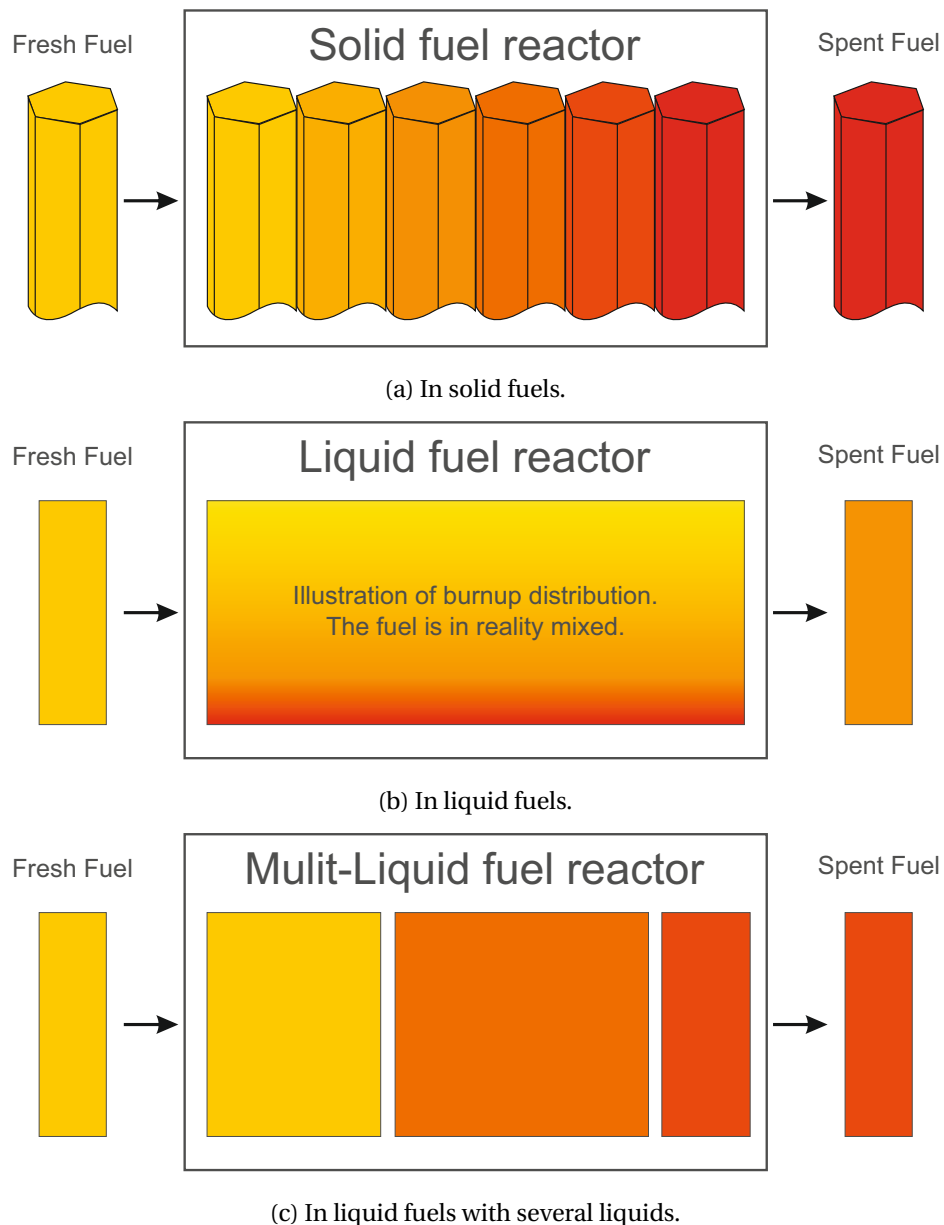


Figure 6.2 – Comparison of the evolution burn-up of liquid and solid fuels.

Additionally, Kasam and Shwageraus (2017) investigated the feasibility of implementing a B&B cycle in an internally-cooled MSR in which the fuel is contained in separate tubes and cooled by another salt, based on Moltex Energy's Stable Salt Reactor concept (Scott, 2017).

This different implementation was not explicitly considered in the present work, however, as it is closer to the implementation of B&B in a solid-fuel reactor.

6.2.1 Lattice-level calculations

The ability of selected salts to sustain B&B must first be established on a cell level, neglecting neutron leakage as a first approximation. For this purpose, a novel method based on the neutron excess method was developed. It uses a single cell depletion starting from the fresh fertile salt to approximately 100 %FIMA. The details of the derivation of the method were previously reported in section 3.2.6. An approximation of the equilibrium k_{∞} can be obtained using equation (3.20) made by a convolution with the residence time distribution of equation (3.16).

Fluoride salts

Fluoride salts have the advantage of having been much more investigated for use as fuel salts than chloride salts, as well as containing more actinides per unit volume than many chloride salts. Moreover, the softer neutron spectrum decreases leakage compared to the case of chloride salts. Additionally, they can be used in a thermal spectrum. In this section, they were evaluated for use in a graphite-moderated lattice and in a fast spectrum (no moderator).

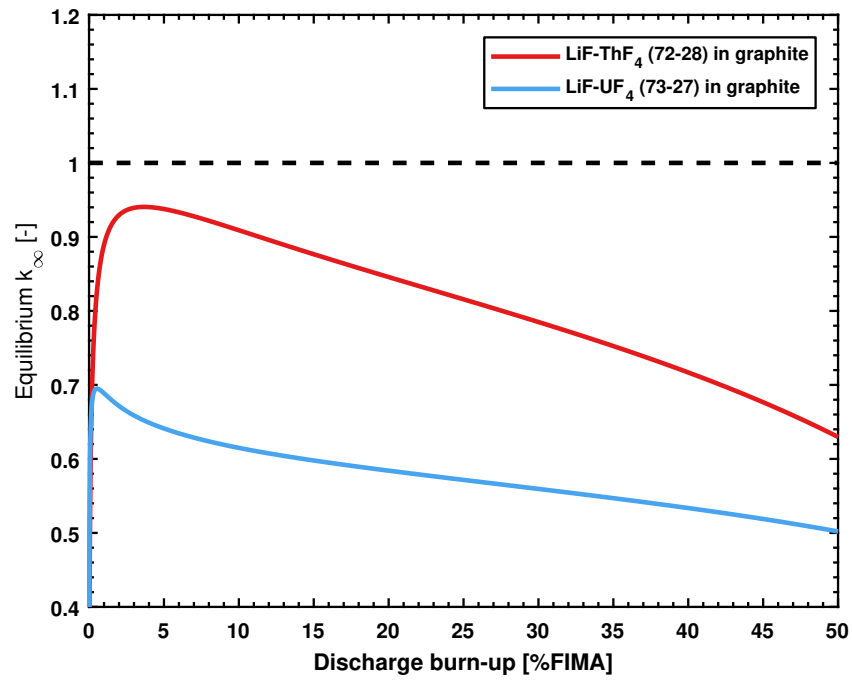
An hexagonal lattice composed of 90 % of graphite and 10 % fluoride-based fuel salt per volume was used to investigate the possibility of a graphite-moderated B&B MSR. The maximum k_{∞} achievable at equilibrium computed using equation (3.20), while the same fluoride salts were investigated in a fast neutron spectrum, with the results depicted on figure 6.3 below.

Neither salts reaches criticality in an infinite lattice, although $\text{LiF}-\text{ThF}_4$ performs substantially better than $\text{LiF}-\text{UF}_4$ in a thermal spectrum. The difference between Th and U cycle is noticeably smaller than in a thermal spectrum. However, in both cases the fuel salts fails to reach net neutron generation and the equilibrium k_{∞} remains below unity, precluding their use in a B&B reactor. It is therefore unlikely to obtain a B&B-capable reactor using fluoride salts.

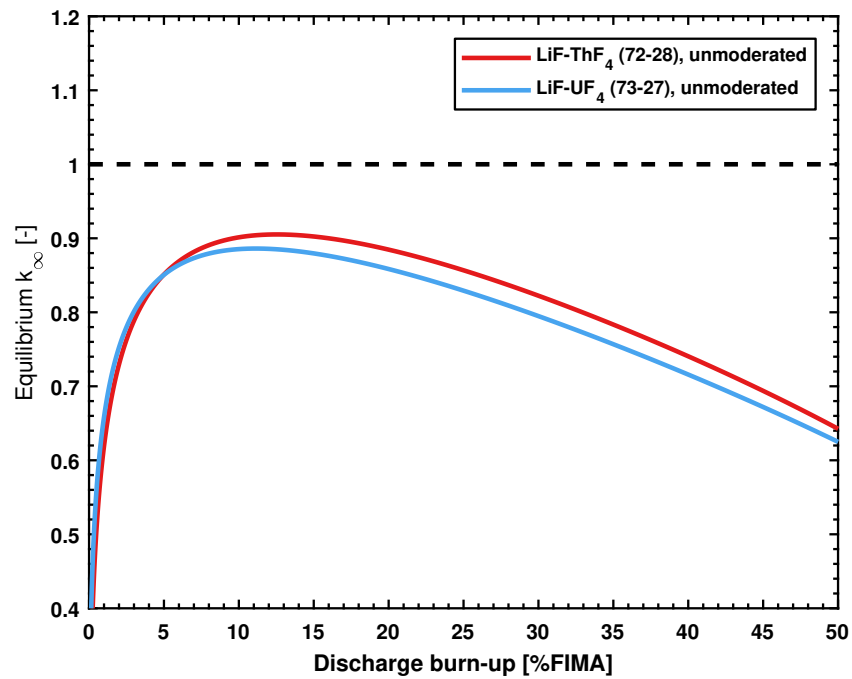
Chloride salts

In (Hombourger et al., 2015), it was found that chlorine in chloride salts must be enriched in its ^{37}Cl isotope to obtain acceptable performance due to the large capture cross-section of ^{35}Cl . In the present, chloride-based salts were investigated in a fast spectrum using chlorine enriched to 100% ^{37}Cl (unless otherwise stated). The results derived using the simplified method are reported graphically on figure 6.4 as well as numerically on Table 6.1 below.

The results show that a pure Th-cycle B&B reactor is not practical due to the too low equilibrium k_{∞} that is achievable. The pure U-cycle salts perform substantially better, with higher

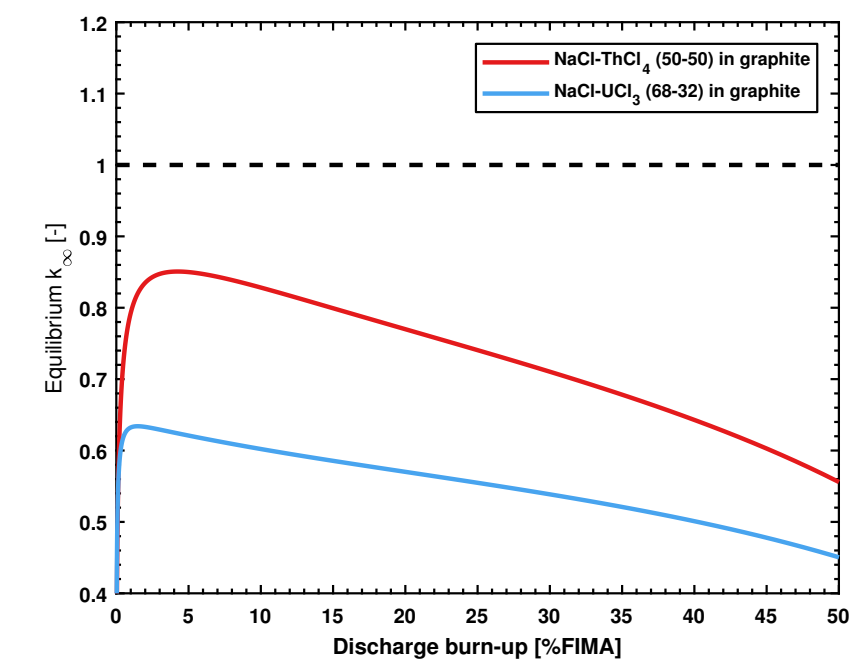


(a) In graphite

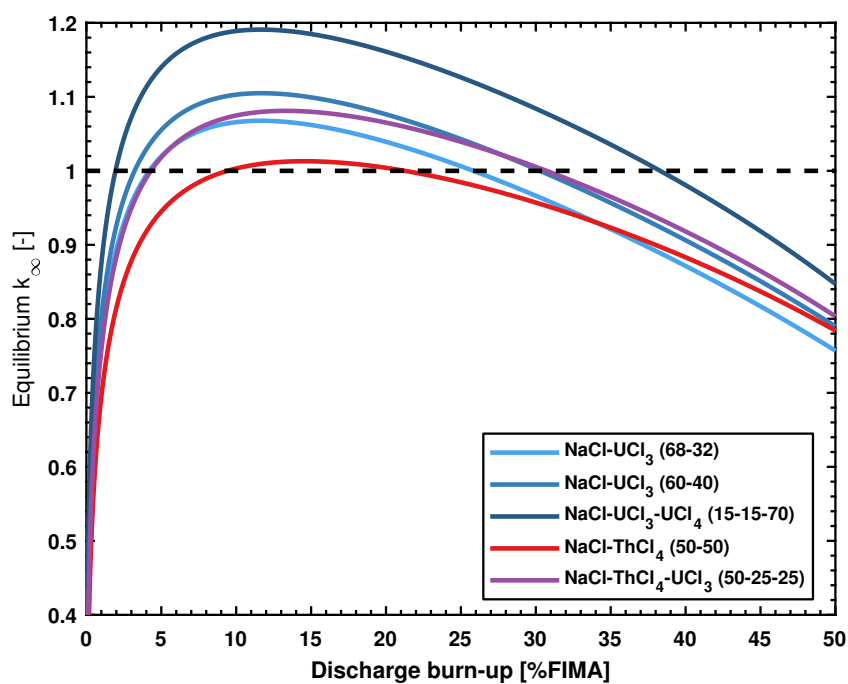


(b) In a fast spectrum

Figure 6.3 – Achievable equilibrium k_{∞} as function of the discharge burn-up for fluoride salts in a graphite-moderated lattice and a fast spectrum.



(a) In graphite



(b) In a fast spectrum

Figure 6.4 – Achievable equilibrium k_{∞} as function of the discharge burn-up for chlorides salts in a graphite-moderated lattice and a fast spectrum.

Table 6.1 – Zero-dimensional estimates of minimum and maximum burn-ups and burn-up at maximum reactivity achievable with enriched chloride salts.

Burn-up	Min.	Max.	Max. k_{∞}
	[%FIMA]		
NaCl–UCl ₃ (68-32)	4.2	25.8	11.7
NaCl–UCl ₃ (60-40)	3.2	30.3	11.8
NaCl–ThCl ₄	9.4	21.3	14.4
NaCl–ThCl ₄ –UCl ₃	4.3	30.7	13.1
NaCl–UCl ₃ –UCl ₄	1.9	38.3	11.7

reactivity the higher their actinide density is, due to diminished parasitic captures and spectrum hardening. The mixed NaCl–ThCl₄–UCl₃ performs slightly better than NaCl–UCl₃ (68-32%mol.) due to the presence of Thorium which increases the maximum burn-up. The expected advantage is that the melting point of the NaCl–ThCl₄–UCl₃ mixture should be below 500 °C.

The maximum reactivity at equilibrium (and thus smallest core size) is obtained for fuel discharged at a burn-up in the range of 10 %FIMA to 15 %FIMA for all salts. It is therefore possible to operate a chloride-fueled MSR on a B&B cycle.

6.2.2 Full-core calculations

Having ascertained the possibility of operating a chloride-fueled MSR on a B&B cycle in an infinite lattice, a more realistic three dimensional design can be investigated and optimized.

To minimize the physical size of the core, an adequate reflector material must first be selected; a challenging task due to the neutron transparency of chlorides salts which combine a low actinide density compared to solid fuels with a hard neutron spectrum, making finite-sized cores highly susceptible to neutron leakage and therefore quite large. In (Hombourger et al., 2017), several candidate reflector materials (Fe, Zr, Pb and ²⁰⁸Pb) were evaluated and it was found that ²⁰⁸Pb results in the lowest core size and inventory but with a marginal improvement over Pb, at the cost of isotopic enrichment. Therefore, Pb was selected in the present work as main reflector material.

The four candidate salts that proved to be usable in a B&B MSR, that is, NaCl–UCl₃ (68-32), NaCl–ThCl₄–UCl₃ (50-25-25) and NaCl–UCl₃–UCl₄ (15-15-70) were investigated at BOL, at equilibrium (EQL) and during the transition to said equilibrium and their performance compared.

Equilibrium core dimensions

A simple cylindrical vessel of 3 cm thickness made out of Hastelloy N and a 100 cm Pb reflector were further assumed, while the cooling loops were not accounted for, since they do not change the fuel cycle behavior of the reactor beyond increasing the salt inventory. For each possible salt, core dimensions critical at equilibrium at a discharge burn-up of maximum predicted k_{∞} were computed. The calculated values for the diameters, core volume and heavy metal inventories are depicted on figure 6.5.

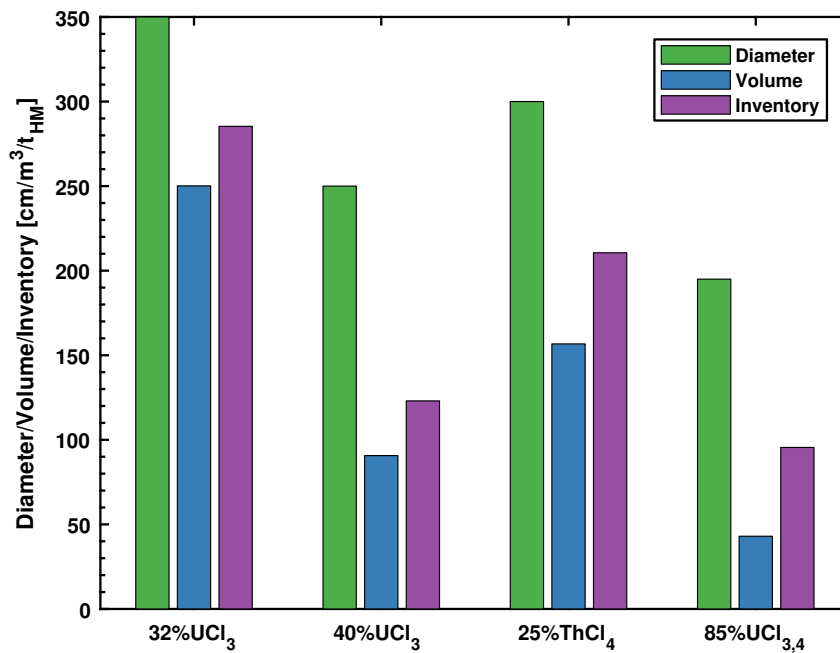


Figure 6.5 – Equilibrium core dimension for each selected candidate salts.

The minimum values are obtained for the most actinide-dense salt, NaCl–UCl₃–UCl₄. An acceptably low volume and inventory is obtained with NaCl–UCl₃ (60-40), while other salts result in substantially large fuel volumes and inventories.

Start-up inventory

For the initial core load, both enriched uranium and LWRPu with the composition described in table 2.4 were considered. In the first case, the enrichment was varied so as to achieve criticality. In the second case, the quantity of LWRPu was varied to obtain a critical configuration, the rest of the actinide vector being composed of ²³⁸U. In the case of the Th-containing salt, half of the actinide vector is composed of ²³²Th.

Table 6.2 – Critical LEU and LWRPu fraction for each candidate salt.

^{235}U or Pu fraction	LEU	LWRPu
NaCl–UCl ₃ (32-68)	10.65%	11.3%
NaCl–UCl ₃ (40-60)	10.7%	11%
NaCl–UCl ₃ –ThCl ₄	23.6%	23.2%
NaCl–UCl ₃ –UCl ₄	10.35%	9.85%

Doubling time

In the transition to equilibrium, reactivity is controlled by discharging slightly supercritical fuel and replacing it with fertile feed. Therefore, once the cumulative volume of fuel discharged reaches the initial equilibrium critical volume, and additional initial inventory has been bred. The time needed to reach this point is the doubling time of the reactor.

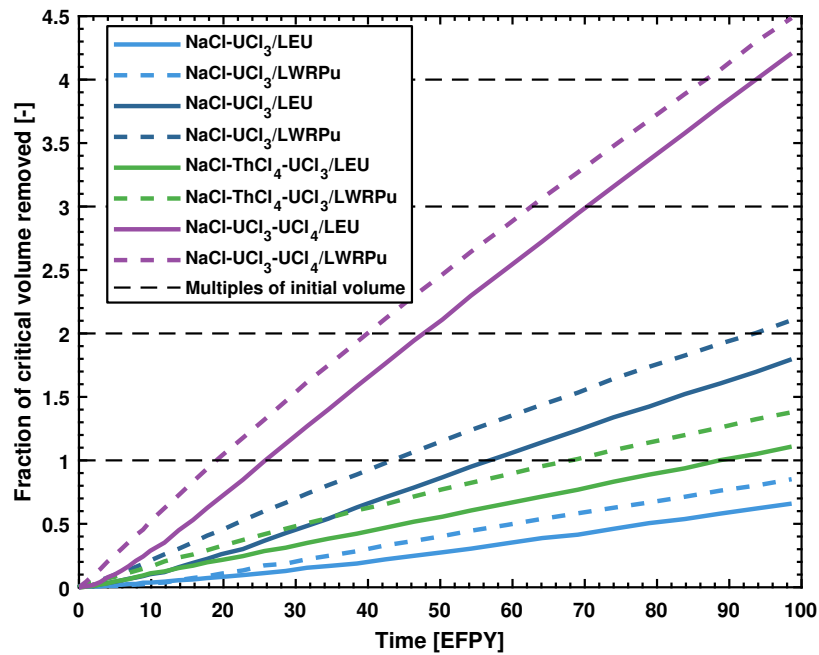


Figure 6.6 – Evolution of the cumulative volume of fuel salt discharged during the transition to equilibrium.

More actinide-dense salts improve the doubling time substantially over less dense salts and a LWRPu start-up results in a lower doubling time than a LEU start-up.

Table 6.3 – First doubling times for candidate salts as function of the start-up fuel.

Doubling time	LEU	LWRPu
	[EFPY]	
NaCl–UCl ₃ (32-68)	142	113
NaCl–UCl ₃ (40-60)	56.8	43.3
NaCl–UCl ₃ –ThCl ₄	88.6	68
NaCl–UCl ₃ –UCl ₄	25.8	19

Reactivity coefficients

In an homogenous fast-spectrum MSR, the main reactivity feedback is that of fuel salt expansion with higher temperature, which expels fissile nuclides out of the core and into an expansion tank, thereby lowering reactivity.

The reactivity coefficient α can be calculated using the following equation:

$$\alpha = \frac{\Delta \rho}{\Delta T} = 10^5 \frac{1}{T_{\text{hot}} - T_{\text{nom}}} \left(\frac{1}{k_{\text{nom}}} - \frac{1}{k_{\text{hot}}} \right) \quad (6.1)$$

in which T_{nom} and k_{nom} are the nominal temperature and multiplication factor and T_{hot} and k_{hot} the temperature and multiplication factor at higher temperature.

Reactivity coefficients were computed at BOL and EQL using (6.1) by increasing the temperature of the cross-section library by 300 K and decreasing the density to that computed for the new temperature using (3.8). They are summarized on Table 6.4 below.

Table 6.4 – Reactivity coefficients of selected salts at BOL and EQL.

	BOL		EQL
	LEU	LWRPu	
NaCl–UCl ₃ (32-68)	–5.2 pcm/K	–5.3 pcm/K	–5.1 pcm/K
NaCl–UCl ₃ (40-60)	–5.8 pcm/K	–6.8 pcm/K	–8.8 pcm/K
NaCl–UCl ₃ –ThCl ₄	–7.0 pcm/K	–6.4 pcm/K	–8.9 pcm/K
NaCl–UCl ₃ –UCl ₄	–13.8 pcm/K	–14.5 pcm/K	–16.6 pcm/K

It is clear that the reactivity coefficients are negative for all cases and remain rather stable between BOL and EQL. Salts with higher actinide chloride densities result in cores with more negative reactivity coefficients.

6.3 Once-through Cycle

Finally, a last alternative mode of operating a MSR is on a once-through cycle, i.e. a cycle in which the reactor is first loaded with fuel, which is then burnt until the reactor cannot be kept critical anymore, and then discharged without recycling the actinide vector.

This fuel cycle can be applied to the chloride-fueled reactors designed for an isobreeding closed fuel cycle of the previous chapter starting from their initial critical load. It can be applied to the B&B designs of the previous section in their equilibrium state as well, to simulate a transition to a burner mode instead of the normal breeding mode producing excess fissile material in B&B.

As the aforementioned designs are breeders, the reactivity will first increase in time and then decrease until it reaches unity, at which point the reactor cannot be further operated without discharging at least part of the fuel and refueling the reactor. In the following calculations, it was assumed that no further feed of actinides will take place and that no FP removal other than the removal of volatile and insoluble FPs is performed. Moreover, the reactivity is not compensated for by changing the fuel composition to match the assumption of a lack of reprocessing capability. It is assumed that reactivity can be compensated for using other means, which could include:

- additional neutron absorbers such as control organs or burnable poisons,
- increased neutron leakage using a mobile reflector or,
- inherent reactivity feedbacks, provided that other parameters (power, temperatures, flow rates) can be kept within safe margins.

The reactivity evolution of such cores in a once-through cycle is depicted on figure 6.7 below and the burn-ups reached are given in table 6.5.

Table 6.5 – Achievable burn-ups in a once-through fuel cycle.

	Core volume [m ³]	Burn-up [%FIMA]
NaCl–UCl ₃ (^{nat} Cl)	134	16.8
NaCl–UCl ₃ (³⁷ Cl)	19.1	18.3
NaCl–ThCl ₄ (³⁷ Cl)	65.8	32.3
NaCl–UCl ₃ –ThCl ₄ (B&B EQL)	157	23.2
NaCl–UCl ₃ –UCl ₄ (B&B EQL)	250	29.8

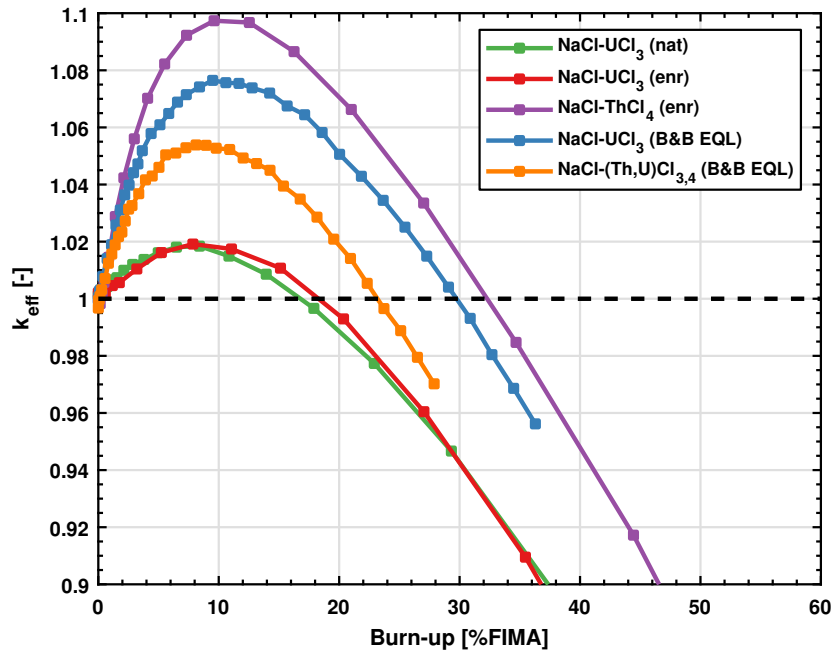


Figure 6.7 – Reactivity evolution of the closed-cycle chloride cores and of selected B&B chloride cores.

6.4 Conclusions

In this chapter, the possibility of operating chloride-fueled MSR in open fuel cycles without fuel processing was investigated from a neutronics point of view.

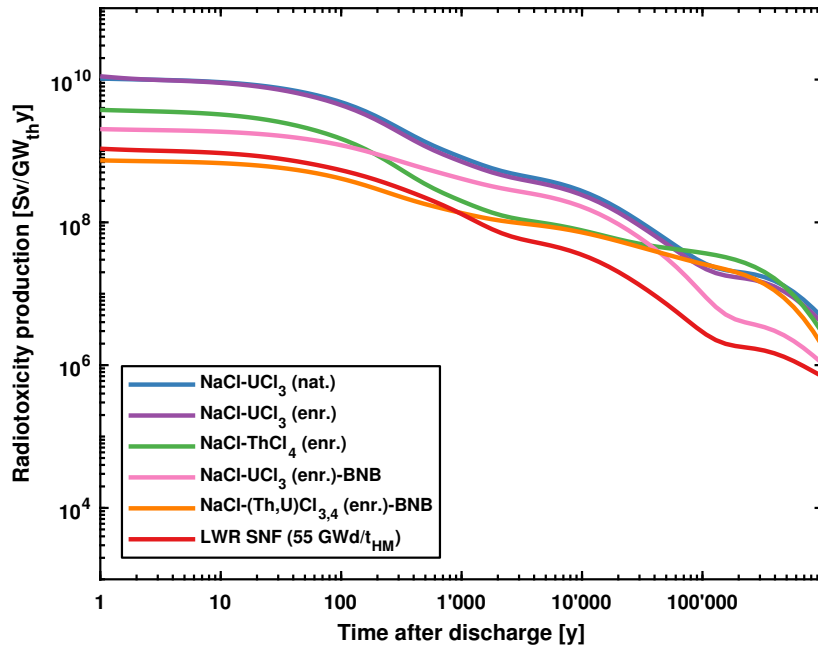
The first type of open cycle studied in this chapter is the sustainable B&B in which the core is designed to breed sufficiently to compensate for FP build-up, and the fuel is progressively discharged and replaced by fertile fuel, after which it can be reused to start a second reactor. This mode of operation proved to be feasible provided that enriched chloride salts are used. Discharge burn-ups of 10 %FIMA to 15 %FIMA are achievable in this way, providing an interested alternative to a closed fuel cycle if fuel reprocessing is unavailable for technical or proliferation-related reasons.

The second type of open cycle that was investigated is that of a simple, once-through fuel cycle, which is arguably the least efficient and least sustainable type of fuel cycle studied in this thesis. In this mode, an alternative reactivity control mechanism was assumed to be feasible to compensate for the increase in reactivity due to the high breeding rate of the investigated cores. However, under this assumption, it proved to be feasible with burn-ups ranging from 16.8 %FIMA to 32.3 %FIMA depending on the case. Thorium-fueled cases showed the highest burn-ups and reactivity swings. The burn-ups could be improved by replacing removed volatile FPs by fertile feed of Thorium or natural Uranium.

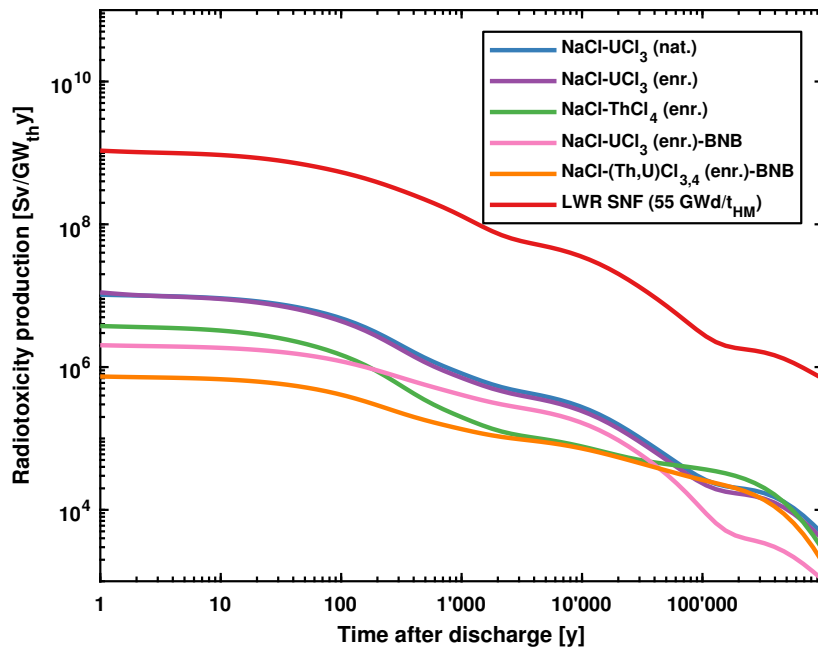
The once-through cycle was also applied to selected B&B cores to simulate an end to the stockpiling of excess fissile material that comes with B&B cycles. Burn-ups beyond 20 %FIMA were shown to be feasible in this particular case.

In these cases the fuel cycle could be closed by reprocessing fuel in a batch-wise manner after it has been discharged. However, this was not assumed in this study. Nevertheless, operating on an open cycle is bound to produce substantial amounts of radiotoxicity due to the actinides being discharged and not recycled. Similarly to what was done in the previous chapter, the radiotoxicity produced by discharging the entire core can be averaged over the energy produced by operating the reactor from zero burn-up to the maximum burn-up achievable and then compared to the radiotoxicity production of discharged LWR SNF. The results are depicted on figure 6.8 below.

As can be expected, nearly all cases produce more radiotoxicity on an open cycle than that of LWR SNF. However, it must be mentioned that no credit was given for the incineration of the TRUs present in the initial load. In the case of fuel being reprocessed after discharge however, the radiotoxicity due to losses is comparable to that of a closed fuel cycle.



(a) Without final recycling



(b) With final recycling

Figure 6.8 – Radiotoxicity production per unit energy produced due to discharged cores in an open fuel cycle with and without final recycling.

7 Conclusions

7.1 Summary

The work presented in this thesis focused on researching conceptual MSR designs that could sustain a sustainable isobreeding closed fuel cycle while being capable of incinerating existing TRU waste from LWR SNF during their transition to equilibrium.

To this end, the open literature was reviewed and the numerous concepts proposed in the past have been investigated to obtain a better understanding of the possible designs.

For the purpose of simulating the fuel cycles of MSRs, a MATLAB and Serpent-based procedure known as EQL0D was developed. It is capable of performing zero-dimensional depletion calculations for MSRs or of directly searching for the equilibrium state of the fuel cycle. Additional capabilities include criticality control, redox potential adjustment and various nuclide removal and addition operations, making it suitable to simulate the transition of a given design to its equilibrium.

The procedure was first applied to several candidate fuel salts and moderators in an infinite lattice to evaluate their respective performance in a closed Thorium-Uranium or Uranium-Plutonium fuel cycle. The ability of configurations to incinerate TRU waste was quantified by their excess reactivity at equilibrium, which is a measure of the size of the available neutron budget.

While several moderators performed well at equilibrium in a Thorium-Uranium cycle by having substantial amounts of excess reactivity, they are incompatible with the salt and must thus be clad with a corrosion-resistant materials. The impact of several such materials on available reactivity was shown to be substantial enough to make an isobreeding fuel cycle impossible. In the Uranium-Plutonium cycle, thermal-spectrum configurations were shown to be incapable of isobreeding. Unmoderated cases were studied as well, showing substantial available reactivity at equilibrium in both cycles, particularly in the case of chloride salts. The influence of other variables such as power density and reprocessing cycle time was

Chapter 7. Conclusions

investigated separated using selected cases. The results show that thermal-spectrum fluoride-fueled reactors are particularly sensitive to high power densities due to parasitic captures on Protactinium, which can be alleviated by its separation and isolation to let it decay outside of the neutron flux. Fast-spectrum configurations were shown to be much less sensitive to power density and fission products concentration.

Selected core designs were then investigated during their transition to a closed fuel cycle equilibrium. Three fluoride-fueled cases, including the historic single- and two-fluid MSBR and more recent fast-spectrum MSFR and three simplified chloride-fueled designs based on the results of the infinite lattice study were selected for this purpose.

The fluoride-fueled reactors could however not be fueled using TRUs due to the too low solubility of trifluorides in their fuel salts. Nevertheless, the hypothetical transitions were computed, as well as transitions using other potential fuels including high- and low-enriched uranium, ^{233}U and weapons-grade plutonium. Several of these transitions were found to be impossible as well, either on ground of solubility problems or because of the too high amounts of fuel needed to sustain a critical core during the transition.

No such limitation is present in chloride-fueled reactors however, and the cores designed for isobreeding could be directly started using TRUs. The transition to equilibrium could be carried out without further additions of fuel due to the high breeding capabilities of the cores, confirming the possibility of burning the initial load and producing energy on a fertile feed essentially indefinitely.

However, the feasibility of such a closed fuel cycle relies on the assumption that adequate reprocessing techniques are available to remove fission products and return actinides to the core. The possibility of running MSRs on two types of open cycles without fuel processing was therefore investigated. Firstly, the Breed-and-Burn fuel cycle, in which fuel containing both actinides and FPs is regularly discharged and replaced by the fertile feed to keep the reactor critical, was demonstrated to be feasible provided that one uses enriched chloride salts. The resulting core dimensions and inventories are nevertheless substantially larger than those necessary in closed fuel cycle. Due to the neutron budget of the reactor being so sensitive to neutron leakage and capture, salts with high actinide densities must be used to lower the inventories, not all of which may be adequate in reality due to the simultaneous requirement of low melting point for the salt mixture. Finally, the maximum burn-ups achievable in a once-through cycle in which the fuel is not reprocessed during the core lifetime were evaluated for the closed-cycle and B&B cores. The results indicate that burn-ups as high as 30 %FIMA may be possible.

In conclusion, chloride-fueled reactors may be the most adequate type of MSRs for the incineration of TRU TRUs waste and the subsequent establishment of an isobreeding closed fuel cycle. In particular, configurations using enriched chloride salts on an Uranium-Plutonium cycle yielded the smallest core inventories. Alternatively, chloride-fueled MSRs could be operated on a B&B if actinide separation processes are unavailable or unwanted.

7.2 Future work

This thesis strictly focused on the neutronics and fuel cycle aspects of MSR designs, which represents only a small fractions of the considerations needed to deploy such reactors. Other domains such as static and transient behavior, fuel chemistry, and material behavior in a high-temperature, high-corrosion and radiation environment are paramount to the development of this technology. It remains that unlike in the more conventional solid-fueled reactors, numerous phenomena present in MSRs involve different physics that are interrelated and that thus cannot be treated separately as it has often been done in the earlier days of nuclear power research.

One particular area that was not addressed in this thesis is that of multiple-fluid MSR which could show an improvement in performance over single-fluid concepts, particularly in B&B.

To truly demonstrate the feasibility of a given concept, a much more substantial amount of data must be obtained. During the course of this work, many questions in these various domains were stumbled upon and often could not be answered satisfactorily using the available open literature. Therefore, assumptions had to be made to circumvent these obstacles. It is however likely that several of these hypotheses are not valid in reality.

In particular, issues concerning salt chemistry necessitate substantial further research:

- The potential fuel salt compositions using fluoride salts could be optimized to allow for higher solubility of trifluorides at the required temperatures.
- The potential fuel salt compositions using chloride salts could be optimized by adding more salt components to maximize their actinide density for a given melting temperature.
- The feasibility of using chloride salts containing large amounts of uranium tetrachloride is very uncertain due to its potential corrosiveness on the one hand and to its low boiling point on the other.
- The feasibility of enriching chlorine to high enrichment levels in an economical manner must be demonstrated.
- The corrosion behavior of chloride salts containing impurities (fission products, actinides, sulfur) must be investigated, as there is currently no such data, unlike fluoride salts.
- The conversion of actinides contained in spent LWR fuels into chlorides must be demonstrated on a large scale.
- The potential of a multiple-fluid B&B concept should be investigated.

However, these issues only cover uncertainties related to the chloride-fueled concepts that have been researched in this thesis. Other issues related to MSRs in general should also be mentioned:

- The steady-state and transient behavior of homogeneous fast-spectrum MSRs is not as

Chapter 7. Conclusions

well understood as that of graphite-moderated MSRs due to their large open cavities involving complex thermal-hydraulics compared to individual fuel channels.

- The fuel reprocessing technology must be further developed to reach the efficiencies necessary to minimize losses causing substantial amounts of radiotoxicity to be released to the waste stream.
- Materials that have high-temperature strength, are corrosion resistant and tolerant of neutron irradiation must be developed, tested and qualified for lifetimes necessary for economical operation of MSRs.
- A novel safety concept must be established on solid experimental bases to demonstrate the effectiveness of the inherent safety features of MSRs and inform the design process.

Bibliography

- Alexander, L. G. (1958). Nuclear Aspects of Molten-salt Reactors. In MacPherson, H. G., editor, *Fluid Fuel Reactors*, Atoms for Peace, pages 626–660. Addison-Wesley, Boston.
- Allen, T., Ball, S., Blandford, E., Downar, T., Flanagan, G., Forsberg, C., Greenspan, E., Holcomb, D., Hu, L.-W., Matzie, R., and others (2013a). Fluoride-Salt-Cooled, High-Temperature Reactor (FHR) Subsystems Definition, Functional Requirement Definition, and Licensing Basis Event (LBE) Identification. White Paper UCBTH-12-001, University of California, Berkeley, Berkeley, CA, USA.
- Allen, T., Blandford, E., Cao, G., Chapin, D., Denman, M., Downar, T., Flanagan, G., Forget, B., Forsberg, C., Greenspan, E., and others (2013b). Fluoride-Salt-Cooled, High-Temperature Reactor (FHR) Methods and Experiments Program White Paper. White Paper UCBTH-12-002, University of California, Berkeley, Berkeley, CA, USA.
- Aufiero, M., Cammi, A., Fiorina, C., Leppänen, J., Luzzi, L., and Ricotti, M. (2013). An extended version of the SERPENT-2 code to investigate fuel burn-up and core material evolution of the Molten Salt Fast Reactor. *Journal of Nuclear Materials*, 441(1–3):473–486.
- Bateman, H. (1910). Solution of a System of Differential Equations Occurring in the Theory of Radioactive Transformations. *Proceedings of the Cambridge Philosophical Society*, 15:423–427.
- Bauer, C., Frischknecht, R., Eckle, P., Flury, K., Neal, T., Papp, K., Schori, S., Simons, A., Stucki, M., and Treyer, K. (2012). Umweltauswirkungen der Stromerzeugung in der Schweiz. Technical report, Bundesamt für Energie.
- Beneš, O., Beilmann, M., and Konings, R. J. M. (2010). Thermodynamic assessment of the LiF–NaF–ThF₄–UF₄ system. *Journal of Nuclear Materials*, 405(2):186–198.
- Beneš, O. and Konings, R. (2008a). Thermodynamic evaluation of the NaCl–MgCl₂–UCl₃–PuCl₃ system. *Journal of Nuclear Materials*, 375(2):202–208.
- Beneš, O., Konings, R., Sedmidubský, D., Beilmann, M., Valu, O., Capelli, E., Salanne, M., and Nichenko, S. (2013). A comprehensive study of the heat capacity of CsF from T = 5 K to T = 1400 K. *The Journal of Chemical Thermodynamics*, 57:92–100.

Bibliography

- Beneš, O. and Konings, R. J. M. (2008b). Actinide burner fuel: Potential compositions based on the thermodynamic evaluation of MF–PuF₃ (M = Li, Na, K, Rb, Cs) and LaF₃–PuF₃ systems. *Journal of Nuclear Materials*, 377(3):449–457.
- Beneš, O. and Konings, R. J. M. (2008c). Thermodynamic study of LiF–BeF₂–ZrF₄–UF₄ system. *Journal of Alloys and Compounds*, 452(1):110–115.
- Beneš, O. and Konings, R. J. M. (2009). Thermodynamic properties and phase diagrams of fluoride salts for nuclear applications. *Journal of Fluorine Chemistry*, 130(1):22–29.
- Berthou, V., Slessarev, I., and Salvatores, M. (2001). The TASSE Concept (Thorium-based Accelerator-driven System with Simplified Fuel Cycle for Long-term Energy Production). In *Proceedings of GLOBAL '01*, Paris, France. American Nuclear Society.
- Bettis, E. S., Cottrell, W. B., Mann, E. R., Meem, J. L., and Whitman, G. D. (1957a). The Aircraft Reactor Experiment—Operation. *Nuclear Science and Engineering*, 2:841–853.
- Bettis, E. S. and Robertson, R. C. (1970). The Design and Performance Features of a Single-Fluid Molten-Salt Breeder Reactor. *Nuclear Applications and Technology*, 8(2):190–207.
- Bettis, E. S., Schroeder, R. W., Cristy, G. A., Savage, H. W., Affel, R. G., and Hemphill, L. F. (1957b). The Aircraft Reactor Experiment—Design and Construction. *Nuclear Science and Engineering*, 2(6):804–825.
- Bowman, C. D. (1998). Accelerator-Driven Systems for Nuclear Waste Transmutation. *Annual Review of Nuclear and Particle Science*, 48(1):505–556.
- Bullmer, J. J. (1956). Fused Salt Fast Breeder: Feasibility Study. Technical Report CF-56-8-204, Oak Ridge National Laboratory, Oak Ridge, TN, USA.
- Capelli, E., Beneš, O., and Konings, R. J. M. (2014). Thermodynamic assessment of the LiF–NaF–BeF₂–ThF₄–UF₄ system. *Journal of Nuclear Materials*, 449(1–3):111–121.
- Compere, E. L., Kirslis, S. S., Bohlmann, E. G., Blankenship, F. F., and Grimes, W. R. (1975). Fission Product Behavior in the Molten Salt Reactor Experiment. Technical Report ORNL-4865, Oak Ridge National Laboratory, Oak Ridge, TN, USA.
- Cury, R. (2007). *Étude Métallurgique des Alliages Ni-W et Ni-W-Cr : Relation entre Ordre à Courte Distance et Durcissement*. Ph.D. Thesis, Université Paris-XII Val-de-Marne, Paris, France.
- Danckwerts, P. V. (1953). Continuous flow systems: Distribution of residence times. *Chemical Engineering Science*, 2(1):1–13.
- Delpech, S., Merle-Lucotte, E., Heuer, D., Allibert, M., Ghetta, V., Le-Brun, C., Doligez, X., and Picard, G. (2009). Reactor physic and reprocessing scheme for innovative molten salt reactor system. *Journal of Fluorine Chemistry*, 130(1):11–17.

- Desyatnik, V. N., Mel'nikov, Y. T., Raspopin, S. P., and Sushko, V. I. (1971). Ternary systems containing sodium, potassium, and calcium chlorides, and uranium tri- and tetrachloride. *Soviet Atomic Energy*, 31(6):1423–1424.
- Desyatnik, V. N., Vorobei, M. P., Kurbatov, N. N., Kalashnikov, I. S., and Siiba, O. V. (1975). Melting diagrams of ternary systems containing sodium and potassium chlorides, thorium tetrachloride, and plutonium trichloride. *Soviet Atomic Energy*, 38(3):219–221.
- Dirian, J. and Saint-James, R. (1959). Les Sels Fondus dans les Réacteurs Nucléaires. Rapport CEA 1194, Commissariat à l'Énergie Atomique, Saclay, France.
- Engel, J. R., Bauman, H. F., Grimes, W. R., Dearing, J. F., McCoy, E. H., and Rhoades, W. A. (1980). Conceptual Design Characteristics of a Denatured Molten-Salt Reactor with Once-Through Fuelling. Technical Report ORNL/TM-7207, Oak Ridge National Laboratory, Oak Ridge, TN, USA.
- England, T. R. and Rider, B. F. (1994). Evaluation and Compilation of Fission Product Yields. ENDF-349 LA-UR-94-3106, Los Alamos National Laboratory, Los Alamos, NM, USA.
- Ergen, W. K., Callihan, A. D., Mills, C. B., and Scott, D. (1957). The Aircraft Reactor Experiment—Physics. *Nuclear Science and Engineering*, 2:826–840.
- Facilitators, M. I. T. and Facilitators, U. M. (2013a). Fluoride-Salt-Cooled, High-Temperature Reactor (FHR) Development Roadmap and Test Reactor Performance Requirements. White Paper UCBTH-12-004, Massachusetts Institute of Technology, Boston, MA, USA.
- Facilitators, U. M. and Facilitators, M. I. T. (2013b). Fluoride-Salt-Cooled, High-Temperature Reactor (FHR) Materials, Fuels and Components. White Paper UCBTH-12-003, University of Wisconsin - Madison, Madison, WI, USA.
- Feinberg, S. M. and Kunegin, E. P. (1958). Discussion Comments. In *Proceedings of the Second United Nations International Conference on the Peaceful Uses of Atomic Energy*, volume 9, pages 446–447, Geneva, Switzerland. International Atomic Energy Agency.
- Ferris, L. M., Mailen, J. C., and Smith, F. J. (1971). Solubility of PuF₃ in molten 2 LiF-BeF₂. *Journal of Chemical & Engineering Data*, 16(1):68–69.
- Forsberg, C. W., Peterson, P. F., and Pickard, P. S. (2003). Molten-salt-cooled advanced high-temperature reactor for production of hydrogen and electricity. *Nuclear Technology*, 144(3):289–302.
- Fraas, A. P. and Savolainen, A. W. (1956). Design Report on the Aircraft Reactor Test. Technical Report ORNL-2095, Oak Ridge National Laboratory, Oak Ridge, TN, USA.
- Fuchs, K. and Hessel, H. (1961). Über die Möglichkeiten des Betriebs eines Natururanbrutreaktors ohne Brennstoffaufbereitung. *Kernenergie*, 4(8):619–623.

Bibliography

- Furukawa, K., Lecocq, A., Kato, Y., and Mitachi, K. (1990). Thorium Molten-Salt Nuclear Energy Synergetics. *Journal of Nuclear Science and Technology*, 27(12):1157–1178.
- Furukawa, K., Mitachi, K., and Kato, Y. (1992). Small molten-salt reactors with a rational thorium fuel-cycle. *Nuclear Engineering and Design*, 136(1):157–165.
- Greene, S. R., Gehin, J. C., Holcomb, D. E., Carbajo, J. J., Ilas, D., Cisneros, A. T., Varma, W. K., Corwin, W. R., Wilson, D. F., Yoder Jr., G. L., Qualls, A. L., Peretz, F. J., Flanagan, G. F., Clayton, D. A., Bradley, E. C., Bell, G. L., Hunn, J. D., Pappano, P. J., and Cetiner, M. S. (2010). Pre-Conceptual Design of a Fluoride Salt-Cooled Small Modular Advanced High-Temperature Reactor (SmaHTR). Technical Report ORNL/TM-2010/199, Oak Ridge National Laboratory, Oak Ridge, TN, USA.
- Grimes, R. (1970). Molten Salt Reactor Chemistry. *Nuclear Applications and Technology*, 8(2):137–155.
- Grimes, W. R. (1966). Reactor Chemistry Division Annual Progress Report For Period Ending December 31, 1965. Annual Progress Report ORNL-3913, Oak Ridge National Laboratory, Oak Ridge, TN, USA.
- Groupe de Travail CEA-EDF "Concept RSF" (1983). Dossier Concept. Note CEA 002381, Commissariat à l'Énergie Atomique (CEA).
- Haubenreich, P. N. and Engel, J. R. (1970). Experience with the Molten-Salt Reactor Experiment. *Nuclear Applications and Technology*, 8(2):118–136.
- Heidet, F. and Greenspan, E. (2012). Neutron Balance Analysis for Sustainability of Breed-and-Burn Reactors. *Nuclear Science and Engineering*, 171(1):13–31.
- Hejzlar, P., Petroski, R., Cheatham, J., Touran, N., Cohen, M., Truong, B., Latta, R., Werner, M., Burke, T., Tandy, J., Garrett, M., Johnson, B., Ellis, T., Mcwhirter, J., Odedra, A., Schweiger, P., Adkisson, D., and Gilleland, J. (2013). TERRAPOW, LLC TRAVELING WAVE REACTOR DEVELOPMENT PROGRAM OVERVIEW. *Nuclear Engineering and Technology*, 45(6):731–744.
- Hery, M. and Lecocq, A. (1983). Réacteurs à Sels Fondus : Synthèse des Études réalisées entre 1973 et 1983. Note CEA 002381, Commissariat à l'Énergie Atomique.
- Heuer, D., Merle-Lucotte, E., Allibert, M., Brovchenko, M., Ghetta, V., and Rubiolo, P. (2014). Towards the thorium fuel cycle with molten salt fast reactors. *Annals of Nuclear Energy*, 64:421–429.
- Hirschberg, S., Burgherr, P., Spiekerman, G., and Dones, R. (2004). Severe accidents in the energy sector: comparative perspective. *Journal of Hazardous Materials*, 111(1):57–65.
- Hombourger, B., Krepel, J., Mikityuk, K., and Pautz, A. (2015). Fuel Cycle Analysis of a Molten Salt Reactor for Breed-and-Burn Mode. In *Proceedings of ICAPP '15*, Nice, France. American Nuclear Society.

- Hombourger, B., Krepel, J., Mikityuk, K., and Pautz, A. (2017). On the Feasibility of Breed-and-Burn Fuel Cycles in Molten Salt Reactors. In *Proceedings of FR17*, Yekaterinburg, Russian Federation. International Atomic Energy Agency.
- Hron, M. (2005). Project SPHINX spent hot fuel incinerator by neutron flux (the development of a new reactor concept with liquid fuel based on molten fluorides). *Progress in Nuclear Energy*, 47(1):347–353.
- Huke, A., Ruprecht, G., Weißbach, D., Czerski, K., Gottlieb, S., Hussein, A., and Herrmann, F. (2017). 25 - Dual-fluid reactor. In Dolan, T. J., editor, *Molten Salt Reactors and Thorium Energy*, pages 619–633. Woodhead Publishing.
- IAEA. Power Reactor Information System.
- IAEA (2008). *Thermophysical properties of materials for nuclear engineering: a tutorial and collection of data*. International Atomic Energy Agency, Vienna.
- IEA (2016). Key World Energy Statistics. Technical report.
- Ignatiev, V., Feynberg, O., Gnidoi, I., Merzlyakov, A., Smirnov, V., Surenkov, A., Tretiakov, I., Zakirov, R., Afonichkin, V., and Bovet, A. (2007). Progress in development of Li, Be, Na/F molten salt actinide recycler & transmuter concept. In *Proceedings of ICAPP '07*, Nice, France. American Nuclear Society.
- Ignatiev, V., Feynberg, O., Gnidoi, I., Merzlyakov, A., Surenkov, A., Uglov, V., Zagnitko, A., Subbotin, V., Sannikov, I., Toropov, A., Afonichkin, V., Bovet, A., Khokhlov, V., Shishkin, V., Kormilitsyn, M., Lizin, A., and Osipenko, A. (2014). Molten salt actinide recycler and transforming system without and with Th–U support: Fuel cycle flexibility and key material properties. *Annals of Nuclear Energy*, 64:408–420.
- Ignatiev, V., Surenkov, A., Gnidoi, I., Fedulov, V., Uglov, V., Afonichkin, V., Bovet, A., Subbotin, V., Panov, A., and Toropov, A. (2008). Compatibility of Selected Ni-Based Alloys in Molten Li,Na,Be/F Salts with PuF₃ and Tellurium Additions. *Nuclear Technology*, 164(1):130–142.
- Ignatiev, V., Surenkov, A., Gnidoi, I., Kulakov, A., Uglov, V., Vasiliev, A., and Presniakov, M. (2013). Intergranular tellurium cracking of nickel-based alloys in molten Li, Be, Th, U/F salt mixture. *Journal of Nuclear Materials*, 440(1–3):243–249.
- Isotalo, A. E. and Aarnio, P. A. (2011). Higher order methods for burnup calculations with Bateman solutions. *Annals of Nuclear Energy*, 38(9):1987–1995.
- Kang, J. and Hippel, F. N. v. (2001). U-232 and the proliferation-resistance of U-233 in spent fuel. *Science & Global Security*, 9(1):1–32.
- Kasam, A. and Shwageraus, E. (2017). Feasibility studies of a Breed and Burn Molten Salt Reactor. In *Proceedings of ICAPP 2017*, Fukui and Kyoto, Japan. Atomic Energy Society of Japan.

Bibliography

- Kasten, P. R., Gat, U., Schulze Horn, S., and Vornhusen, H. W. (1965). Design concepts for the core structure of a MOSEL (MOlten Salt Experimental) reactor. *Nuclear Structural Engineering*, 2(2):224–232.
- Kato, Y., Nitawaki, T., and Fujima, K. (2003). Zero Waste Heat Release Nuclear Cogeneration System. In *Proceedings of ICAPP '03*, Córdoba, Spain. American Nuclear Society.
- Keiser, J. R. (1977a). Compatibility Studies of Potential Molten-Salt Breeder Reactor Materials in Molten Fluoride Salts. Technical Report ORNL/TM-5783, Oak Ridge National Laboratory, Oak Ridge, TN, USA.
- Keiser, J. R. (1977b). Status of Tellurium–Hastelloy N Studies in Molten Fluoride Salts. Technical Report ORNL/TM-6002, Oak Ridge National Laboratory, Oak Ridge, TN, USA.
- Kerlin, T. W., Ball, S. J., Steffy, R. C., and Buckner, M. R. (1971). Experiences with Dynamic Testing Methods at the Molten-Salt Reactor Experiment. *Nuclear Technology*, 10(2):103–117.
- Koomey, J. and Hultman, N. E. (2007). A reactor-level analysis of busbar costs for US nuclear plants, 1970–2005. *Energy Policy*, 35(11):5630–5642.
- Leppänen, J., Pusa, M., Viitanen, T., Valtavirta, V., and Kaltiaisenaho, T. (2015). The Serpent Monte Carlo code: Status, development and applications in 2013. *Annals of Nuclear Energy*, 82:142–150.
- Lopez-Solis, R. and François, J.-L. (2017). The breed and burn nuclear reactor: A chronological, conceptual, and technological review. *International Journal of Energy Research*.
- Losa, E., Košťál, M., Rypar, V., Novák, E., and Juříček, V. (2015). Effect of inserted fluoride salts on criticality in the LR-0 reactor. *Annals of Nuclear Energy*, 81:18–25.
- Lovering, J. R., Yip, A., and Nordhaus, T. (2016). Historical construction costs of global nuclear power reactors. *Energy Policy*, 91:371–382.
- McCoy, H. E. (1969). The INOR-8 Story. *ORNL Review*, 3(2):35–50.
- MOST Project (2005). MOST Project Final Report. Technical report, European Commission.
- Mourogov, A. and Bokov, P. (2006). Potentialities of the fast spectrum molten salt reactor concept: REBUS-3700. *Energy Conversion and Management*, 47(17):2761–2771.
- Nelson, P. A., Butler, D. K., Chasanov, M. G., and Meneghetti, D. (1967). Fuel Properties and Nuclear Performance of Fast Reactors Fueled with Molten Chlorides. *Nuclear Applications*, 3(9):540–546.
- Olson, L. C., Ambrosek, J. W., Sridharan, K., Anderson, M. H., and Allen, T. R. (2009). Materials corrosion in molten LiF–NaF–KF salt. *Journal of Fluorine Chemistry*, 130(1):67–73.

- Ottewitte, E. H. (1982). *Configuration of a Molten Chloride Fast Reactor on a Thorium Fuel Cycle to Current Nuclear Fuel Cycle Concerns*. Ph.D. Thesis, University of California in Los Angeles (UCLA), Los Angeles, CA, USA.
- Pachauri, R. K., Allen, M. R., Barros, V. R., Broome, J., Cramer, W., Christ, R., Church, J. A., Clarke, L., Dahe, Q., Dasgupta, P., and others (2014). *Climate Change 2014: Synthesis Report. Contribution of Working Groups I, II and III to the Fifth Assessment Report of the Intergovernmental Panel on Climate Change*.
- Petroski, R., Forget, B., and Forsberg, C. (2011). Using the Neutron Excess Concept to Determine Starting Fuel Requirements for Minimum Burnup Breed-and-Burn Reactors. *Nuclear Technology*, 175(2):388–400.
- Pusa, M. and Leppänen, J. (2013). Solving Linear Systems with Sparse Gaussian Elimination in the Chebyshev Rational Approximation Method. *Nuclear Science and Engineering*, 175(3):250–258.
- Qvist, S., Hou, J., and Greenspan, E. (2015). Design and performance of 2d and 3d-shuffled breed-and-burn cores. *Annals of Nuclear Energy*, 85:93–114.
- Robertson, R. C. (1965). Part I: Description of Reactor Design. Technical Report ORNL-TM-728, Oak Ridge National Laboratory, Oak Ridge, TN, USA.
- Robertson, R. C. (1971). Conceptual Design Study of a Single-fluid Molten-salt Breeder Reactor. Report ORNL-4541, Oak Ridge National Laboratory, Oak Ridge, TN, USA.
- Robertson, R. C., Smith, O. L., Briggs, R. B., and Bettis, E. S. (1970). Two-fluid Molten-salt Breeder Reactor Design Study. Technical Report ORNL-4528, Oak Ridge National Laboratory, Oak Ridge, TN, USA.
- Rosenthal, M. W. (1969). Molten-Salt Reactor Program Semiannual Progress Report For Period Ending February 28, 1969. Semiannual Progress Report ORNL-4396, Oak Ridge National Laboratory, Oak Ridge, TN, USA.
- Scott, I. (2017). 21 - Stable salt fast reactor. In Dolan, T. J., editor, *Molten Salt Reactors and Thorium Energy*, pages 571–580. Woodhead Publishing.
- Sekimoto, H., Ryu, K., and Yoshimura, Y. (2001). CANDLE: The New Burnup Strategy. *Nuclear Science and Engineering*, 139(3):306–317.
- Smith, J. and Simmons, W. E. (1974). An Assessment of a 2500 MWe Molten Chloride Salt Fast Reactor. Technical Report AEEW-R956, United Kingdom Atomic Energy Authority, Atomic Energy Establishment, Winfrith, Dorchester, Dorset.
- Snead, L. L., Nozawa, T., Katoh, Y., Byun, T.-S., Kondo, S., and Petti, D. A. (2007). Handbook of SiC properties for fuel performance modeling. *Journal of Nuclear Materials*, 371(1):329–377.

Bibliography

- Sooby, E., Baty, A., Beneš, O., McIntyre, P., Pogue, N., Salanne, M., and Sattarov, A. (2013). Candidate molten salt investigation for an accelerator driven subcritical core. *Journal of Nuclear Materials*, 440(1–3):298–303.
- Sood, D. D., Iyer, P. N., Prasad, R., Vaidya, V. N., Roy, K. N., Venugopal, V., Singh, Z., and Ramaniah, M. V. (1975). Plutonium Trifluoride as a Fuel for Molten Salt Reactors-Solubility Studies. *Nuclear Technology*, 27(3):411–415.
- Taube, M. (1974). A Molten Salt Fast Thermal Reactor System with no Waste. Technical Report EIR-Bericht 249, Eidgenössisches Institut für Reaktorforschung, Würenlingen, Switzerland.
- Taube, M. (1978). Fast Reactors Using Molten Chloride Salts as Fuel. Technical Report EIR-Bericht 332, Eidgenössisches Institut für Reaktorforschung, Würenlingen, Switzerland.
- Taube, M., Bucher, K. H., and Ligou, J. (1975). The Transmutation of Fission Products (Cs-137, Sr-90) in a Liquid Fuelled Fast Fission Reactor with Thermal Column. Technical Report EIR-Bericht 270, Eidgenössisches Institut für Reaktorforschung, Würenlingen, Switzerland.
- Taube, M. and Heer, W. (1980). Reactor with Very Low Fission Product Inventory. Technical Report EIR-Bericht 411, Eidgenössisches Institut für Reaktorforschung, Würenlingen, Switzerland.
- Taube, M. and Ligou, J. (1974). Molten Plutonium Chlorides Fast Breeder Reactor Cooled by Molten Uranium Chloride. *Annals of Nuclear Science and Engineering*, 1(4):277–281.
- Taube, M., Mielcarski, M., Poturaj-Gutniak, S., and Kowalew, A. (1967). New Boiling Salt Fast Breeder Reactor Concepts. *Nuclear Engineering and Design*, 5:109–112.
- Teller, E., Ishikawa, M., and Wood, L. (1995). Completely automated nuclear power reactors for long-term operation. In *Proceedings of the Frontier in Physics Symposium*, Lubbock, TX, USA.
- Thoma, R. E. (1959). Phase Diagrams of Nuclear Reactor Materials. Technical Report ORNL-2548, Oak Ridge National Laboratory, Oak Ridge, TN, USA.
- Treyer, K., Bauer, C., and Simons, A. (2014). Human health impacts in the life cycle of future European electricity generation. *Energy Policy*, 74, Supplement 1:S31–S44.
- Varma, V. K., Holcomb, D. E., Peretz, F. J., Bradley, E. C., Ilas, D., Qualls, A. L., and Zaharia, N. M. (2012). AHTR Mechanical, Structural, and Neutronic Preconceptual Design. Technical Report ORNL/TM-2012/320, Oak Ridge National Laboratory, Oak Ridge, TN, USA.
- Vergnes, J. and Lecarpentier, D. (2002). The AMSTER concept (Actinides Molten Salt TransmutER). *Nuclear Engineering and Design*, 216(1–3):43–67.
- Weinberg, A. M. (1994). *The First Nuclear Era: The Life and Times of a Technological Fixer*. American Institute of Physics.

- Williams, D. F., Toth, L. M., and Clarno, K. T. (2006). Assessment of Candidate Molten Salt Coolants for the Advanced High-Temperature Reactor (AHTR). Technical Report ORNL/TM-2006/12, Oak Ridge National Laboratory, Oak Ridge, TN, USA.
- Yamanaka, S., Yoshioka, K., Uno, M., Katsura, M., Anada, H., Matsuda, T., and Kobayashi, S. (1999). Thermal and mechanical properties of zirconium hydride. *Journal of Alloys and Compounds*, 293–295:23–29.
- Zhu, H., Holmes, R., Hanley, T., Davis, J., Short, K., and Edwards, L. (2015). High-temperature corrosion of helium ion-irradiated Ni-based alloy in fluoride molten salt. *Corrosion Science*, 91:1–6.

List of Abbreviations

Abbrev.	Description	Page
ADS	Accelerator-Driven System	12
AERE	Atomic Energy Research Establishment	24
AHR	Aqueous Homogeneous Reactor	12
AHTR	Advanced High Temperature Reactor	22
ALISIA	Assessment of LIquid Salts for Innovative Applications	28
ANP	Aircraft Nuclear Propulsion Program	17
ARE	Aircraft Reactor Experiment	37
ART	Aircraft Reactor Test	18
B&B	Breed-and-Burn	52
BOL	Beginning of Life	94
BOS	Beginning of Step	63
BWR	Boiling Water Reactor	5
CAS	Chinese Academy of Sciences	27
CE/LI	Constant Extrapolation/Linear Interpolation	63
CEA	Commissariat à l'Énergie Atomique	23
CNRS	Centre National de la Recherche Scientifique	23
DMSR	Denatured Molten Salt Reactor	21
DOE	Department of Energy	10
EDF	Électricité de France	23
EIR	Eidgenössisches Institut für Reaktorforschung	25
EOS	End of Step	63
EVOL	Evaluation and Viability Of Liquid fuel fast reactor system	27
FCVS	Filtered Containment Venting System	6

List of Abbreviations

Abbrev.	Description	Page
FHR	Fluoride-cooled High temperature Reactor	15
FLi	LiF–AnF ₄ salt mixture	36
FLiBe	LiF–NaF–AnF ₄ salt mixture	36
FLiNa	LiF–BeF ₂ –AnF ₄ salt mixture	36
FNaBe	NaF–BeF ₂ –AnF ₄ salt mixture	36
FNaK	NaF–KF–AnF ₄ salt mixture	36
FP	Fission Product	7
GFR	Gas-cooled Fast Reactor	11
GHG	Greenhouse Gases	1
GIF	Generation IV International Forum	6
HEU	High-Enriched Uranium	38
HTR	High Temperature Reactor	16
IAEA	International Atomic Energy Agency	9
JAERI	Japanese Atomic Energy Research Institute	25
LEU	Low-Enriched Uranium	38
LFR	Lead-cooled Fast Reactor	11
LMFR	Liquid Metal Fuel Reactor	12
LWR	Light Water Reactor	1
LWRPu	Light Water Reactor Plutonium	38
MOSART	MOlten Salt Actinide Recycler and Transmuter	27
MOST	Review of Molten Salt Reactor Technology	28
MOU	Memorandum Of Understanding	25
MOX	Mixed Oxide	5
MSBR	Molten Salt Breeder Reactor	19
MSBR(2f)	Two-fluid Molten Salt Breeder Reactor	58
MSFR	Molten Salt Fast Reactor	23
MSR	Molten Salt Reactor	2
MSRE	Molten Salt Reactor Experiment	16
MSRP	Molten Salt Reactor Program	17
NPP	Nuclear Power Plant	2
ORNL	Oak Ridge National Laboratory	15

Abbrev.	Description	Page
PUREX	Plutonium-Uranium Redox Extraction	12
PWR	Pressurized Water Reactor	5
RE	Reductive Extraction	122
RTD	Residence Time Distribution	52
SAMOFAR	Safety Assessment of the MOlten salt FAst Reactor	28
SCWR	Supercritical Water Reactor	11
SFR	Sodium-cooled Fast Reactor	11
SINAP	Shanghai Institute of Applied Physics	27
SMR	Small Modular Reactor	1
SNF	Spent Nuclear Fuel	7
SPHINX	SPent Hot fuel Incinerator in Neutron fluX	33
SWR	Standing Wave Reactor	106
TASSE	Thorium-based Accelerator-driven System with Simplified fuel cycle for long-term Energy production	23
TRU	TRansUranic elements	38
TWR	Travelling Wave Reactor	105
UKAEA	United Kingdom Atomic Energy Authority	24
VHTR	Very High Temperature Reactor	11
WGPu	Weapons-grade Plutonium	38

Boris Hombourger

Address: Seminarstrasse 19, 5400 Baden AG, Switzerland
Contact: + 41 (0)78 898 41 82, boris.hombourger@protonmail.com
Citizenships: Swiss, French

OBJECTIVE

I am a dedicated and enthusiastic nuclear engineer with experience in Reactor Physics simulations. I am seeking to leverage my expertise in Molten Salt Reactor design to find an internship or permanent position in the field.

TECHNICAL SKILLS

- 4 years of experience in reactor physics simulations, with focus on neutronics and fuel cycle
- Nuclear Engineering codes: Serpent, MCNP, ERANOS, CASMO, SIMULATE, TRACE
- General computing: C++, MATLAB, Python, git, LaTeX, Microsoft Office

EDUCATION

- Doctorate of Science in Physics** *Federal Institute of Technology Lausanne, Switzerland* 2013–2018
- Dissertation entitled "Conceptual Design of a Sustainable Waste-burning Molten Salt Reactor"
 - Developed the MATLAB and Serpent-based EQL0D procedure for MSR fuel cycle simulation
 - Earned the best student paper (Europe) award at the ICONS 22 conference in Prague, Czech Republic
- Master of Science in Nuclear Engineering** *Federal Institute of Technology Lausanne & Zurich, Switzerland* 2011–2013
- Bachelor of Science in Physics** *Federal Institute of Technology Lausanne, Switzerland* 2008–2011

WORK EXPERIENCE

- Paul Scherrer Institute, Federal Institute of Technology Lausanne** *Villigen, Switzerland* 2013–2017
Helped teach 2 graduate Nuclear Engineering and 1 Operators school courses, co-supervised of 3 Master's theses. Doctoral assistant
- Capricorn Investment Group** *New York City, USA* June 2017
Facilitated due diligence interviews with several Molten Salt Reactor companies. Consultant
- Terrestrial Energy** *Oakville, Canada* August 2015
Supported the use of the EQL0D code developed during my thesis work. Consultant
- Swiss Federal Nuclear Safety Inspectorate** *Brugg, Switzerland* 2012–2013
Renewed the Large-break Loss of Coolant Analyses for the Gösgen Nuclear Power Plant using TRACE. Intern
- Federal Institute of Technology Lausanne** *Lausanne, Switzerland* 2009–2011
Prepared and lead exercises sessions for 8 different undergraduate Physics classes. Teaching assistant

SELECTED PUBLICATIONS

- B. Hombourger, J. Křepel, K. Mikityuk, and A. Pautz. On the Feasibility of Breed-and-Burn Fuel Cycles in Molten Salt Reactors. In *Proceedings of FR17*, Yekaterinburg, Russia, June 2017. International Atomic Energy Agency
- B. Hombourger, J. Křepel, K. Mikityuk, and A. Pautz. Fuel Cycle Analysis of a Molten Salt Reactor for Breed-and-Burn Mode. In *Proceedings of ICAPP '15*, Nice, France, May 2015. American Nuclear Society
- B. A. Hombourger, J. Křepel, K. Mikityuk, and A. Pautz. Parametric Lattice Study of a Graphite-Moderated Molten Salt Reactor. *Journal of Nuclear Engineering and Radiation Science*, 1(1):011009, Jan. 2015

LANGUAGES

French native, **English** fluent (spoken, written and read), **German** fluent (spoken, written and read), **Italian** conversational (spoken).

MEMBERSHIPS

American Nuclear Society (2016–Present), **Swiss Nuclear Society** (2012–Present), **EPFL Alumni Association** (2013–Present).